Dissertation

on

TURBULENCE STUDIES BY REFLECTED

ELECTROMAGNETIC WAVES

presented

by

S. L. ALLEMAN

for

the degree of

DOCTOR OF PHILOSOPHY

of

THE OHIO STATE UNIVERSITY

043

B2519

May 1963

PHYSICAL RESEARCH LABORATORY

Avco-Everett

PREFACE

The present dissertation embodies the investigations made by the author at the Physical Research Laboratory, Ahmedabad. It is presented in two main sections.

Section I deals with the studies on the propagation of low frequency radio waves (164 Kc/s) over a distance of about 810 Km from Baghdad, Iraq to Ahmedabad. Analysis of about two years' data reveals distinct diurnal and seasonal variations of the longwave field intensity during daylight hours. It is found that during local summer the field intensity varies regularly with the position of the sun in the sky attaining a maximum around noon and tapering off on either side. During the rest of the year the overall intensity in the day is higher with oscillatory features near sunrise and sunset.

The effect of Sudden Ionospheric Disturbances on the propagation of the low frequency radio wave is investigated with the help of 114 SID's observed during March, 1960 to December, 1960. Broadly, SID's during the local summer started off with a sudden enhancement of the longwave field intensity while those occurring during the rest of the year commenced with a very sharp absorption followed by an enhancement. Most of the SID's recorded showed appreciable absorption after the maximum enhancement. This aspect of the

low frequency work was studied in collaboration with Mr.J.S.Shirke.

In Section II the influence of lunar tide on the critical frequency and the height of maximum electron density of the F_2 layer of the ionosphere over Ahmedabad during March, 1953 to February, 1956 is studied. This analysis is supported by probable error circles on harmonic dials.

The above analysis is followed by an investigation of the lunar tidal effect on the critical frequency of the F_2 layer over stations in a narrow longitudinal belt in the American zone. They are Panama (a northern tropical latitude station), Huancayo (a magnetic equatorial station) and Buenos Aires (a southern tropical latitude station).

Briefly, the maximum amplitude of the semi-diurnal lunar tide in f_0F_2 at Ahmedabad and Panama occurs around noon with its phase between 10 to 12 lunar hours. At Huancayo it takes place around noon having its phase at about 04 lunar hour. The lunar tide in f_0F_2 at Buenos Aires, however, exhibits very different behaviour. The maximum semi-diurnal tide occurs around 16 hour and its phase around 07 lunar hour. In contrast to the other stations, Buenos Aires experiences appreciable lunar tidal effects even at night.

Author

S.R.Khadekar

Countersigned

K.R.Ramanathan

18/5/63

ACKNOWLEDGEMENTS

The work presented in this thesis was carried out under the financial assistance from the Indian Council of Scientific and Industrial Research and the Department of Atomic Energy of the Government of India. My grateful thanks are due to Dr.S.S. Kastogi for suggesting the problem incorporated in Section II of this dissertation and also for occasional helpful discussions. I am thankful to Mr.J.S.Shirke for collaboration in the initial stages of the work on the low frequency propagation. Thanks are also due to Mr.K.N.Thakare and Mr.Sawtant for their valuable help in extensive computations on the IBM 1401.

I record my deep gratitude to Professor K.R.Ramanathan, Director, Physical Research Laboratory, Ahmedabad, for his valuable guidance throughout the period of investigation.

References and acknowledgements to other workers and authors have been made in appropriate places.

S.K.Alurkar

(S.K. Alurkar)

CONTENTS

			Pages
SECTION I -		Studies on the low frequency propagation of electromagnetic waves	
	Chapter 1 -	Experimental set-up for recording the field intensity of 164 Kc/s transmission	1 - 6
	Chapter 2 -	Diurnal and seasonal variations of daytime field intensity	1 - 24
	Chapter 3 -	Effects of sun spots and SID's on the propagation of 164 Kc/s radio waves	1 - 22
	Chapter 4 -	Summary and discussion	1 - 7
SECTION II -		Lunar tidal oscillations in the F_2 layer of the ionosphere	
	Chapter 1 -	Introduction	1 - 16
	Chapter 2 -	Lunar tidal variations in the F_2 layer of the ionosphere over Ahmedabad	1 - 14
	Chapter 3 -	Lunar tidal oscillations in the critical frequency f_0F_2 of the F_2 layer of the ionosphere over Panama, Huancayo and Buenos Aires	1 - 30
	Chapter 4 -	Summary and discussion	1 - 7

Contents

CHAPTER 1

		Page
1.	Introduction	1
2.	Experimental setup at Ahmedabad	2
3.	Antenna	2
4.	Receiver	4
5.	D-C Amplifier	7
6.	Pen Recorder	8
7.	Calibration of records	8

CHAPTER 1

EXPERIMENTAL SET-UP FOR RECORDING THE FIELD INTENSITY OF 164 Kc/s TRANSMISSION FROM TASHKENT (41°N, 69°E) TO AHMEDABAD (23° 01' N, 72° 38' E)

1. Introduction

The lowest portion of the ionosphere, the D region, has been studied for many decades with the help of low (30 - 300 Kc) and very low (3 - 30 Kc) frequency radio waves. The changes produced in the waves by propagation through the lower atmosphere and reflection by the ionosphere are inferred from a study of the amplitude, phase and polarization characteristics of the reflected waves. Different techniques are employed for each of the above parameters. In this chapter the equipment used at Ahmedabad for measuring the variations in the intensity of the down-coming skywave of 164 Kc/s CW-transmission from Tashkent, USSR is described. One of the objects of starting this continuous recording of the longwave field intensity was to observe its response to solar flares, since low frequency waves propagating over long distances are known to be very sensitive to the X-ray emissions of the sun during flares. In addition this experiment enabled us to study the diurnal and seasonal variations of the daytime signal amplitude of the low frequency transmission.

2. Experimental set-up at Ahmedabad

The set-up incorporated a directive wave or Beverage antenna oriented in the E-W direction, a superheterodyne communication receiver, a d-c amplifier, a recording milliammeter and a standard signal generator to calibrate the recorded field intensity. Their arrangement is shown in the block-diagram of Figure 1.

We shall now describe the various components one by one.

3. Antenna

When regular field strength recording was started in March, 1960, the aerial was of the simple inverted - L type. Though it could receive the low frequency signals quite efficiently, due to its omnidirectional property it used to receive stray pick-ups from all directions, thus spoiling the records. To reduce unwanted signals, a low frequency aerial having its principal radiation (or reception) pattern oriented in only one direction was employed. This is the wave-antenna described below.

3.1. General description of a wave antenna

The wave or Beverage antenna has for many years been an important low frequency directive antenna for fixed frequency operations, particularly for frequencies less than 100 Kc/s. It is aperiodic (broad band) and works on the

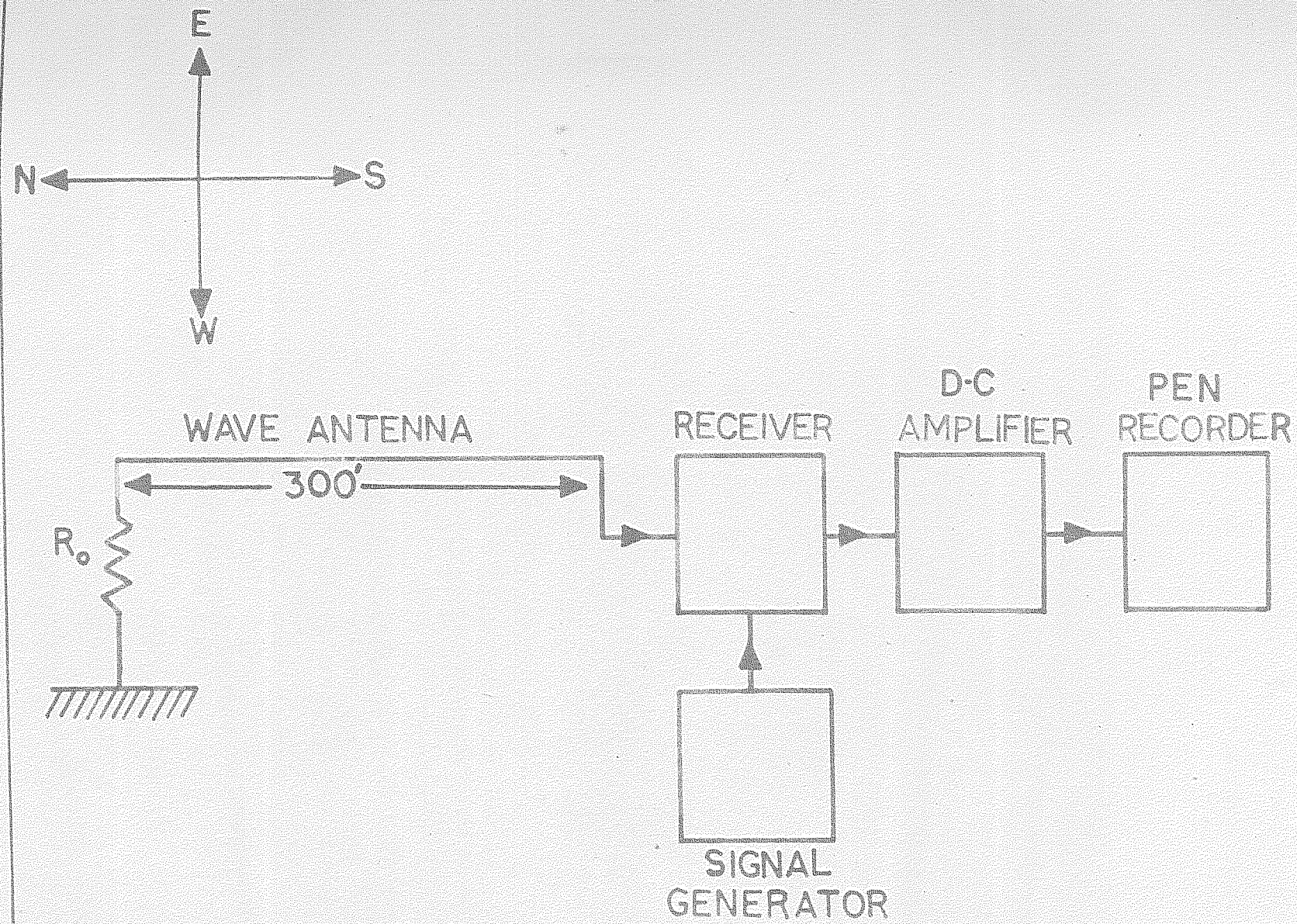

E
N
S
W
WAVE ANTENNA
300'
R_o
RECEIVER
D-C
AMPLIFIER
PEN
RECORDER
SIGNAL
GENERATOR

FIGURE-1.

travelling wave principle. Used for reception it consists of a horizontal wire one or more wavelengths long and oriented in the direction of the wave under consideration. Unlike other antennas, it requires ground with low conductivity and is normally erected at a height of 15 to 30 feet from the ground. It is terminated in its characteristic impedance to ground at the end nearest to the transmitting station. It is effective in the case of vertically polarised waves because the electric vectors of an advancing wavefront, while passing over imperfectly conducting ground, are tilted forward in the direction of the wave as shown in Figure 2. This produces a horizontal component E_H of field strength. In a small element of wire dx there will be an e.m.f. E_H. dx. This will cause currents to flow in either direction from the element of wire. In the direction of propagation the current from the first element adds to that from the next element and so on. In the opposite direction, however, there is no additive effect. Here the signals interfere and produce no resultant. The cumulative current develops a voltage across the input impedance of the receiver which is approximately proportional to E_H and the length of the wire.

The length of the antenna wire can be increased upto the point where the phase of the wave in the aerial begins to interfere with that of the incoming wave. This optimum condition is decided by the conductivity of the soil surrounding the antenna, the operating frequency and the orientation

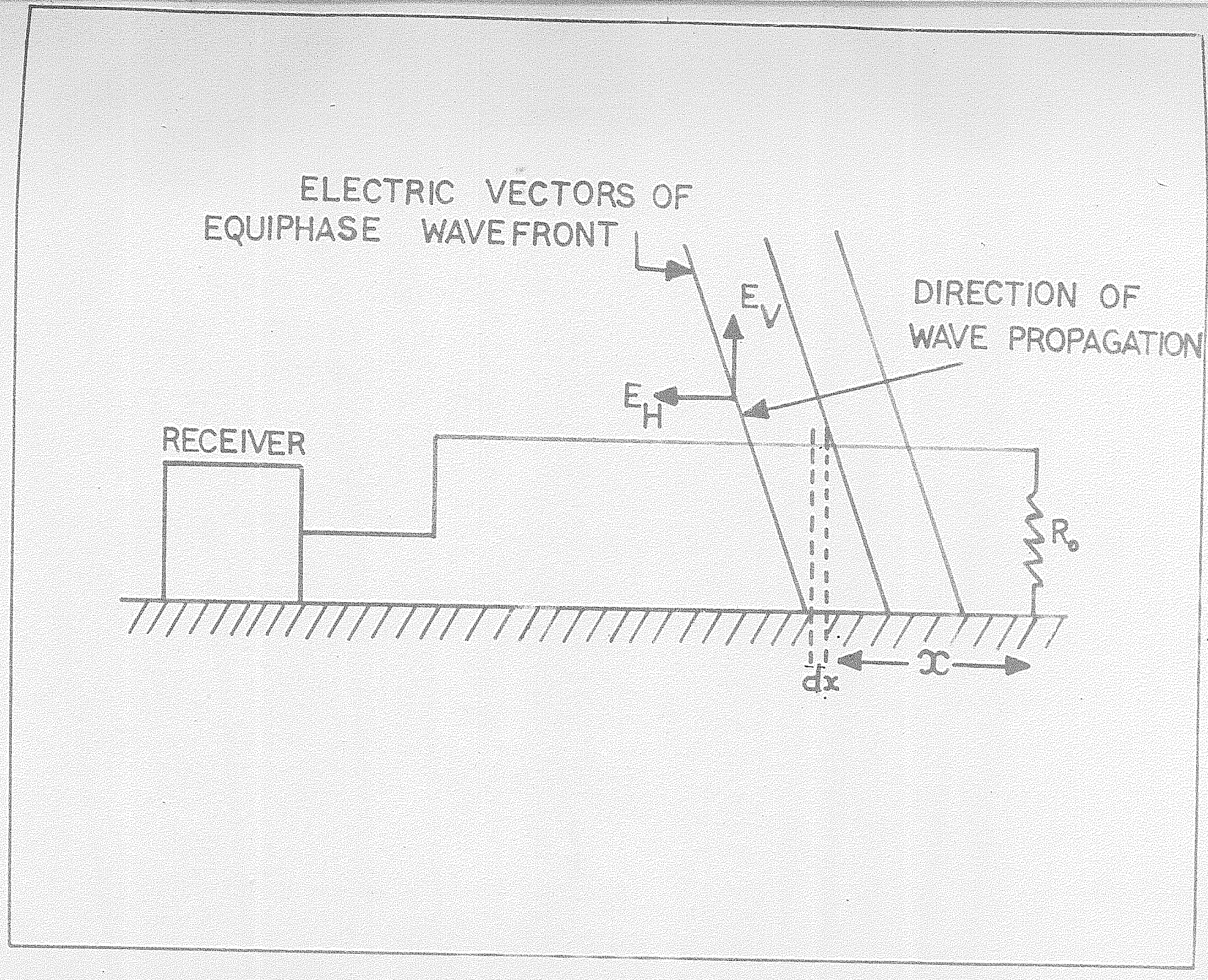

ELECTRIC VECTORS OF
EQUIPHASE WAVEFRONT
DIRECTION OF
WAVE PROPAGATION
E_V
E_H
RECEIVER
R_b
dx
x

FIGURE-2.

of the antenna with respect to the direction of wave propagation in cases where the antenna is not oriented in that direction. This latter condition is responsible in rendering the antenna highly directive, provided its far end is terminated in its characteristic impedance which dissipates energy travelling in the opposite direction in the antenna.

The Beverage aerial is not as efficient as a vertical aerial designed to receive the vertical component. It is most suitable as a directional antenna over a large area of poor conductivity soil. At low frequencies the ratio of the horizontal to vertical component is about 2 % for good soil and 0 % for poor soil.

If the incoming waves are exactly vertically polarised no E.M.F. will be induced in such an antenna, but at Ahmedabad the soil is sandy and usually dry and this may be expected to give the received wave a considerable forward tilt. A horizontal component which induces E.M.F. in each element of the antenna wire is generally found to exist.

4. Receiver

A U.S. Army Signal Corps BC-342D receiver was adapted for the field strength measurement on 164 Kc/s. It is a 9-tube superheterodyne receiver having a frequency coverage of 150 Kc to 1500 Kc divided into four bands. The receiver was originally meant for amplitude modulated (AM) or continuous-wave (CW) code signals over the above range. For our purpose the CW-oscillator was disconnected.

The receiver has the following tube line-up with the respective functions:-

Valve type	Function
6K7 (VT60)	1st and 2nd RF amplifiers
6K7 (VT57)	1st detector or mixer
6C6 (VT65)	RF oscillator
6K7 (VT60)	1st and 2nd IF amplifiers
6H7 (VT59)	2nd detector, AVC, 1st Audio amplifier
6F6 (VT66)	Audio output amplifier
5Y3GT	Rectifier

4.1. Antenna connections

The antenna is coupled to the grid of the first RF amplifier through the grid-tank circuit. The input impedance of the receiver is of the order of 300 ohms.

4.2. RF amplifiers and mixer

There are two conventional RF stages with fixed cathode bias preceding the mixer as shown in Figure 3. Since most of the receiver noise origination is the mixer stage the mixer gain was reduced in order to maintain a good signal to noise ratio at the output of the receiver. The AVC control on these stages was removed since we are measuring both quick and slow changes in the received signal amplitude.

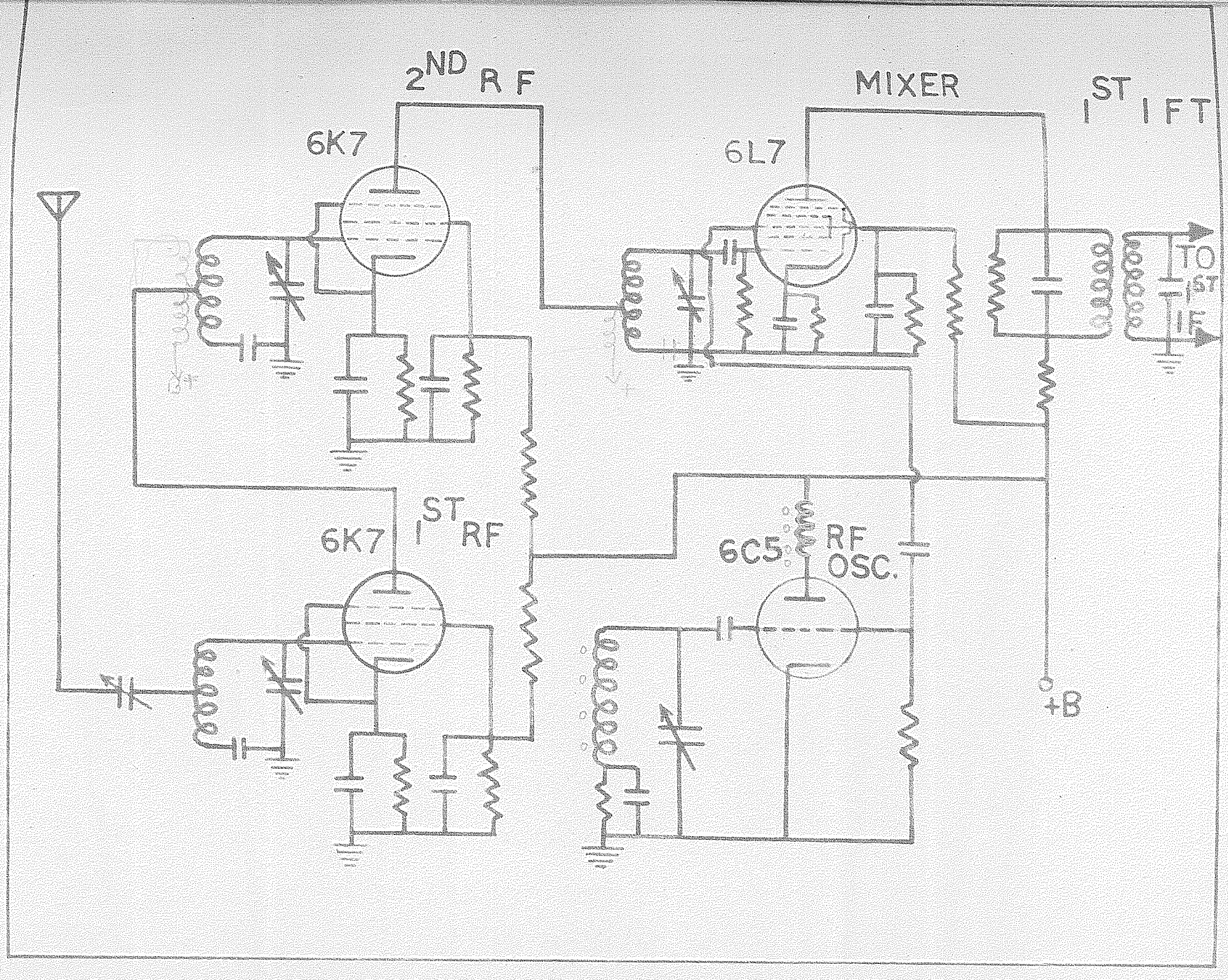


FIGURE-3. RF AMPLIFIER, OSCILLATOR AND MIXER

4.3. RF Oscillator

The RF oscillator stage is originally highly stabilised and carefully shielded.

4.4. IF Amplifiers

The receiver has two intermediate frequency amplifiers having two coupling transformers with two pentode amplifier tubes of the remote cut-off type. The input to the 1st IF amplifier tube is derived from the 1st detector transformer. The IF amplifiers together with the 2nd detector are shown in Figure 4. The AVC from the IF amplifiers was removed and cathode bias was employed to achieve increased gain.

4.5. Gain control

The gain of the RF and mixer was fixed which gave good signal to noise ratio. The receiver gain was controlled by a wire-wound potentiometer, common to the cathodes of the IF amplifier tubes.

4.6. Second detector

The detector employed a conventional double diode triode tube, whose detected output was fed to a recording milliammeter after d-c amplification.

The overall bandwidth of the receiver is about 2 kc at 6 db down. To maintain good stability a constant voltage transformer was used to assure 230 volts AC mains. This was further lowered to 110 volts AC by a step-down transformer

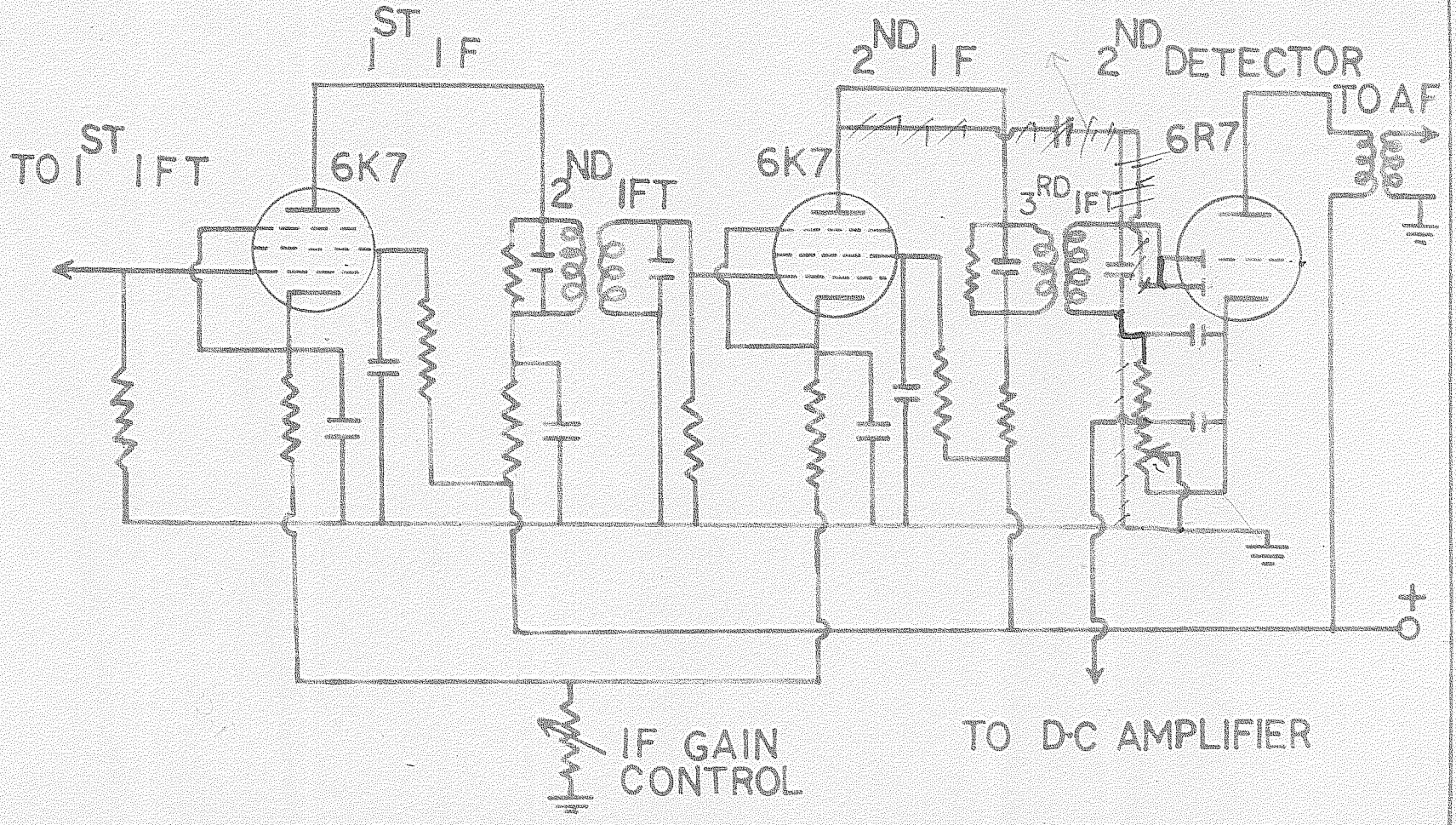


FIGURE-4. IF AMPLIFIER AND 2ND DETECTOR

since the receiver operates on 110 volts mains. Because of good stability of the receiver and the relatively strong signal received, additional care, such as an electronically stabilized power supply, was not warranted.

The detected signal is usually not large enough to produce a recordable current in recording milliammeters. It is, therefore, amplified after detection to give a recordable output current.

5. D-C Amplifier

A direct-coupled amplifier is one in which the input, output and interstage couplings are conductive, i.e. they employ direct connections or resistive network. No blocking condensers or coupling transformers are used. Thus, they amplify dc signals dropping the bandpass characteristics to zero at zero frequency.

The conductive coupling used throughout results in certain practical difficulties. The 'zero adjustment' problem is the most difficult one. A non-conductively coupled amplifier gives zero output for zero input regardless of circuit parameters such as resistors, supply voltages, tube characteristics and so on. In the case of a d-c amplifier, however, the dc output at a given dc input (e.g. zero) does depend on these parameters. A certain output voltage or current is usually required for a specified input. To achieve this a 'zero adjustment' is necessary to

compensate for variations in the above parameters.

The d-c amplifier used in the present case is a difference type of amplifier shown in Figure 6. The d-c amplifier employs a twin triode tube and amplifies the difference between the detector output voltage and a suitable steady reference voltage, viz. the ground voltage.

6. Pen recorder

The receiver output after d-c amplification is fed to a 0-1 mA range milliammeter manufactured by Evershed and Vignoles Co., England. It is operated by a synchronous motor with a normal chart speed of 1 inch per hour. The time constant of the pen recorder is 1 second and is slightly variable by means of a damping arrangement provided.

7. Calibration of records

The charts read signal intensities in terms of milliamperes. These are converted into microvolts by calibrating against a voltage derived from a GR Standard Signal Generator of the type 805-B. The calibration was repeated twice a week.

To measure the intensity of a given record some kind of 'zero marker' is necessary. This was done by mistuning the receiver in the neighbouring band for a minute or two. The level thus noted is the noise level of the receiver

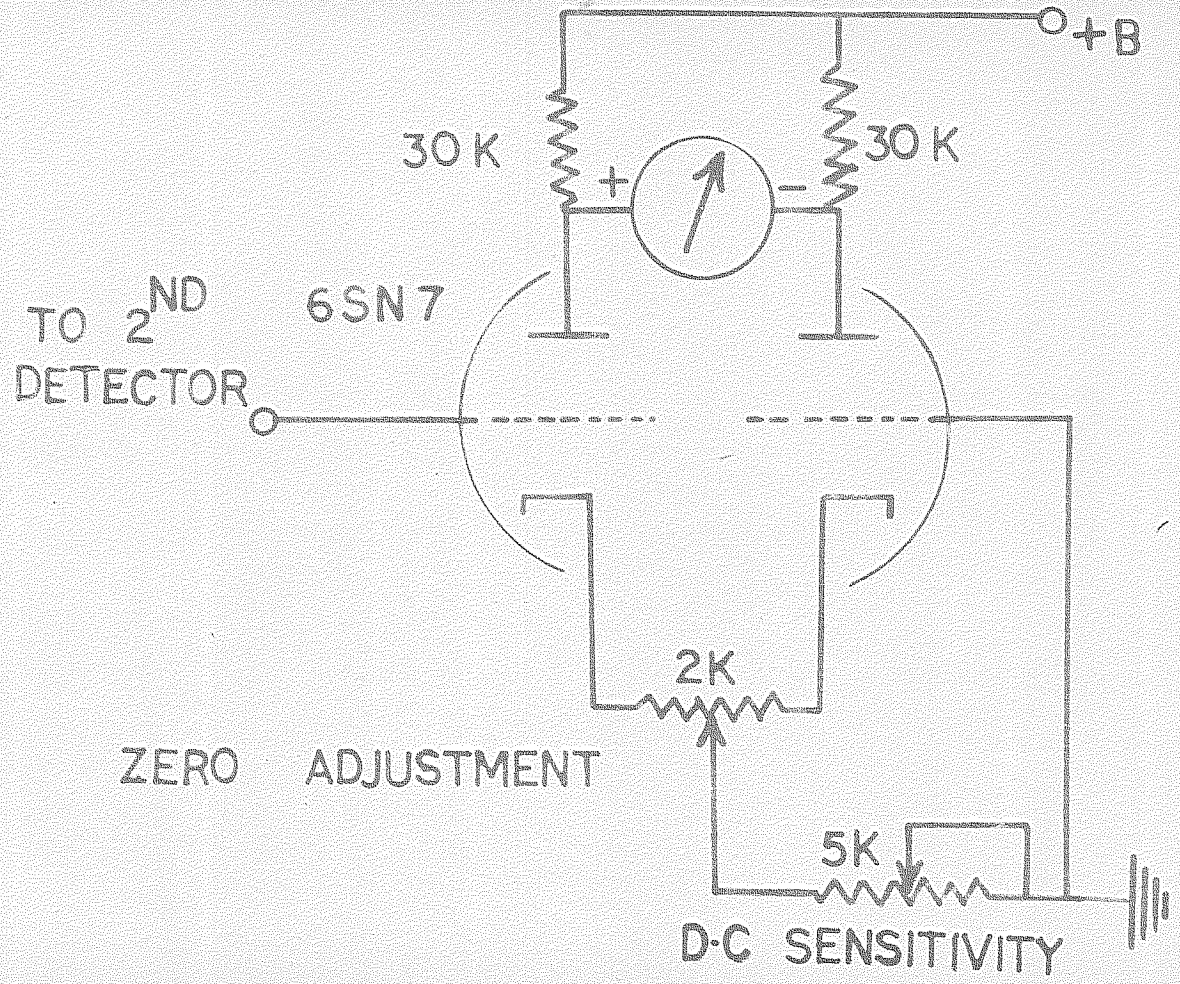


FIGURE-5. D-C AMPLIFIER

plus the noise picked up by the aerial which is almost constant over a wide frequency band. The zero meters were repeated more than once in a day.

Since the signal intensities at night and in the day differ very much from each other, two different settings of the gain control were fixed up. These two positions were changed one before layer sunrise and the other after sunset.

*** ooo ***

CONTENTS

CHAPTER 2

		Page
1.	Introduction	1
2.	Brief summary of previous experimental work	1
3.	Height of the reflecting region	4
4.	Low frequency work at Ahmedabad	5
5.	Diurnal and seasonal variations of the field intensity at Ahmedabad	6
6.	Dependence of the diurnal field intensity on the solar zenith distance	16
7.	Sudden drop in intensity at the time of layer sunrise	18
8.	Height of the ionospheric region corresponding to the commencement of the fall in intensity at the time of layer sunrise	19
9.	Minima in intensity near sunrise and sunset	21

CHAPTER 2

DIURNAL AND SEASONAL VARIATIONS OF DAYTIME FIELD INTENSITY

1. Introduction

Low frequency (30 - 300 Ke/s) and very low frequency (3 - 30 Ke/s) radio waves are used in long distance telegraphy, time broadcasting and navigation services. For these applications one should know the strength of the signal, received at a given point from a given transmitter and also its variations with the time of day, season and phase of the solar cycle.

The theoretical treatment of the problem is rather difficult, since one has to consider the effect of the earth's curvature and its magnetic field. With increasing wavelength the optical ray theory becomes practically inapplicable since the ionospheric constants vary substantially within the length of a wave and full-wave theory must therefore be used. We shall deal mainly with the experimental and observational aspects.

2. Brief summary of previous experimental work

Hollingworth (1930) was one of the first to make detailed studies of long wave propagation over distances less than 1000 Km in U.K. He measured the intensities of waves of frequency 20.0 Ke/s over distances between 300 and

1000 Km and showed the existence of an interference pattern at the ground formed by the combination of the ground wave with the sky wave. The downcoming sky wave was found to be reflected from a height of about 75 Km at midday in summer.

From studies on the ionospheric propagation of low and very low frequency radio waves over distances less than 1000 Km, Bracewell, Budden, et al (1951) from the Cavendish Laboratory, Cambridge, concluded that for distances greater than a few hundred Km, and for frequencies less than 75 Kc/s, the received signal near sunrise and sunset underwent marked minima, and that the signals from distant transmitters in the daytime were stronger and more variable in winter than in summer; a rather sudden seasonal change in propagation conditions occurred in November and corresponding more gradual reverse change in spring.

Budden, Bracewell, Straker and Westcott (1952) studied the characteristic features of 16 Kc/s waves over distances of about 540 Km at Aberdeen. Both the amplitude and phase of the waves showed a fall during morning twilight, but there was still a strong downcoming sky wave during the rest of the day. The diurnal variation of the signal amplitude showed a close solar control. The essential features of the diurnal signal amplitude are (a) a sudden change in amplitude near sunrise and sunset and (b) minima near sunrise and sunset in the period between March and October.

Beginning from about 1945, the scientists of the Cavendish Laboratory did some pioneering work on the propagation of LF and VLF radio waves, particularly in the range 30 - 120 Kc/s. Watson and Stuart (1952) studied the behaviour of the signal amplitudes of frequencies 71.1, 88.4 and 113.3 Kc/s over a distance of about 640 Km. The amplitudes showed marked oscillations near sunrise and sunset. They also observed that the changes in phase and amplitude began well before the time of ground sunrise at the mid-point of the transmission path. The times of occurrence of the first two minima in signal strength were found to be under solar control. The first minimum occurred when the solar zenith angle was $98\frac{1}{2}^{0}$.

Hopkins and Reynolds (1964) worked on 70.3 and 16 Kc/s radio waves over distances up to 100 Km. They showed that (a) in winter, the day to day behaviour of the skywave was very irregular; there were no appreciable difference between day and night signal levels; (b) in midsummer the diurnal variation of the signal amplitude was often repeated from day to day and there was a marked change near sunrise and sunset; the sudden commencement of the early morning fall in amplitude set in about an hour before ground sunrise, and that (c) the October data showed a transition from summer to winter conditions.

Very recently Nargrenven (1969) has studied the diurnal and seasonal variations of the minimum in amplitude

shortly after sunrise. He observed that from June to September the minimum was always shallow. Between December and May the minimum was deeper, indicating a marked sunrise layer, but it was also more variable from day to day. To facilitate interpretations of the diurnal and seasonal variations of 17.80 kc/s signal Hargreaves received it at 841 and 1044 km simultaneously. The daytime signals were comparatively steady and the changes repeated closely from day to day. Most of the diurnal changes occurred near sunrise and sunset, with an asymmetry about noon that was most apparent in winter. The night time signal showed quite irregular variations due apparently to irregular ionosphere at that time. There was a more gradual change from day to night conditions in winter than in summer.

3. Height of the reflecting region

The behaviour of the height of reflection of low and very low frequencies was studied by Nitta (1951) and later by Bracewell, Harwood and Straker (1954). For vertical incidence the law is similar to the one for E and F_1 regions, viz,

$$\Delta h = A \log f(\chi),$$

where $f(\chi)$ is the Chapman function of χ, the solar zenith angle, and approximation to sec χ for $\chi \leq 85^0$. A is approximately a constant. For oblique incidence (beyond 300 km for 16 kc/s waves), however, the height begins to

decrease suddenly about an hour before ground sunrise and remains almost constant throughout the day and increases rapidly near sunset.

Rain, Bracewell, Straker and Westcott (1952) received 16 and 19.4 Kc/s waves over 635 and 400 Km. They obtained 74 and 82 Km as the heights at midday and at night respectively.

A new experiment was performed by Watts and Brown (1954) using a swept frequency recorder covering a range of 50 - 1100 Kc/s. Daytime reflections from apparently discrete levels in the height ranges of 68 - 80 Km, 85 - 90 Km and 98 - 110 Km were observed.

Hargreaves (1952) investigated the behaviour of the reflection height of 19.6 Kc/s waves over 370 and 628 Km at the time of ionospheric sunrise. He observed a temporary reduction of reflection height at sunrise. The fall in the height varied from day to day, and was more marked in winter (about 4 Km) than in summer (about 1 Km or so).

4. Low frequency work at Ahmedabad

Regular field strength recording of 164 Kc/s CW-transmission from Tashkent (41°N, 69°E) has been going on at Ahmedabad since March, 1960. The difference in the longitudes of Ahmedabad and Tashkent is only 5°. The transmitter is on the air for about twenty two hours a day, remaining off for only two hours between 3 a.m. to 5 a.m.

Thus consistent recording of the field intensity is possible.

The great circle distance between Ahmedabad and Teghient is about 2450 Km. The equivalent vertical incidence frequencies for one-hop, two-hop and three-hop transmissions work out to be 24 Kc/s, 28 Kc/s and 36 Kc/s respectively, for an assumed reflection height of 70 Km above the surface of the earth.

The behaviour of the field intensity at night is too irregular to enable any systematic analysis to be made and, therefore, we shall concentrate our attention on daytime observations only.

5. Diurnal and Seasonal variations of the field intensity at Ahmedabad

For convenience, we shall divide the whole year into two periods (a) from June to October and (b) from November to May. The first group represents summer (Northern solstices) while the second one represents, broadly, winter.

5.1. (a) Variations of the diurnal amplitude during the period from June to October

Figure 1 shows the original record on 3rd June, 1960. It is typical of summer conditions. The night-time intensity is quite high and irregular. The transmitter is

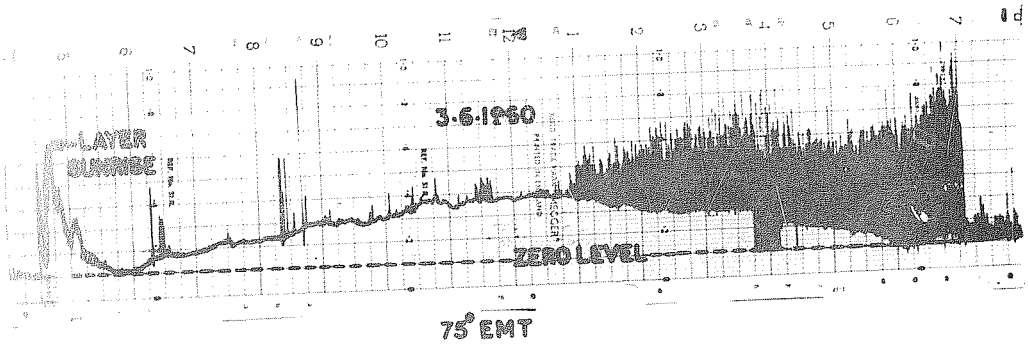
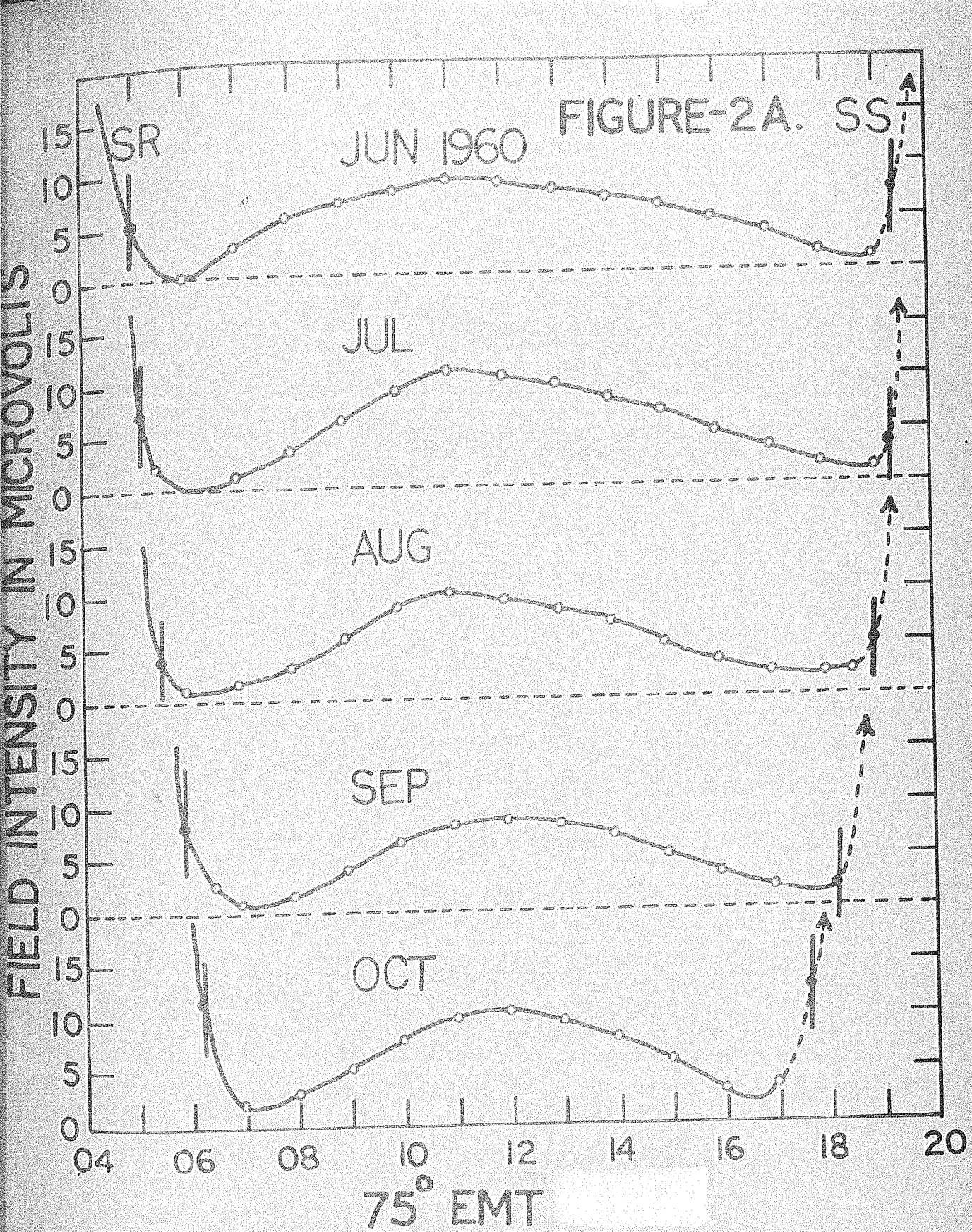


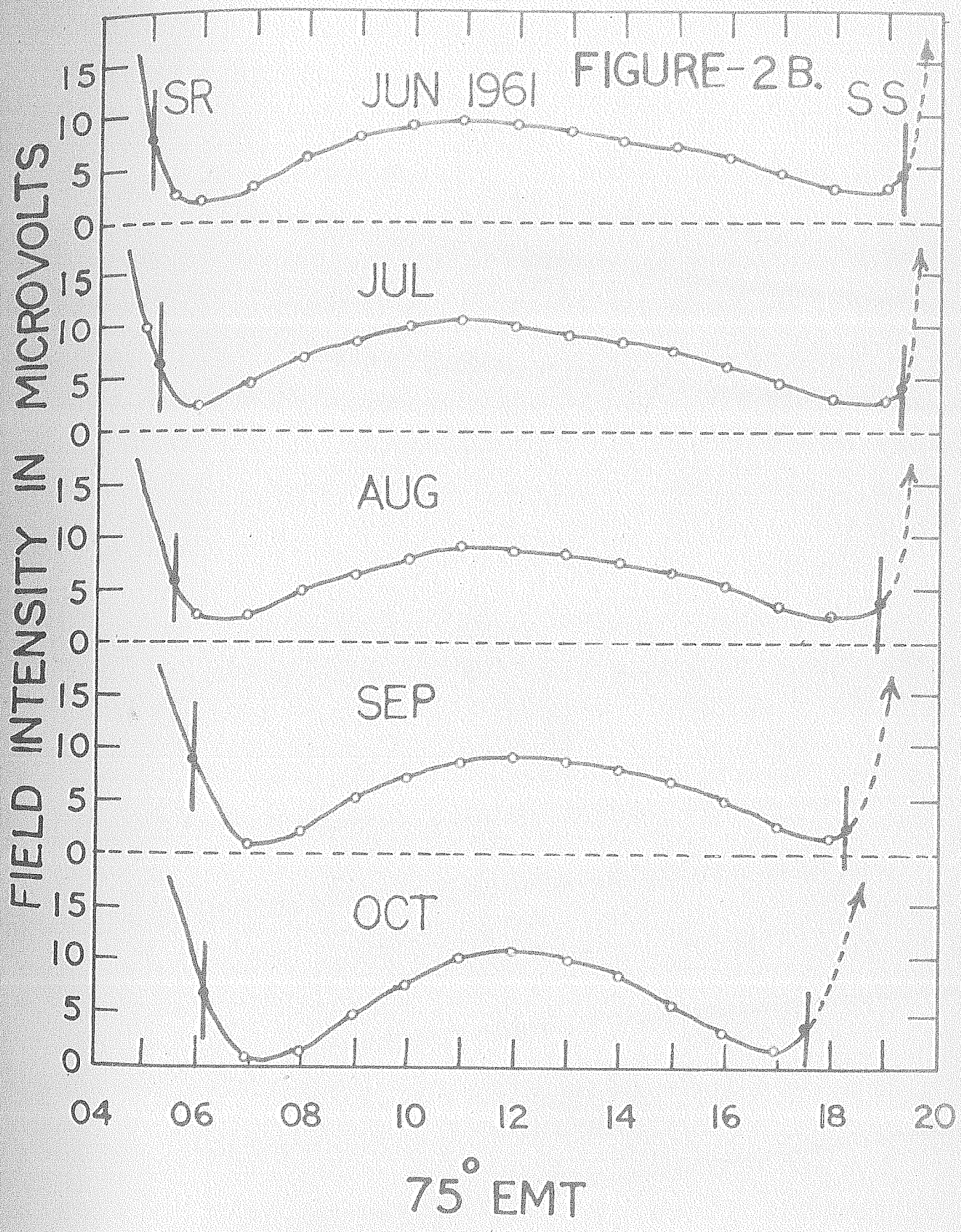
Fig. 1

off between 1 a.m. to 4.00 a.m. 75° EMT. During this interval the receiver noise together with the noise picked up by the aerial are recorded. This serves to indicate the stability of the whole equipment as well as the zero or reference level with respect to which the intensity is measured. At about 0440 the intensity suddenly starts falling till it

attains its minimum about an hour later. The commencement of the drop in intensity is known to coincide with the time at which the solar rays first strike that part of the ionosphere which reflects low frequency waves. It should be noted that before reaching its minimum, the field undergoes a few very sharp minima of intensity, e.g. one at 0400 and the other at 0500. A detailed account of these characteristic fluctuations is presented at the end of the chapter. The intensity then starts rising and after attaining a maximum near about noon again tapers off roughly symmetrically towards the evening. From about 1300 hours the record shows increasingly intense fluctuations which are due to tropical thunderstorms which are active during summer. In this particular record the evening minimum of intensity occurred at about 1900 hours. After this the intensity again goes on increasing gradually to its night time value. It is interesting to see that at the time of the morning and evening minima the signal amplitude almost touched the zero level.

Because of the regular behaviour of the signal amplitude during summer it is possible to compute a significant average diurnal curve for each month from June to October. Figures 2(A) and 2(B) show the monthly mean curves for 1960 and 1961 respectively. SR and SS are the ground sunrise and sunset timings at 32°W, the mid-point of the transmission path. The ordinates are the field intensities expressed in arbitrary units of microvolts.


FIGURE-2A. SS
SR
JUN 1960
JUL
AUG
SEP
OCT
FIELD INTENSITY IN MICROVOLTS
0
5
10
15
04
06
08
10
12
14
16
18
20
75° EMT


FIGURE-2B.
JUN 1961
SR
SS
JUL
AUG
SEP
OCT
FIELD INTENSITY IN MICROVOLTS
15
10
5
0
04
06
08
10
12
14
16
18
20
75° EMT

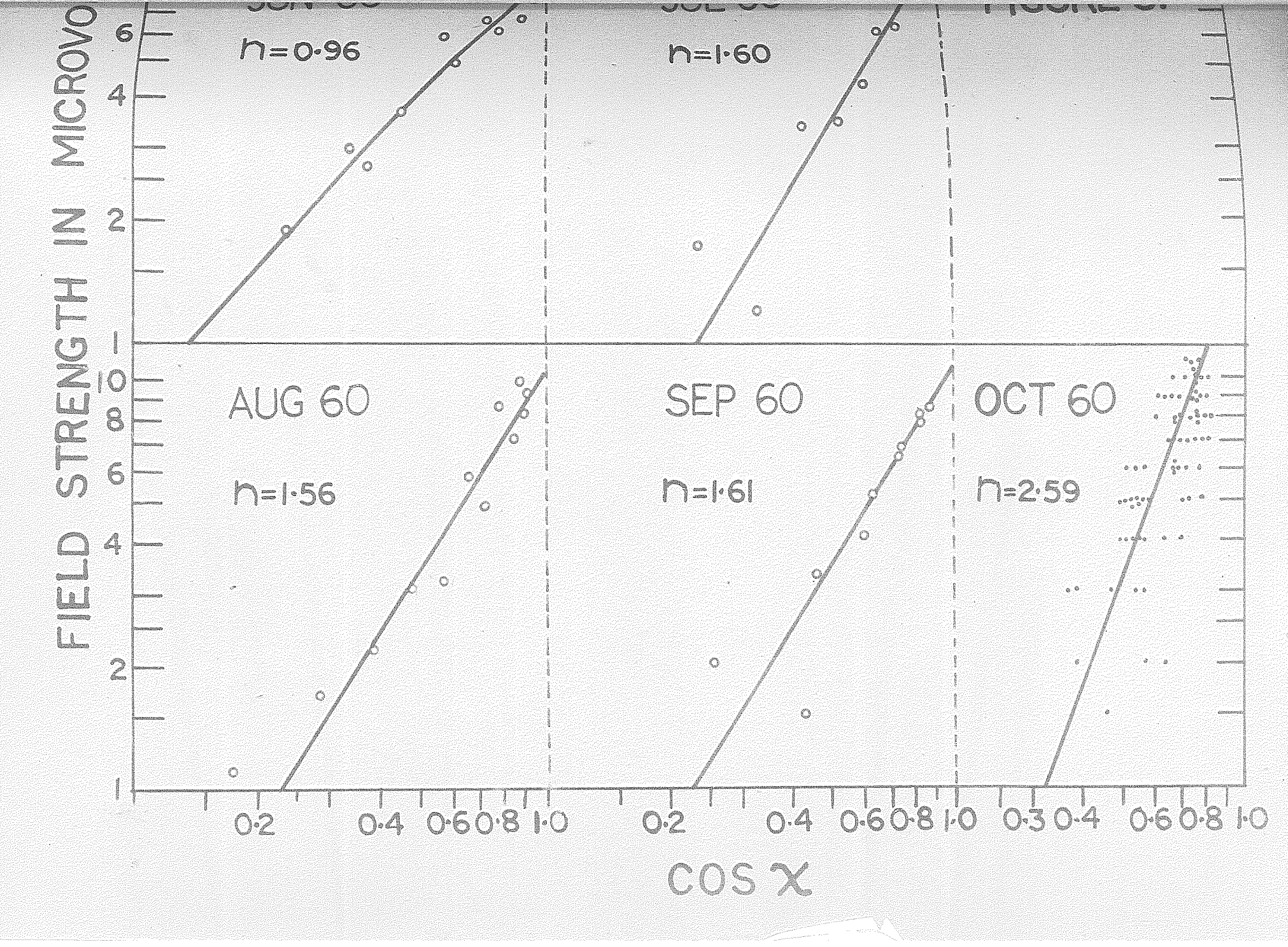
The October curve is averaged over ten days only as against about twenty to twentyfive days during the remaining months, since there is a sudden change-over to winter conditions sometime in the third week of this month. The effect of the sun's declination is clearly brought out by the fact that the time interval between the minima of the field intensity becomes smaller and smaller from June toward October. In all these months the maxima around noon were almost equal, varying between 8 - 10 microvolts. It is interesting to see that these maxima appear later and later as we go from June to October. The monthly mean curves show more rapid increase towards the maxima before noon than the decrease in the afternoon. Also the fall and rise in signal amplitude near sunrise and sunset respectively become steeper and steeper from June to October.

The appearance of the diurnal behaviour of the signal amplitude during summer, as seen from Figures 1 and 2, gives an indication of its dependence on the solar zenith angle. In other words, the daytime pattern appears to follow a law of the form

$$F \propto \cos^n \chi ,$$

where F is the field intensity and χ the solar zenith angle.

In order to test this relation the monthly mean hourly values of the signal amplitude are plotted against the cosine of the solar zenith angle on a logarithmic graph as shown in Figure 3. The points appear to fall, with a


FIELD STRENGTH IN MICROVO
n=0·96
n=1·60
AUG 60
n=1·56
SEP 60
n=1·61
OCT 60
n=2·59
1
2
4
6
8
10
0·2
0·4
0·6
0·8
1·0
0·3
COS χ

little scatter, on a straight line which has a slightly different slope 'n' in each month. The value of n in October is 2.50, which is much higher than those in the previous months. This discrepancy might be ascribed to the fact that the change-over from summer to winter conditions takes place during this month, rendering it rather difficult to make selection of days clearly representing the summer only.

Thus the average daytime field intensity during summer follows the law

$$F \propto \cos^n \chi ,$$

wherein the power n assumes values as shown against each month in Table 1 below:-

Table 1

Month	June	July	August	Sept.	Oct.
n	0.07	1.00	1.50	1.01	2.50

5.3. (b) Variations of the signal amplitude during the period from November to May

The regular behaviour of the daytime signal amplitude discussed in the foregoing paragraphs continues up to

about the beginning of the third week of October every year. A rather sudden change-over takes place from the regular summer conditions to more variable winter conditions. This is clearly seen from Figure 4, which displays a series of original records during October, 1950. The

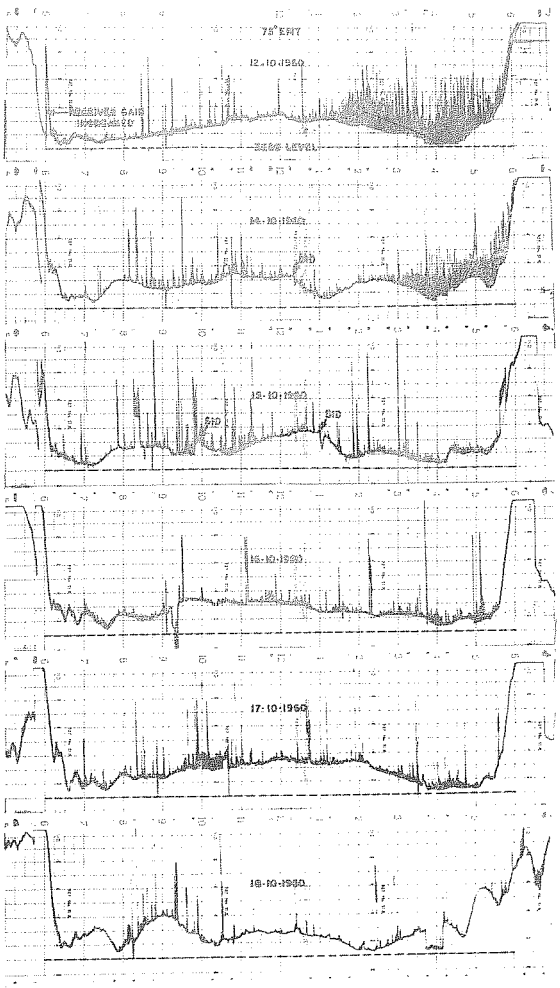


Fig. 4

record on the 18th October shows the summer type of variation of the signal amplitude. On the 19th the transmitter is off most of the time. On the 14th, however, a wavy pattern appears to be formed, the oscillations being clearly seen before 0000 hours and also after about 1600 hours. These crests and troughs become more and more obvious during the following days as one can see them on the 16th October. An interesting point about this pattern is that the interval between about 1015 hours and 1415 hours still resembles a summer type of variation, having a maximum at about 1200 hours. Over and above this there are superimposed maxima on either side, the most prominent of them being one at 0800 hours and the other at 1615 hours. On many days it is seen that the fall in intensity at the time of layer sunrise is much steeper and also smoother than the rise in intensity near sunset.

The gradual variation of the magnitude and phase of these maxima and minima in signal amplitude throughout the period from November to May could be well seen by arranging a series of records of successive days one below the other. Figures 5 and 6 show the results for the winter months and equinoctial months respectively. Both the figures consist of a series of successive records on quiet days only. On and SS are the ground sunrise and sunset times at 90°W, the mid-point of the transmission path.

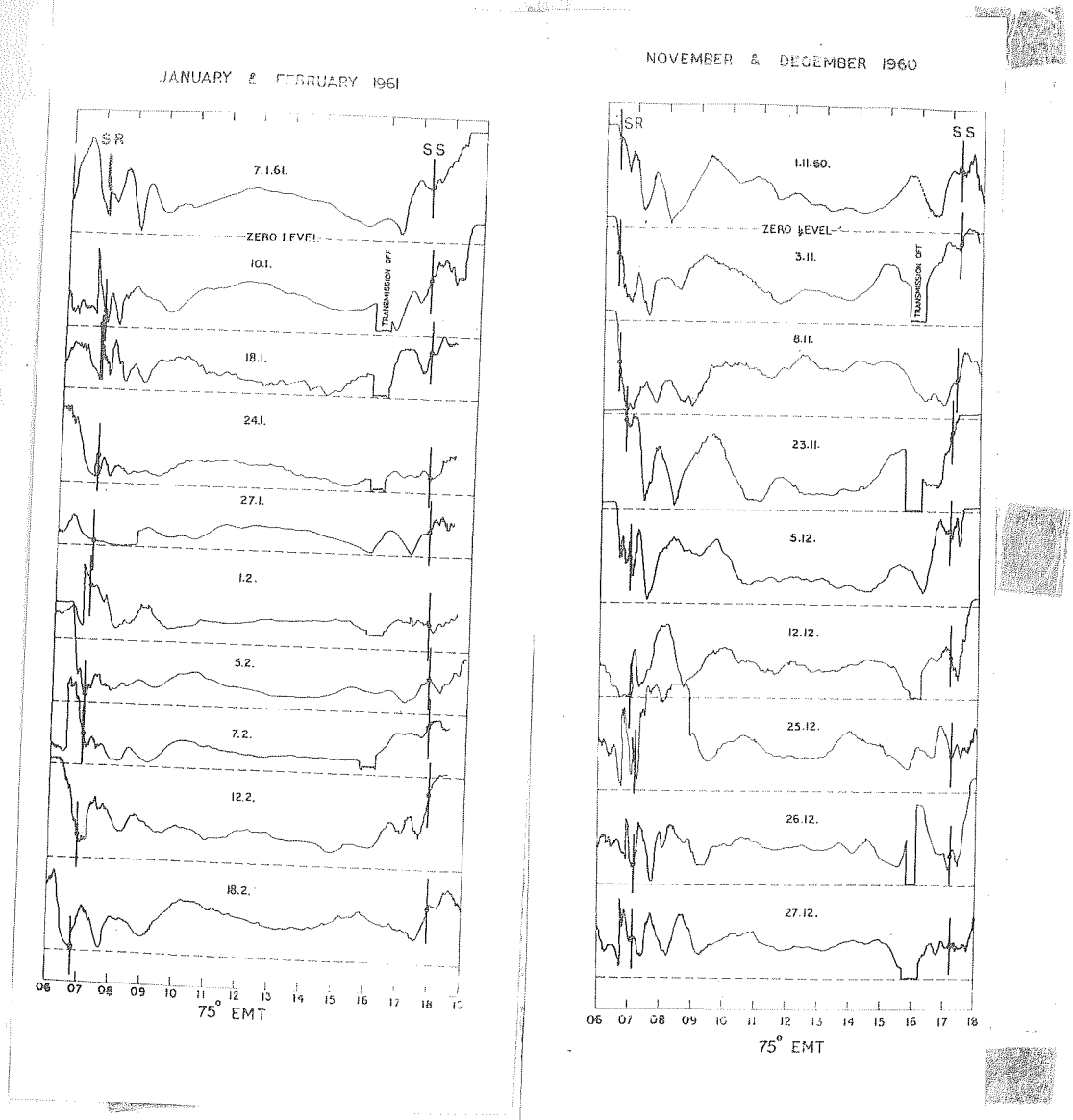
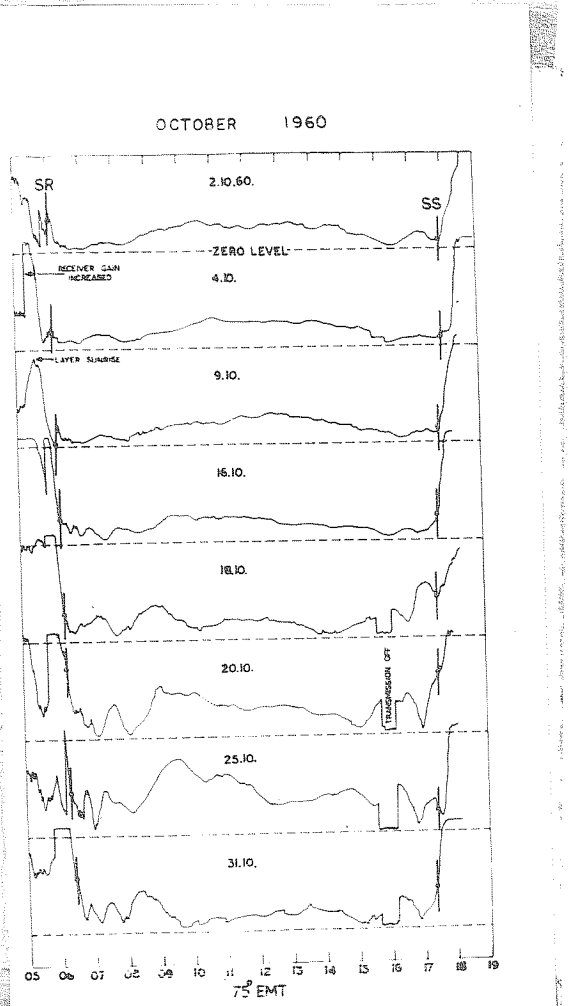


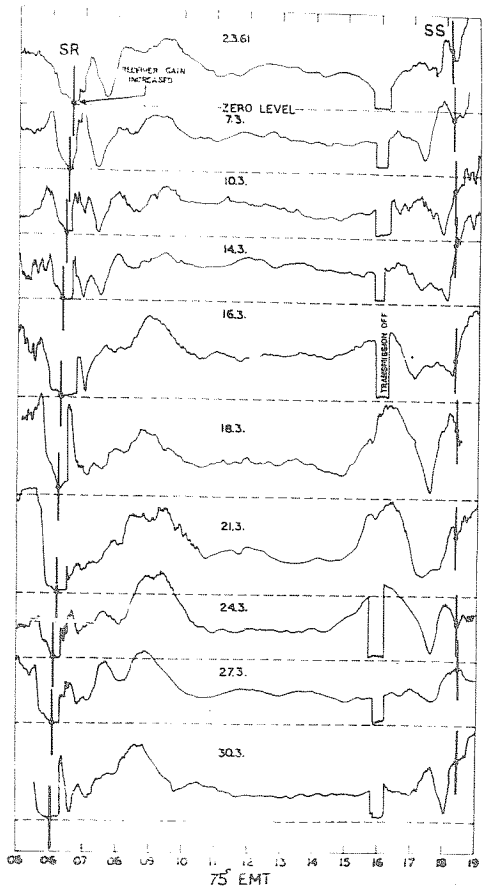
Fig. 5

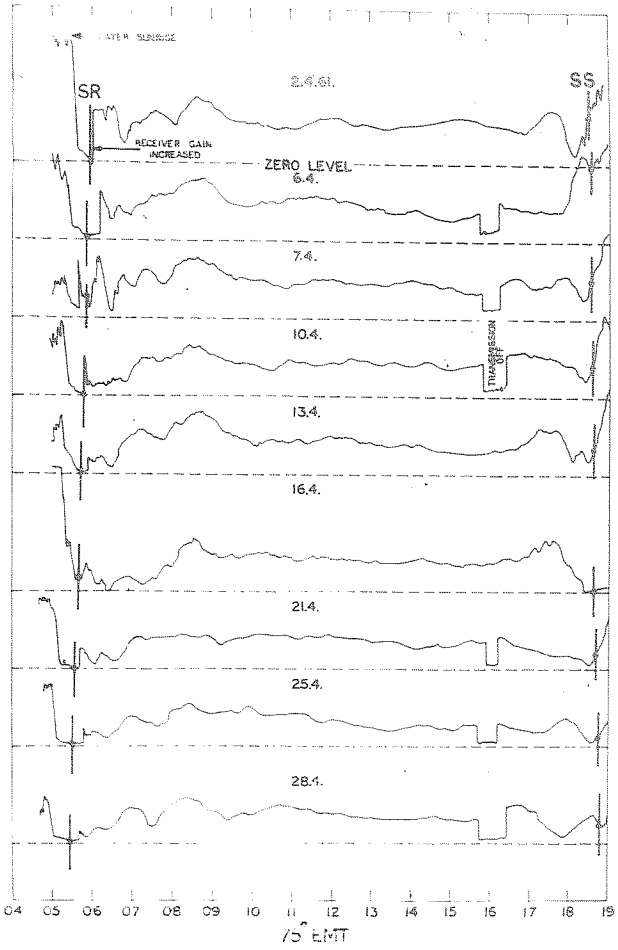
The common feature of the intensity patterns in Figure 5 is their high variability a few hours after sunrise and before sunset. Consider the record on the 1st November, 1960. Two prominent maxima, one at about 0013 hours and the other at about 1048 hours, are evident. The solar control of these maxima could be noticed as we

nova towards the end of December, e.g. on the 27th December the nova maxima appear at about 1100 hours and 1430 hours respectively. Again on the 24th February, 1961 they are seen at about 0930 hours and 1600 hours respectively.

Please turn over for Figure 6


OCTOBER 1960
SR
2.10.60.
SS
ZERO LEVEL
RECEIVER GAIN INCREASED
4.10.
LAYER SUNRISE
9.10.
16.10.
18.10.
20.10.
TRANSMISSION OFF
25.10.
31.10.
05 06 07 08 09 10 11 12 13 14 15 16 17 18 19
75° EMT


MARCH 1961
SR
2.3.61
SS
WEATHER GAIN INCREASED
ZERO LEVEL
7.3.
10.3.
14.3.
16.3.
TRANSMISSION OFF
18.3.
21.3.
24.3.
27.3.
30.3.
05 06 07 08 09 10 11 12 13 14 15 16 17 18 19
75° EMT


APRIL 1961
LAYER SUNRISE
SR
2.4.61.
SS
RECEIVER GAIN INCREASED
ZERO LEVEL
6.4.
7.4.
10.4.
TRANSMISSION OFF
13.4.
16.4.
21.4.
25.4.
28.4.
04 05 06 07 08 09 10 11 12 13 14 15 16 17 18 19
75° EMT

Similarly in Figure 6 consider the records on the 7th March, 1961 and 16th April, 1961. The two prominent maxima of intensity occur at about 0900 and 1630 hours and 0830 and 1730 hours respectively. Thus it is seen that these maxima of intensity glide on the diurnal curve according to the declination of the sun.

Considering both the figures 5 and 6 together, it is seen that intercepted between these two prominent maxima of intensity there is a portion of the diurnal curve which bears almost a constant value of the signal amplitude. The duration and magnitude of this intercept vary from day to day. For instance, on the 25th December, 1960 this interval is only about an hour and a half and the average value of the signal amplitude is about 23 microvolts of arbitrary units; while on the 16th April, 1961 the duration of the intercept is as much as six to seven hours and its average magnitude is about 24 microvolts of the same arbitrary units. As compared with November and December the month of April shows very few fluctuations in intensity around sunrise and sunset. This is an indication of the change-over to summer conditions. This change-over is rather slower than the one from summer to winter condition, so that, unlike the latter, one finds it very difficult to fix a line of demarcation in the case of the former change-over.

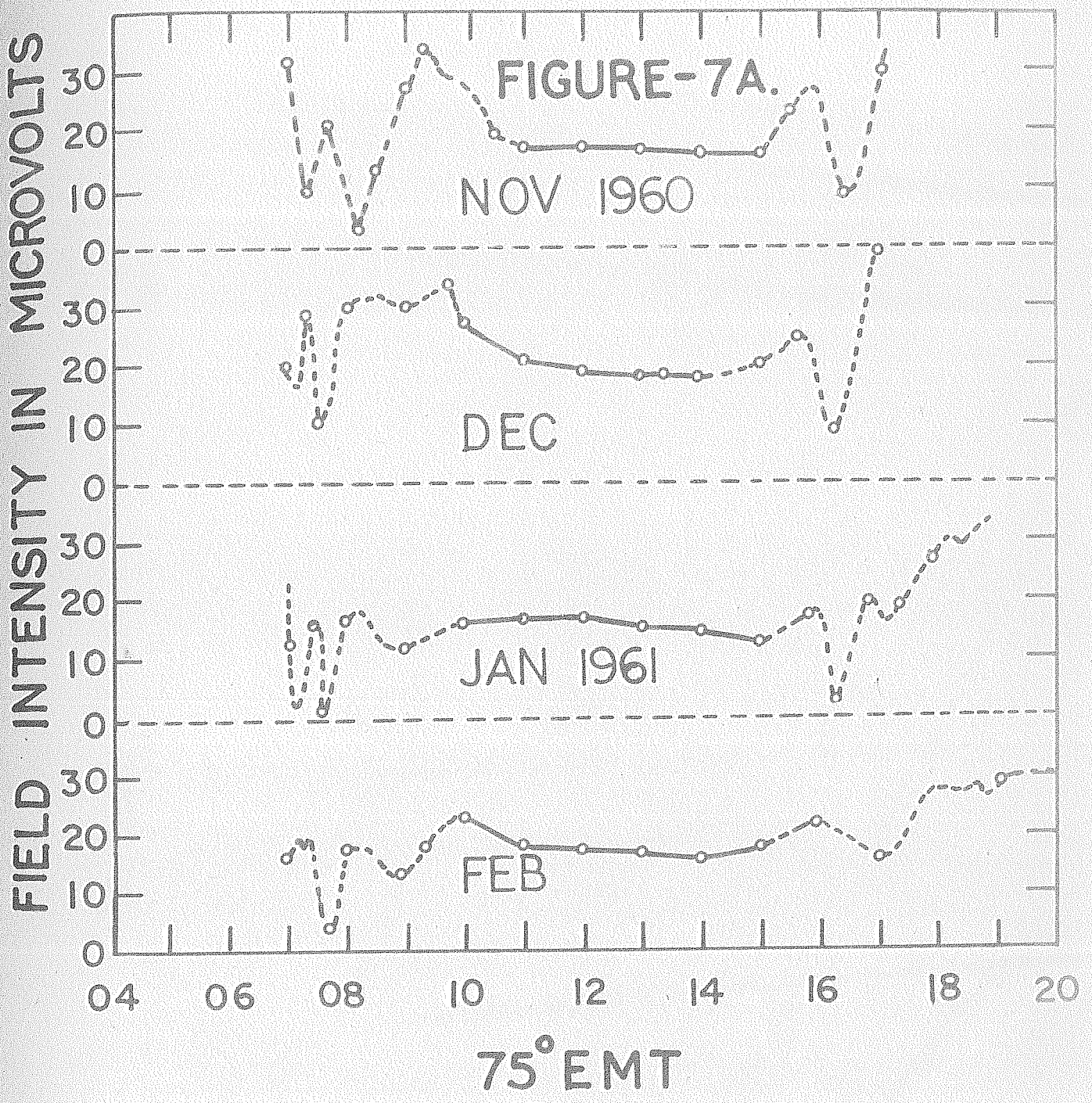
As seen in the foregoing paragraphs, the phases of maxima and minima in intensity undergo appreciable changes

from time to time during winter and equinoxes. It becomes, therefore, meaningless to compute monthly mean hourly values of the signal amplitude, particularly around sunrise and sunset. We have seen, however, that the intercept between the two prominent maxima in intensity does possess more or less a constant value of the field strength on a given daytime curve. Making use of this fact we can compute monthly average intensity curves during that interval.

Figures 7(A) and 7(B) present the results of such an analysis. The solid portions are the hourly values of the signal amplitude averaged over a number of days, about fifteen, in a month. The dotted portions on either side of these, which cannot be averaged over a month, are reproduced from any individual day typical of that month. It can be seen that the average value of the solid portions varies from about 13 microvolts in November, 1960 to about 10 microvolts in May, 1961. These values are about one and a half to two times larger than those around noon during summer months. Thus during the months other than the summer there is an extra contribution to the daytime field intensity. There are minima of intensity near sunrise and sunset which are quite distinct during winter and equinoxes.

6. Dependence of the diurnal field intensity on the solar zenith distance during the period November, 1960 to May, 1961

Consider a diurnal field strength curve e.g. the one on the 5th December, 1960 in Figure 5, typical of


FIGURE-7A.
FIELD INTENSITY IN MICROVOLTS
NOV 1960
DEC
JAN 1961
FEB
30
20
10
0
04
06
08
10
12
14
16
18
20
75° EMT

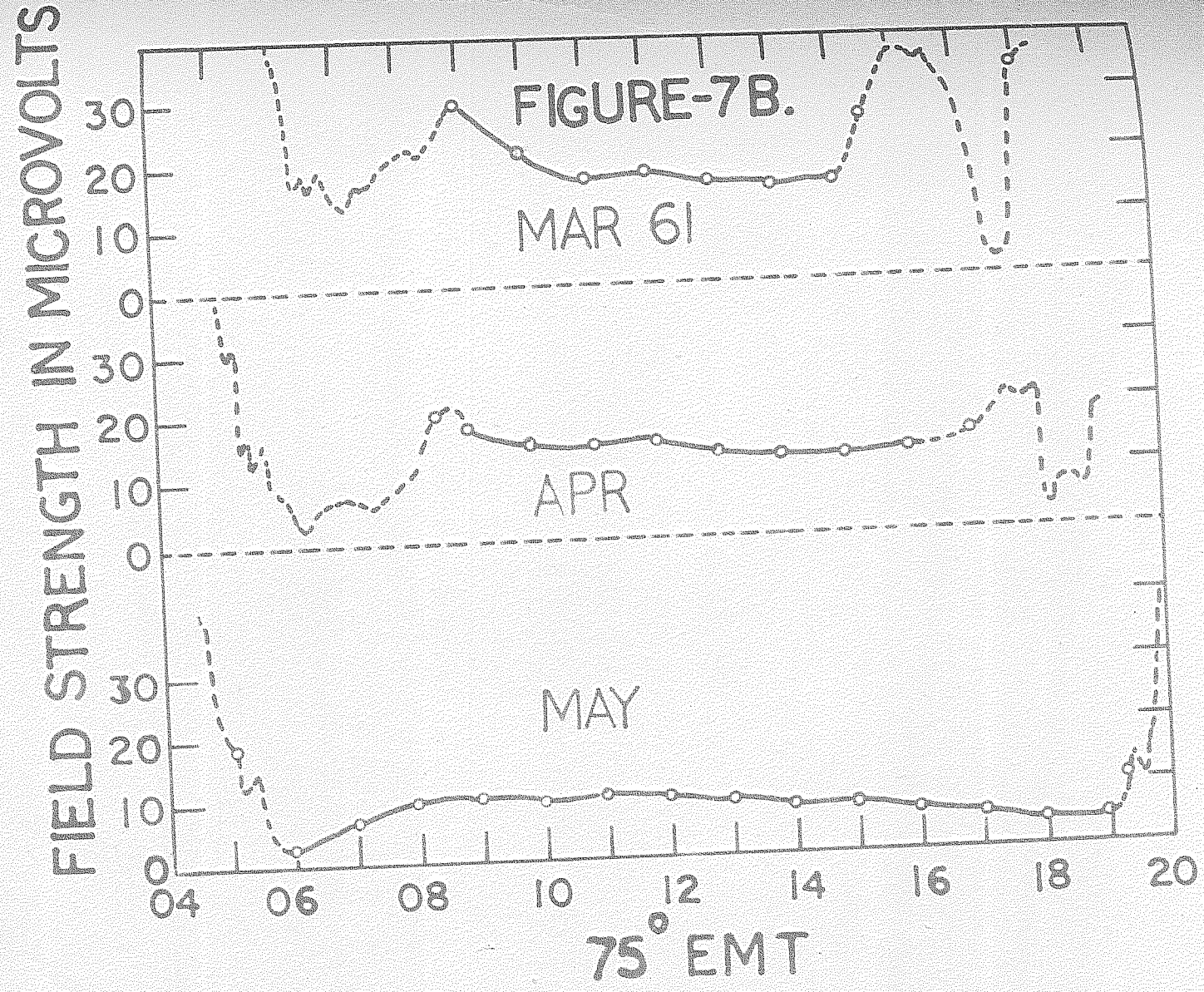
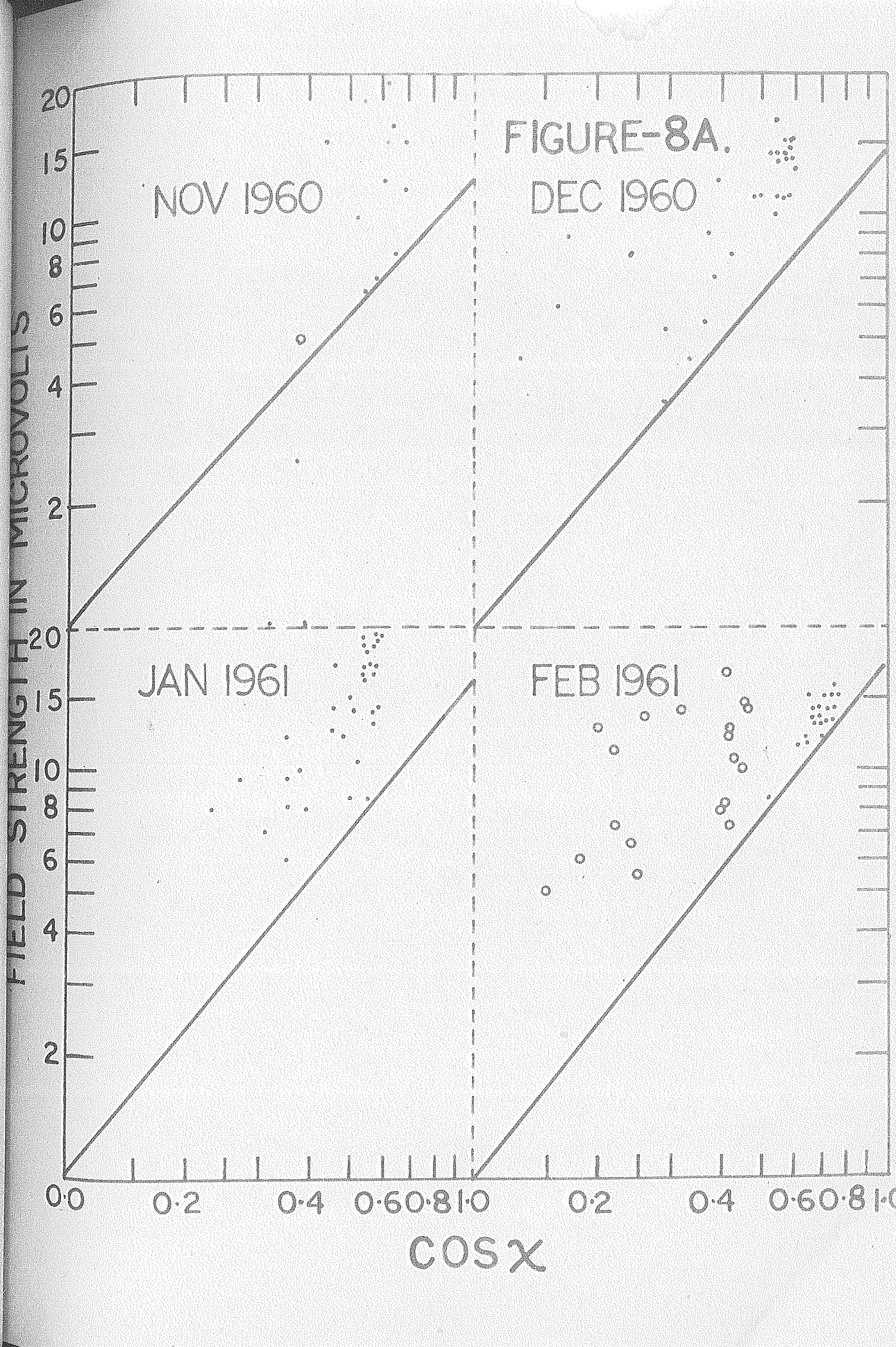

FIELD STRENGTH IN MICROVOLTS
30
20
10
0
MAR 61
APR
MAY
04
06
08
10
12
14
16
18
20
75° EMT

FIGURE-7B.

this period. The shape of the curve suggests that if a smooth curve joining the minima in intensity to the intercept between the two main maxima could be drawn, it would resemble the one during summer. In other words, this basic curve on which the maxima in intensity are superimposed would bear some simple relation with the solar zenith distance, similar to the one during summer, viz. $P \propto \cos^{n} x$.

To investigate this point a number of quiet days were selected from each month from November, 1950 to December, 1951. The field strength of the minima and the hourly values along the intercept between the two prominent maxima were plotted against the cosine of the solar zenith angle corresponding to the respective timings. In Figures 8(A) and 8(B) the result of this analysis is shown plotted on double logarithmic graph paper. The field intensities in microvolts are shown along the ordinates. The solid points correspond to the intensities along the intercept between the two main maxima on a diurnal curve, while the circles correspond to the minima in intensity on either side of the intercept. An appreciable amount of scatter is seen in each month. From the positions of the circles on this mass plot it is seen that the values of the field intensity of the minima are quite high as compared with those for the same solar zenith distance during summer months. Again there is an indication of lower


FIGURE-8A.
NOV 1960
DEC 1960
JAN 1961
FEB 1961
FIELD STRENGTH IN MICROVOLTS
20
15
10
8
6
4
2
0·0
0·2
0·4
0·6
0·8
1·0
COS χ

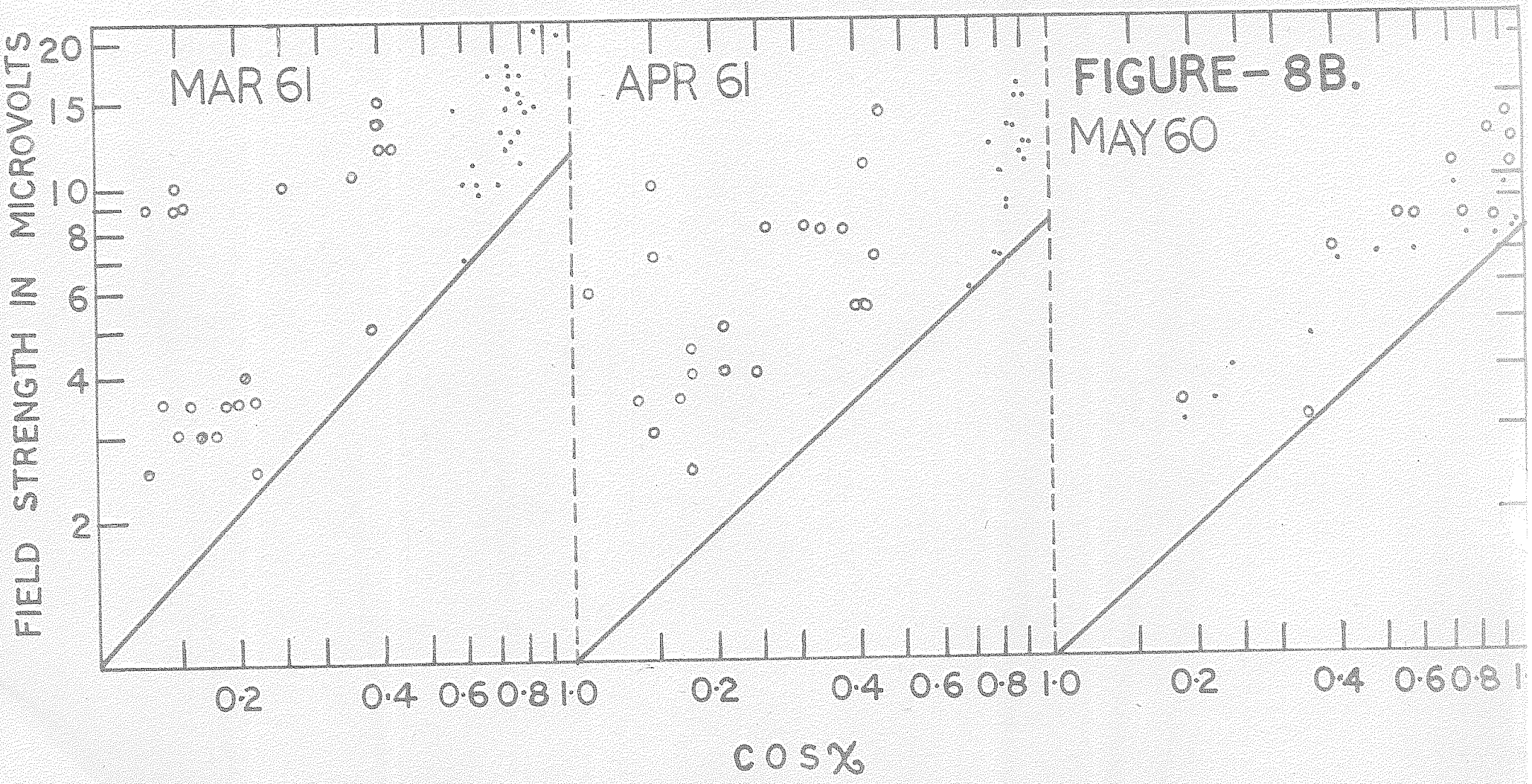

FIELD STRENGTH IN MICROVOLTS
20
15
10
8
6
4
2
MAR 61
APR 61
MAY 60
0·2
0·4
0·6
0·8
1·0
COS χ

FIGURE-8B.

intensities of the minima for the lowest solar zenith distances during March and April, showing thereby that the minima near sunrise and sunset are quite sharp in these months. Thus from Figures 8(A) and 8(B) it can be concluded that during months other than the summer, a hypothetical basic curve, obtained by joining the minima in intensities to the intercept between the two main curves, does not follow any simple relation connecting the field intensities to the corresponding solar zenith distances.

7. Sudden drop in intensity at the time of lower sunrise

It is well known that the night-time field intensities of low and very low frequency radio waves are quite high as compared with that during day-time. This high signal strength decreases very rapidly in the early morning hours. When the solar rays first strike the D region, electrons are produced and absorption sets in thereby decreasing the signal amplitude of the low frequency radio wave passing through the region. This drop in intensity of the radio wave continues till it starts reflecting from the newly formed lower D layer which is known to reflect low and very low frequency radio waves during day-time.

The commencement of this drop can be accurately determined within a minute or so. From the time of the

layer sunrise, it is easy to find the position of the sun below the horizon at the mid-point of the transmission path. A mean plot of these zenith distances computed for the year 1960-61 is shown in Figure 9. The values are grouped closely round a mean of $97^{0}30'$. This value of the mean solar zenith distance may be compared with $97^{0}30'$, obtained by Bain, Bracewell, Straker and Westcott (1962) for 16 Kc/s radio waves propagated over distances of about 540 km in U.K.

It may be mentioned here that the difference in time between the start of the drop in intensity and the ground sunrise at the mid-point of the transmission path remains almost constant throughout the year, the value of the difference being variable from about 37 to 42 minutes.

It is also interesting to note that the rise in intensity near sunset is more gradual than the fall in intensity at the time of layer sunrise. It is, therefore, difficult to pinpoint the time of the beginning of the rise in intensity near sunset.

6. Height of the ionospheric region corresponding to the commencement of the fall in intensity at the time of layer sunrise

The sunrise effect of the fall in intensity provides information on the height of the reflecting layer at that time. From simple geometrical considerations it is easy to

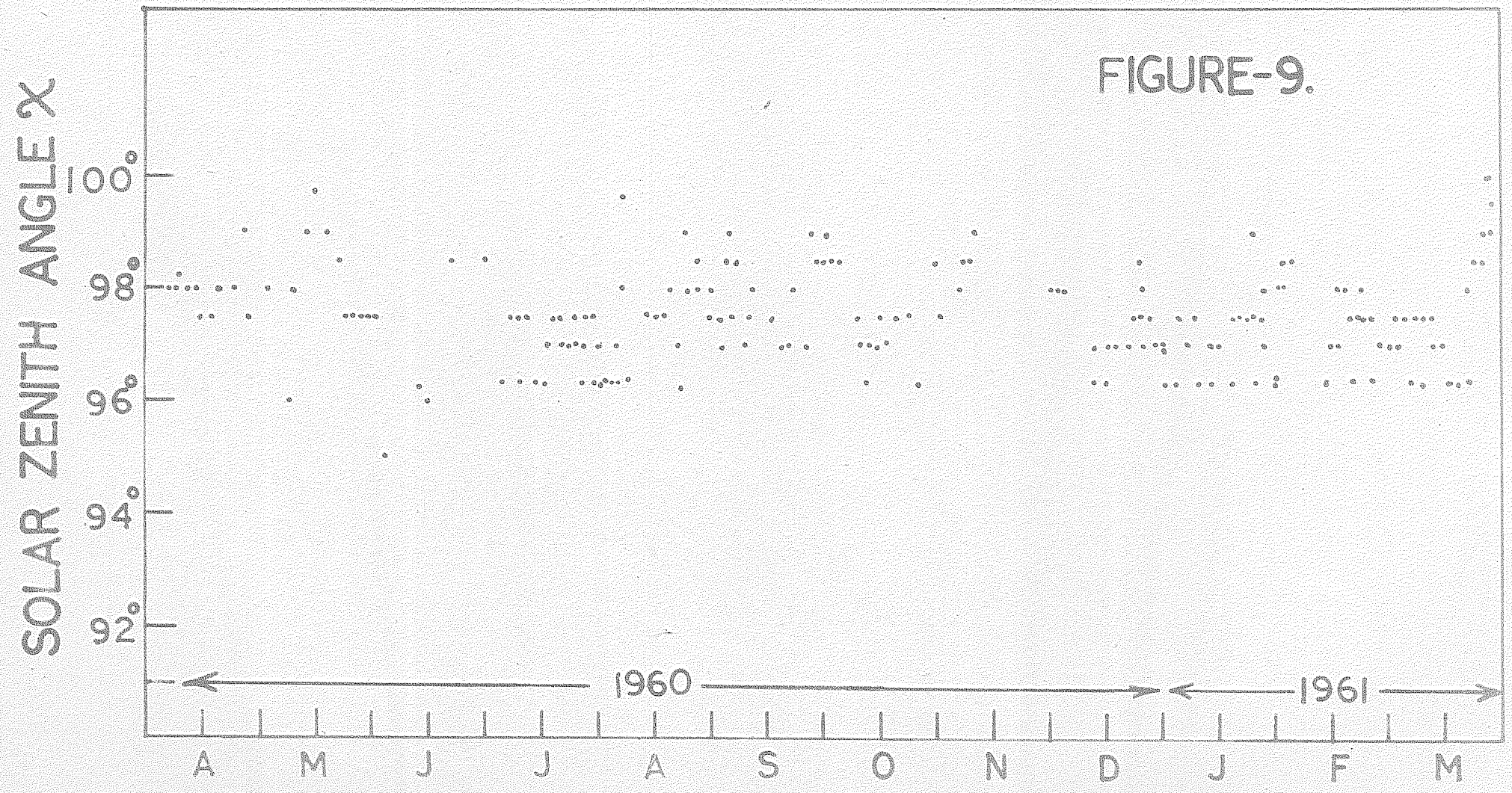


FIGURE-9.

computed the height corresponding to the fall in signal strength at layer sunrise. These have been calculated for a number of days during the period from March, 1960 to February, 1961. Table 2 shows the results. It is obvious

Table 2

Showing height in Km of the ionospheric region at the time of layer sunrise

Date	Mar. 1960	Apr.	May.	Jun.	Jul.	Aug.	Sep.	Oct.	Nov.	Dec.	Jan. 1961	Feb.
1		68	77				70	96	88	70	45	51
2		71				45	70	88		77	V.Low	64
3		71				45	64				45	70
4		75			58	45	90	96		88	Low	64
5		75				58	96				51	
6		84			77	58	88		96		V.Low	
7		80	45			39	96	102			42	
8		80	70		64	96	64		102		V.Low	
9		71			51	51	77	70	105		51	
10		71		58			88	88			Low	
11	88						77	51	100			
12				51				64		51		
13	70	70	77	45	45					58	42	
14	73	71				70		77			30	Low
15	71		100		45	70	77	64		58	42	45
16	85				64					64		45
17	85	72	80		64	70	64	70		64	Low	51
18	73		88		70		58				42	64
19		76				77		70			51	45
20					58		88				51	51
21				39	51	64				70	45	39
22	68			77	51	51	64			77	64	
23	64	73	64		64			70		70	51	51
24			64			77				96	77	51
25	57	71	64		54			64		90		58
26	64	72		100	51		102			64	42	39
27			70		51	88	96			77	51	
28	69				51	90	51				64	45
29			88		61		88			70		
30	67		64	90	51	77		90		70	45	
31					58	77				64	42	
Median	70	72	70	68	60	70	80	74	102	70	48	52

that the heights vary irregularly from day to day and no marked seasonal variation is observed. Nevertheless, there is indication that on many days this height is about 70 km from the surface of the earth at the mid-point of the transmission path between Kashkent and Ahmedabad. The above calculation of the height of the reflecting layer at the time of layer sunrise is based on the assumption of a single hop transmission, though multiple hops are probable over this distance of 2150 km along the great circle. In the latter case the heights will naturally be a little higher.

9. Minima in intensity near sunrise and sunset

Consider the day-time field strength curve on the 4th August, 1950 shown in Figure 10. During the fall in intensity after layer sunrise the signal undergoes a number of sharp crests and troughs. On this record the first two minima occur at about 0621 and 0635 hours 75°EM respectively. These oscillations may be caused either by the interference between the ground wave and a variable downcoming sky-wave or due to interference between multiple reflections from the ionosphere. Figure 11 shows how the time of the first minimum varies throughout the year. For this analysis, days from April, 1950 to May, 1950 are utilised. The solid points are the times of first minima and the triangles are the times of ground sunrise at 67°N, the mid-point of the

transmission path. A marked polar control of the first minimum is evident. Again, during the summer months (Northern solstice) the first minima appear, on an average, 10 to 15 minutes earlier than the second sunrise; while

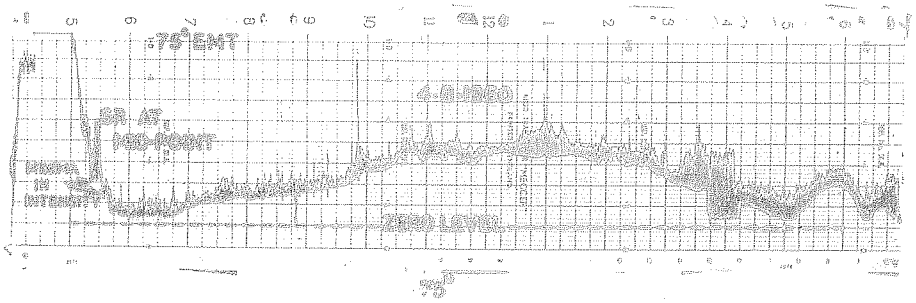
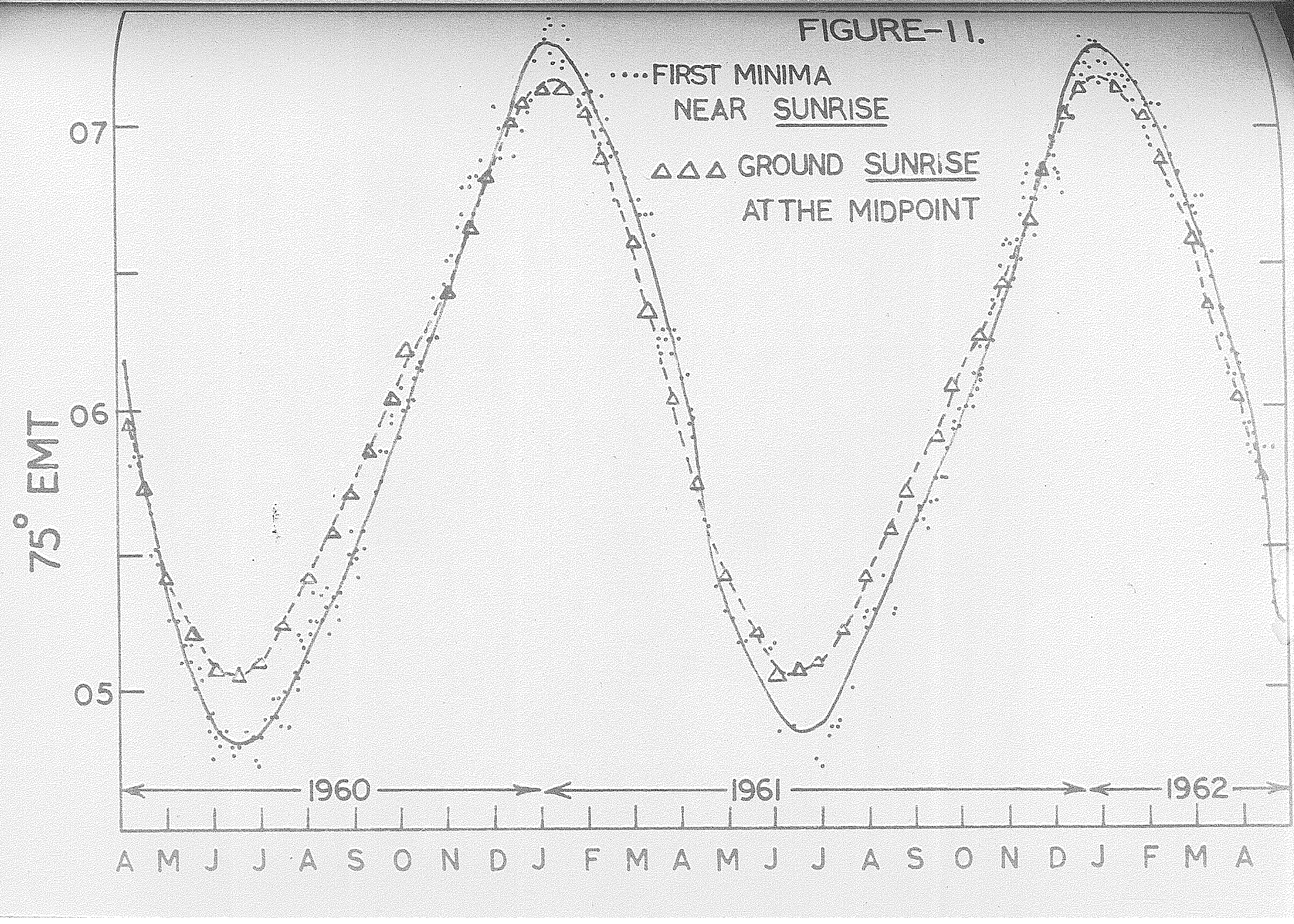


Fig. 10


FIGURE-11.
....FIRST MINIMA NEAR SUNRISE
ΔΔΔ GROUND SUNRISE AT THE MIDPOINT
75° EMT
07
06
05
1960
1961
1962
A M J J A S O N D J F M A M J J A S O N D J F M A

during the winter months (Southern solstices) they appear about 5 to 10 minutes later than the ground sunrise. During the equinoxes, however, the first minima occur almost simultaneously with the ground sunrise. This point is brought out more clearly by plotting these time differences against the dates as shown in Figure 12. The upper and lower halves of the ordinate indicate the time in minutes taken by the minima to appear before and after the ground sunrise respectively. It is seen that the minima occur more than 15 minutes before the ground sunrise in mid-summer and about 5 minutes after the ground sunrise in mid-winter.

Figure 12 suggests another way of looking at the same point. From these time-differences, one can compute the solar zenith distances corresponding to the occurrence of the minima. Figure 13 shows the manner in which these solar zenith distances vary with the time of the year. Thus in the middle of summer, the first minima of intensity occur when the solar zenith angle is about 94° (i.e. 4° below the horizon); while in the middle of winter they appear when the solar zenith angle is about 90°, i.e. when the sun rises about 1° above the horizon at the mid-point of the transmission path.

The above analysis could be extended to the second minima of intensity as well. But it is observed that some

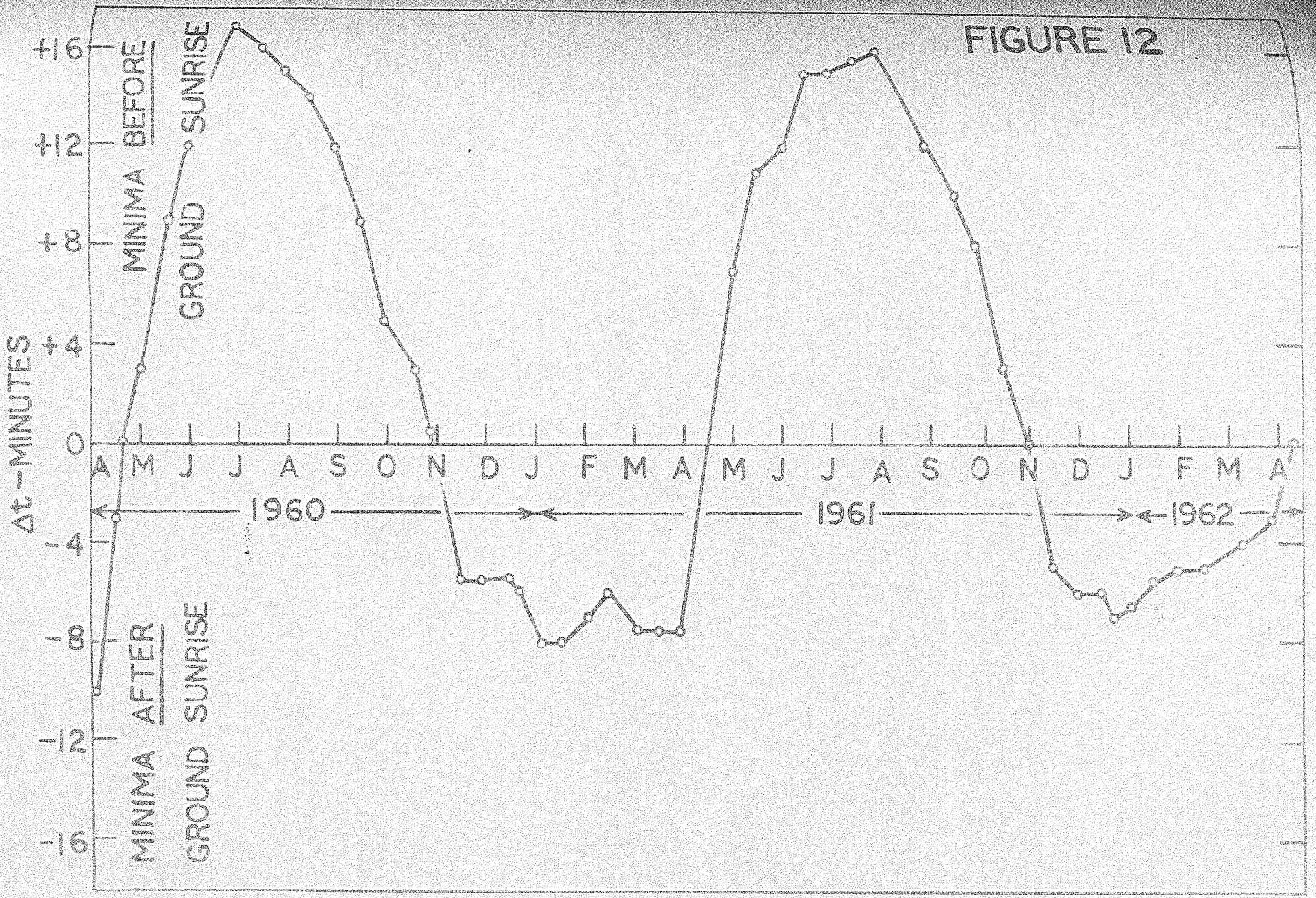
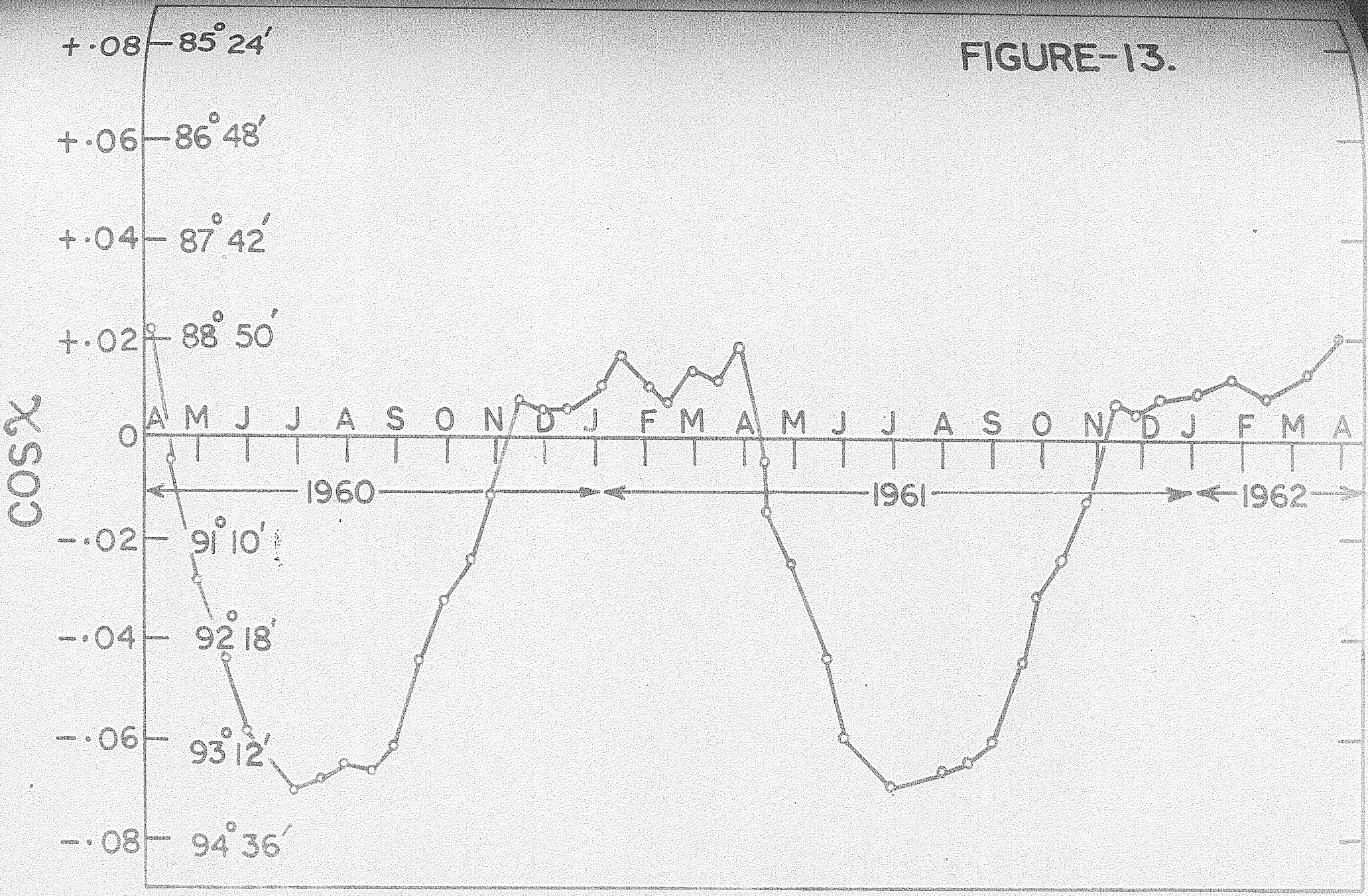

FIGURE 12
Δt - MINUTES
+16
+12
+8
+4
0
-4
-8
-12
-16
MINIMA BEFORE GROUND SUNRISE
MINIMA AFTER GROUND SUNRISE
A M J J A S O N D J F M A M J J A S O N D J F M A
1960
1961
1962

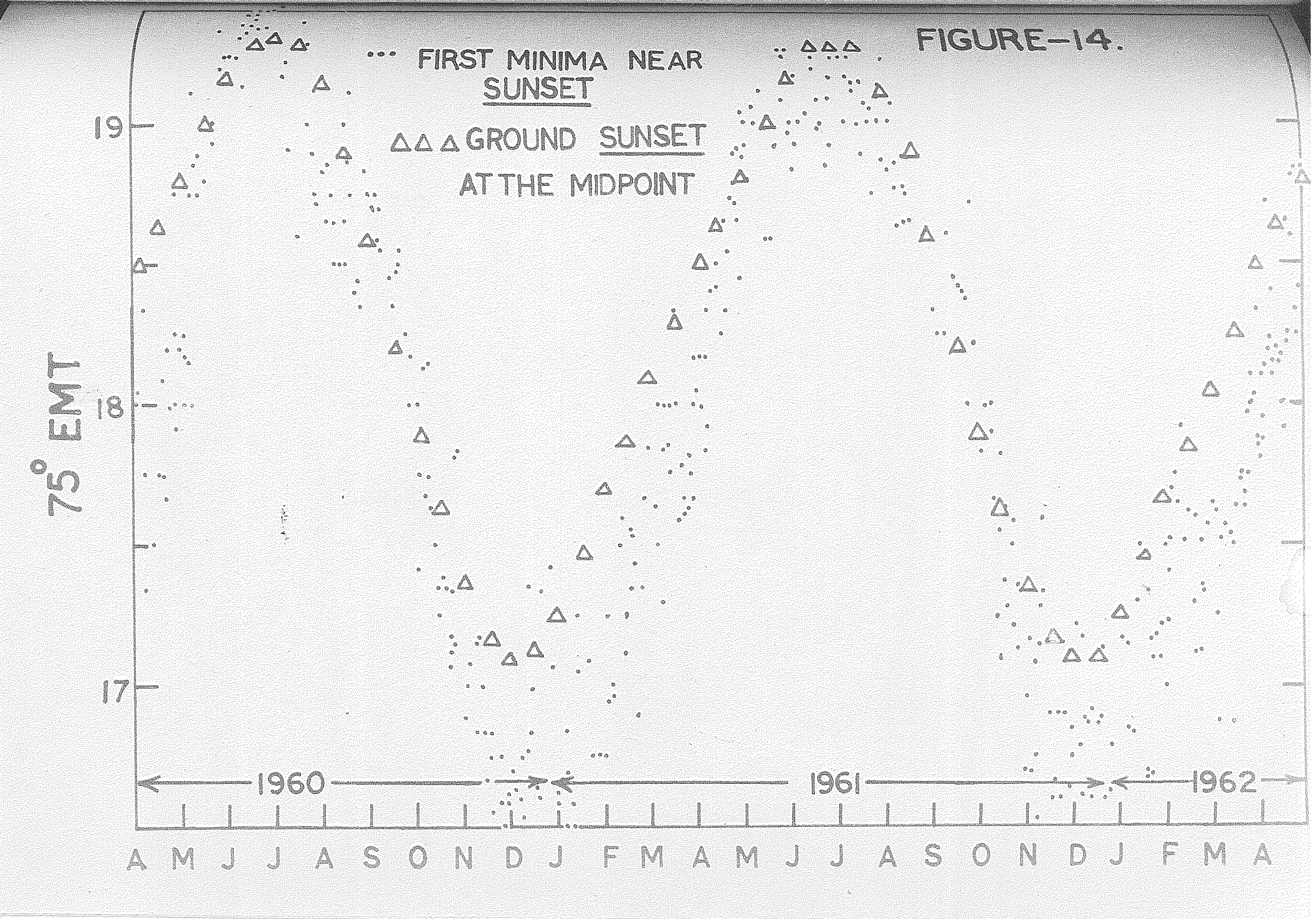
FIGURE-13.


+·08
85° 24′
+·06
86° 48′
+·04
87° 42′
+·02
88° 50′
0
−·02
91° 10′
−·04
92° 18′
−·06
93° 12′
−·08
94° 36′
COSχ
A M J J A S O N D J F M A M J J A S O N D J F M A
1960
1961
1962

of them occur very irregularly, thereby introducing much uncertainty in fixing up their exact timings.

As for the first minima of intensity near sunset, Figure 14 shows the variation of the time of their occurrence for the period from April, 1960 to April, 1962. Though they show a definite dependence on the solar zenith distance, much more scatter is observed showing, therefore, their more irregular behaviour. During November and December they appear on an average about 20 to 25 minutes earlier than the ground sunset. During the summer months, however, the minima seem to occur almost simultaneously with the ground sunset. Thus in mid-winter the first minima of intensity near sunset appear when the solar zenith angle is about 110°, i.e. when the sun is about 20° above the horizon at the mid-point of the transmission path.

Generally it can be remarked that these minima of intensity are less marked in summer than in the rest of the year.


FIGURE-14.
... FIRST MINIMA NEAR SUNSET
ΔΔΔ GROUND SUNSET AT THE MIDPOINT
75° EMT
19
18
17
1960
1961
1962
A M J J A S O N D J F M A M J J A S O N D J F M A

REFERENCES

Hollingworth	1928	J.I.E.E., Vol. 64.
Bracewell, Ratcliffe, Strafer and Wooles	1951	Proc.I.E.E., Part 3, Vol. 98.
Bain, Bracewell, Strafer and Westcott	1952	Proc.I.E.E., Part 3, Vol. 99.
Wooles and Stuart	1952	Proc.I.E.E., Part 3, Vol. 99.
Hopkins and Reynolds	1954	Proc.I.E.E., Part 3, Vol. 101.
Hargreaves	1952	J.A.I.P., Vol. 64.
Mitra	1951	J.Geophys.Res., 56.
Bracewell, Harwood and Strafer	1954	Proc.I.E.E., Part 4, Vol. 101.
Watts and Brown	1954	J.Geophys.Res., 59, 71.

ooo 0 ooo

CONTENTS

CHAPTER 3

		Page
1.	Introduction	1
2.	SID's on 16A Ke/s waves observed at Ahmedabad	4
3.	Classification of SID's on 16A Ke/s	8
4.	Diurnal and seasonal variations of SID's on 16A Ke/s	10
5.	Initial dips and solar zenith angle	10
6.	Post-enhancement decrease in signal strength during SID's	13
7.	SID's on 16A Ke/s in relation to the K_α radiation from solar flares	15
8.	16A Ke/s SID's and Sudden Cosmic Noise absorption on 25 Ke/s	19
9.	SID's and Cosmic Ray Flares	23
	Appendix	1 - 7

CHAPTER 3

EFFECTS OF SOLAR FLARES AND SID's ON THE PROPAGATION OF 16 Kc/s RADIO WAVES FROM TASHKENT TO AHMEDABAD

1. Introduction

The visual observation of solar flares has been going on for a long period of years now. Among the terrestrial effects of these events, the sudden fadeout of short waves was first observed by Mogel in the years 1927 to 1930. Dellinger (1935) ascertained its main features. Sudden enhancements of atmospherics (SEA) have been recorded since 1930 and were extensively studied by Bureau (1937). On 27 Kc/s he observed an increase in atmospherics during solar flares which, he pointed out, did not correspond to an increase in the number of atmospherics, but was due to the improvement in the propagation conditions of very long waves over great distances.

Gardner (1950) and Rowe (1951) reported on attenuation of waves below 10 Kc/s in contrast to the enhancement observed above about 27 Kc/s during SID's.

The behaviour of very long waves (16 Kc/s) over short distances was studied by Budden, Ratcliffe and Wilkes (1950) by measuring the phase changes of the downcoming skywaves. On some occasions they observed sudden

anomalies in phase (SPA) which were shown by Sudden and Ratcliffe (1957) to be correlated to the sudden ionospheric disturbances (SID's) which produced short wave fadeouts (SWF) and sudden enhancements of very low frequency atmospherics (SEA).

Ingcovell and Straker (1960) made an extensive analysis of sudden phase anomalies on 16 Kc/s GBR transmission from Rugby. They showed that these SPA's were closely related to the occurrence of solar flares and provided a considerably better flare patrol than other ionospheric phenomena.

Smith-Rose (1950) reported an increase in the field strength of 101 Kc/s waves over 970 Km during a solar flare. By measuring the phase change of the ionospheric wave, he observed a lowering of the reflection height by about 10 Km.

Ingcovell, Sudden, Ratcliffe, Straker and Weekes (1961) studied the effects of SID's on the amplitude and phase of waves of 16, 70 and 113 Kc/s incident vertically. They observed almost no change in the 16 Kc/s wave amplitude, but the amplitudes of the higher frequency waves showed large decreases. The changes of the apparent heights of reflection, deduced from their phase changes, were essentially the same for all the above frequencies.

Bain (1963) studied the effects of SID's on the phase and amplitude of the skywave of 16 Kc/s transmission over

535 and 415 Km. At 535 Km the majority of the sudden field anomalies (SFA's) showed rapid increase of signal strength followed by a gradual recovery to normal. On a few occasions, however, the effect consisted of a decrease in signal strength, or of a decrease followed by an increase. These unusual SFA's all occurred in the winter months from November to March.

Maslen and Stuart (1960) working on 71.1, 86.4 and 113.8 Kc/s transmissions over a distance of 940 Km observed that during sudden ionospheric disturbances the signal strength was greatly enhanced.

In an analysis made to study the association between SFA's on 27 Kc/s and solar flares Ellison (1959) found that the percentage association was higher during the middle of the day and in the afternoons than in the early morning hours. It was also higher in winter than in summer. He compared the SFA's with the corresponding development curves of the line-width of H_{α} and concluded that there was a lag of about 7 minutes in the response of the D layer to the H_{α} radiation emitted during the flares.

From rocket measurements, Friedman and Gubb (1955) showed that X-rays of wavelength 1 - 8 A^{0} were considerably enhanced during solar flares. They also showed that during a major flare, when the reflection height of low frequency waves fell by as much as 15 Km, X-rays could produce the necessary ionization at about 60 Km.

S.M.Mitra (1950) reported sudden increases of long-wave intensity (SFI) of 164 Kc/s Tashkent transmissions at Delhi during solar flares. He observed that all flares, irrespective of their importance, produced sudden increases in amplitude. He also found good correlation between the development of the line-width of H_α and the corresponding SFI.

2. SFD's on 164 Kc/s waves observed at Ahmedabad

Continuous recording of the longwave field intensity on 164 Kc/s was started at Ahmedabad in March, 1960 mainly to serve as a flare patrol. Upto the end of December 1960, about 135 SFD's were recorded. The present study is based on an analysis of 115 SFD's observed during solar flares.

The diurnal and seasonal behaviour of the signal strength on quiet days during summer and winter was discussed in the preceding chapter. Briefly, we shall repeat that during summer the daytime signal amplitude follows a law of the form

$$F \propto \cos^n \chi ,$$

F being the field intensity and χ the solar zenith angle at the midpoint of the transmission path. n has an average value of about 1.3.

During the months other than summer there is an additional contribution of the signal strength superimposed

on the one during summer. The winter pattern is characterised by intensity fluctuations after sunrise and before sunset.

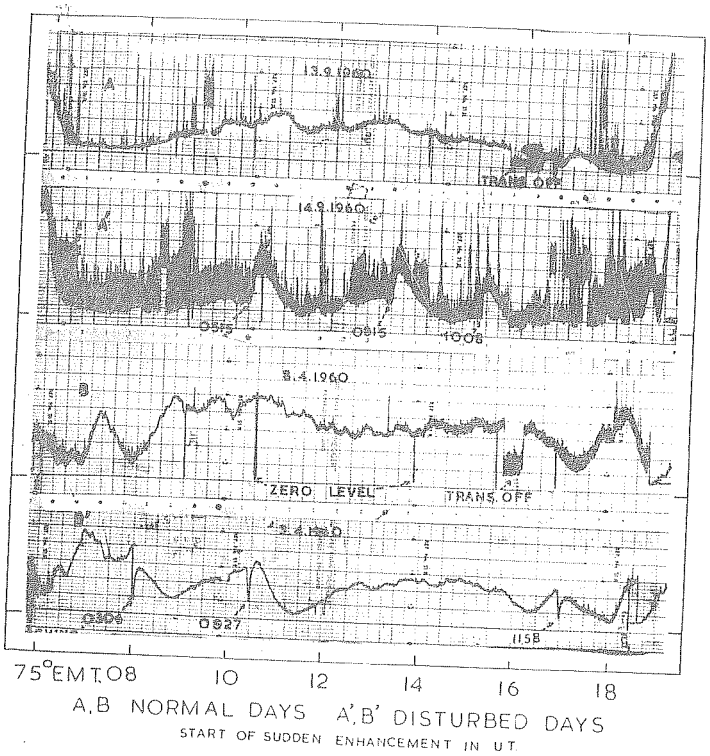


Fig. 1

Figure 1 shows these two types of field strength variations on the 13th September and the 3rd April, 1960

respectively. These are named A, B; the other two curves, A' and B', on the 14th September and the 3rd April, 1960 respectively were obtained on disturbed days having a number of SID's on each day.

On the 14th September, 1960 three SID's were observed starting respectively at 0515, 0815 and 1008 hours U.T. All of them commenced with a sudden enhancement of the longwave field intensity (SWFI). After reaching a maximum they fall gradually towards the normal signal level, after which they continued to fall to a broad minimum and finally started rising slowly towards the normal intensity. This whole process takes on an average about 24 hours or so.

In contrast, the SID's on the 3rd April, 1960 started with a very rapid drop in intensity, which we shall call the initial dip. This lasted only 3 - 5 minutes and was followed by a rise to a maximum; the other features being similar to those in the SID's on the 14th September. It is noteworthy that the post-enhancement decrease in the signal amplitude, observed in all the above cases, reached a very low value.

The details concerning the durations and magnitudes of the various portions for 115 SID's are presented in an appendix at the end of the chapter. Table 1 gives the times of the different portions of SID's relative to sudden enhancements of the low frequency (S.E.L.F.).

Table 1

Times relative to Sudden Enhancements of Low Frequency (S.E.L.F.).

(1) Time of beginning of initial dip (in minutes) before enhancement.

Time in minutes before S.E.L.F.	Number of events.
0	76
1 - 5	28
6 -10	13
11 -16	2

(2) Time of maximum after beginning of enhancement.

Time in minutes after S.E.L.F.	Number of events.
1 - 10	67
11 - 20	24
21 - 30	13

(3) Time of minimum following enhancement.

Time in minutes after S.E.L.F.	Number of events.
1 - 20	0
21 - 40	8
41 - 60	46
61 - 80	20
81 -100	16
100 -120	5
120	8
Uncertain	9

(4) Time for recovery to normal.

Time in minutes after S.E.L.F.	Number of events.
0 - 50	0
51 - 100	30
101 - 150	47
151	10
Doubtful events	37

3. Classification of SID's on 164 Mc/s

The SID's recorded at Ahmedabad can be classified into two main groups as follows:-

A) SID's which commence with a sudden enhancement of the field intensity simultaneously with the onset of a solar flare. On the 14th September, 1960 in Figure 1, three SID's of this type were observed.

B) SID's falling in this group start off with an initial dip in intensity followed by a sudden enhancement to a maximum. Instances of this type were recorded on the 3rd April 1960 in Figure 1, where their initial dips appeared at 0336, 0837 and 1153 hours UT. The magnitude of this initial dip can be as much as 22 db with respect to the preflare level.

The magnitudes of the maximum enhancement of intensity and of the post-enhancement absorption work out to about 7 and 10 db respectively as compared with the preflare level. The average duration between the initial dip and the maximum enhancement is about 10 minutes, while that between the maximum enhancement and the maximum decrease following the enhancement is about an hour.

In addition to the above two principal types of SID's there are instances of still one more type of SID's,

e.g. those shown in Figure 2. On the 27th October, 1960 there was a rapid drop in intensity starting at about 1136 hours 75° EMT. A similar drop occurred at about 1131 hours on 30th January, 1961. Both these sudden drops were not followed by any of the remaining features of a typical SID, viz. sudden enhancement and post-enhancement

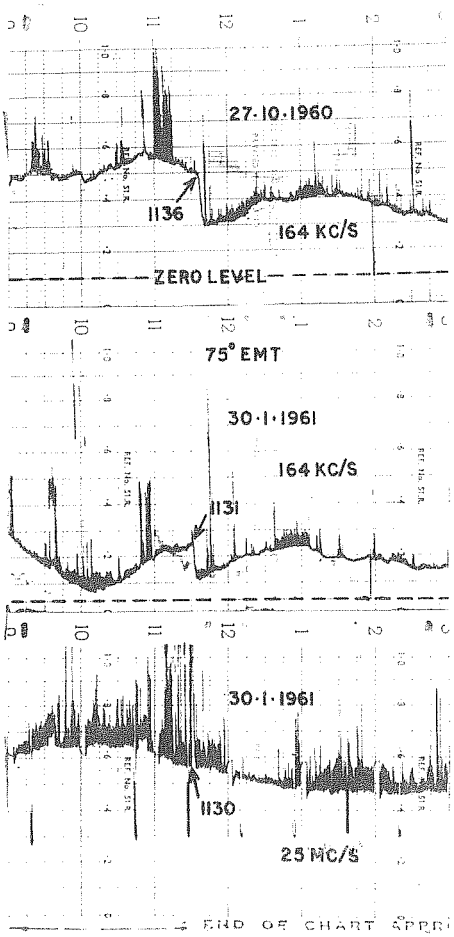


Fig. 2

decrease. After the drop, these SID's built up exponentially to the normal level of the respective daytime intensities. The third record on the 30th January, 1961 showed a solar radio noise burst on 25 Mc/s at about 1130 hours 75^{0}E.T, which is also regularly recorded at Ahmedabad. The Solar Astrophysical Observatory at Kodaikanal reported a solar flare beginning at 0691 hours G.C.T or 1121 hours 75^{0}M.T. For the SID on the 27th October, 1960, however, there was no counterpart on the 25 Mc/s Cosmic Radio Noise.

It is worth mentioning here that this type of SID has been observed only on rare occasions and that too only in winter when the sun is low in the sky.

4. Diurnal and Seasonal variations of SID's on 164 Kc/s

It was shown at the beginning of the chapter that other SID's occurring in summer usually started off with a sudden enhancement of the longwave field intensity with the onset of a solar flare, while those in months other than summer commenced with an initial dip. This point could be studied in detail with the help of Figure 3, which shows how the shape of the SID changes during the course of a day and also during different seasons. Nine selected SID's which occurred at different times of the day in different seasons are arranged in rows and columns.

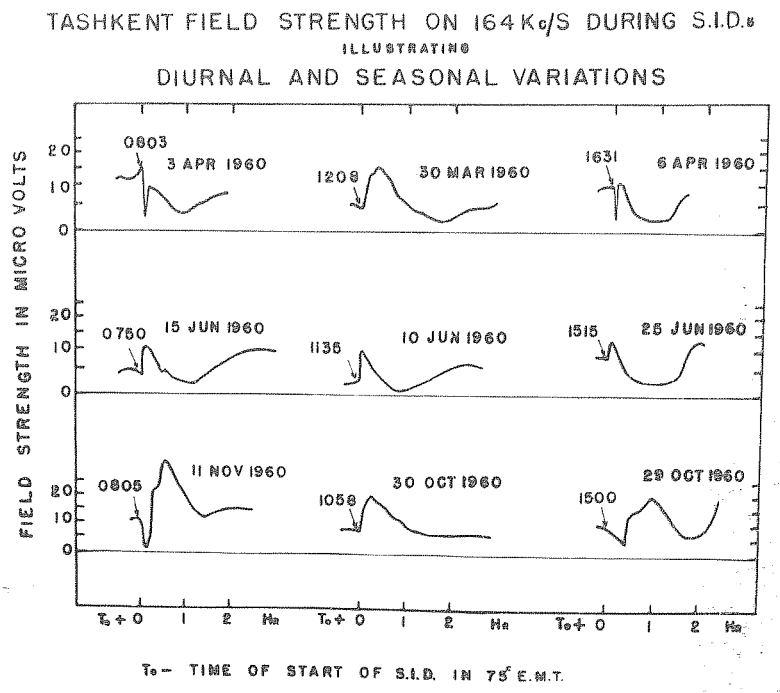


Fig. 3

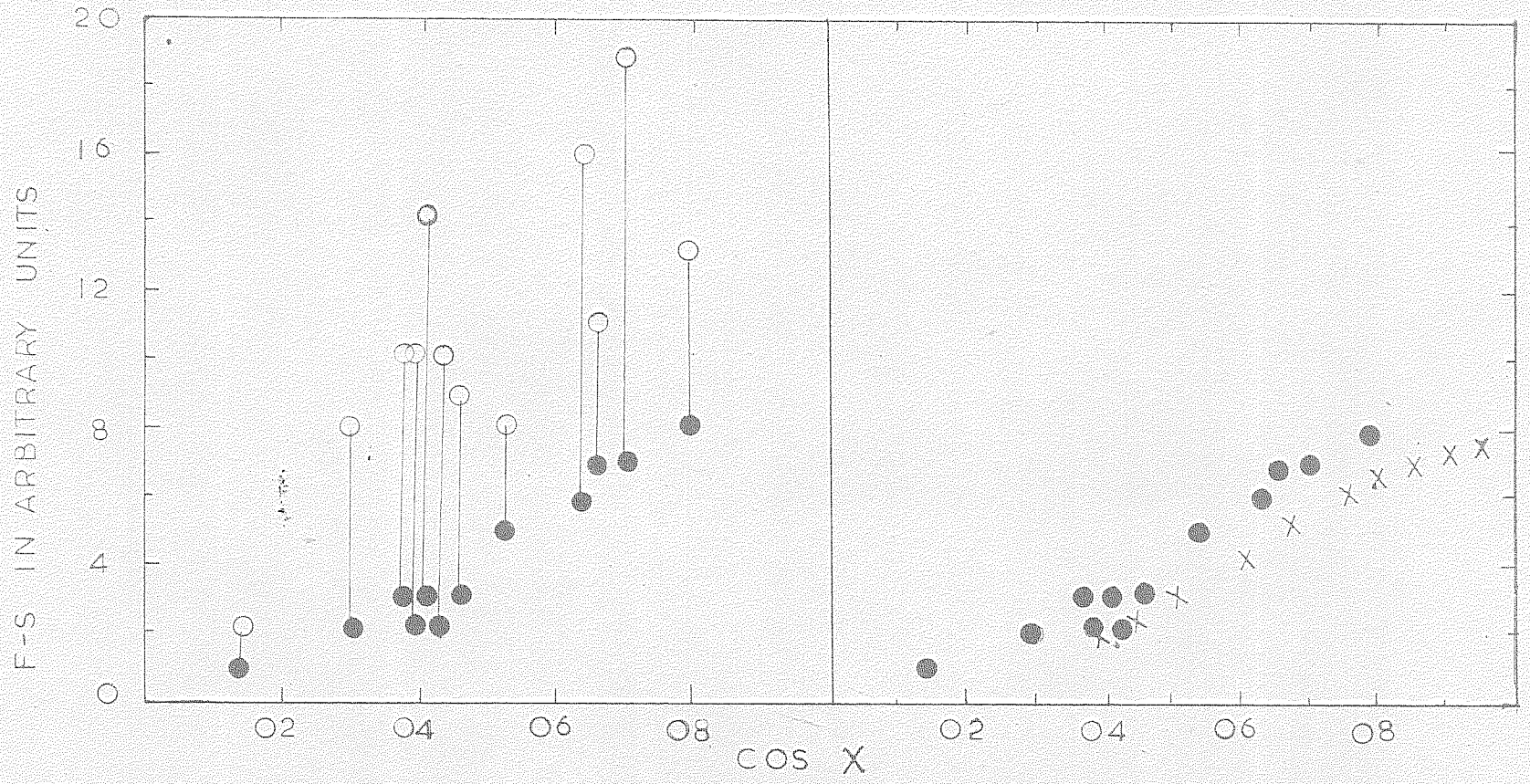
The rows show the three seasons equinoxes, summer and winter respectively, while the columns represent forenoon, noon and afternoon respectively. The first row shows the SID's which occurred between 3rd April to 6th April, 1960. In the figure T_0 is the time of start of SID in 75^0 EMT. Looking along a row it can be seen that the SIDs begin

with an initial dip in the early morning and evening hours when the sun is low in the sky. Around noon, however, the SID's in all the rows show hardly any dip. Again, the seasonal behaviour is seen on examining the diagram columnwise. During equinoxes and winter, first and third row, the initial dips are seen to be pronounced, while during summer the SIDs start off with sudden enhancements with no significant initial dips. It is interesting to see that the SIDs in the middle column and middle row do not show any initial dips.

5. Initial dips and solar zenith angle

It is instructive to check how the amount of initial dip depends on the solar zenith angle. For this, a dozen SID's were taken at random and the field strengths at the start of the initial dips as well as at their ends were plotted against the corresponding solar zenith distance as shown in Figure 4. The hollow circles represent pre-flare signal intensities and the solid ones the field intensity at the start of sudden enhancement. The crosses show the field intensity in microvolts on 3rd June, 1980, a typical summer day. It is clearly seen that the initial dips fall roughly on a straight line, shown by the solid circles, which lie on nearly the same line as that obtained on an undisturbed summer day. In this context it may be recalled that the minima in signal strength which occur near sunrise and sunset during the months other than summer,

VARIATIONS WITH SOLAR ZENITH ANGLE IN THE FIELD-STRENGTH ON 164 Kc/S RECEIVED AT AHMEDABAD DURING THE INITIAL PHASES OF SOLAR FLARES



OOO FIELD-STRENGTH F-S JUST BEFORE START OF FLARE

●●● MINIMUM F-S IMMEDIATELY FOLLOWING FLARE, AFTER WHICH THE ENHANCEMENT BEGINS

XXX NORMAL F-S VARIATION ON AN UNDISTURBED SUMMER DAY

FIG. 4

as seen in the previous chapter, do not fall on a curve similar to the one on a quiet summer day obeying the law $F \propto \cos^n \chi$.

6. Post-enhancement decrease in signal strength during SID's

It was mentioned a little before that all SID's, irrespective of the type to which they belong, produce a decrease in intensity below the normal level after attaining a maximum. On examining a large number of SID's it was observed that the magnitude of this decrease varied from one SID to the other. It was, therefore, felt that a critical examination of this decrease for a number of SID's against their respective solar flare intensities might throw some light on the correlation, if any, between the post-enhancement decrease and solar flare intensities. In Figure 5 a number of SID's are arranged in three columns corresponding to the three classes of flares, viz. 1, 2 and 3 and 3*. The solar flares producing these SID's were taken from the CRPL Solar-Geophysical Data, Part I Volumes. It is seen from Figure 5 that the post-enhancement decreases of the SID's in the columns of Class 1 and Class 2 flares are much more conspicuous than those in the case of Class 3 and Class 3* flares. Consequently the SID's produced by the more intense flares have shorter durations than those caused by the milder ones. How the recovery in the amplitude of the

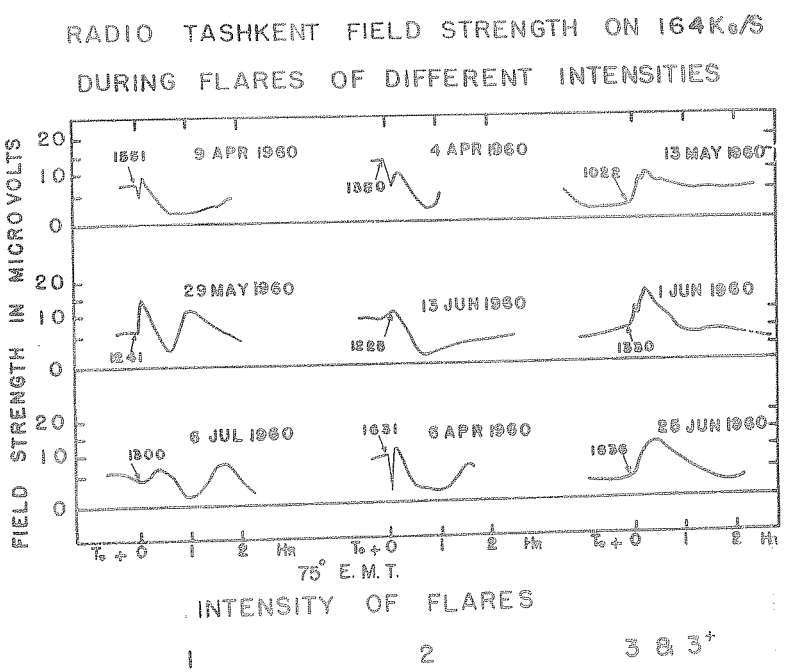


Fig. 5

longwave after a visible flare is over depends upon how quickly the ionization density came back to normal. If this relaxation time is large, obviously it will take a longer time for the SID to come to normal. Thus our observations indicate that in the case of major flares this

relaxation time is small as compared with that for minor flares. It is known that during major flares the reflection heights are lowered by as much as 15 Km as against 3 - 5 Km during minor flares. In this connection it may be remembered that the magnitudes of the initial dips and sudden enhancements do not exhibit any direct correlation with the importance of visible flares.

7. SID's on 164 Kc/s in relation to the Hα radiation from solar flares

It is interesting to see how the shape of an SID changes during the course of a solar flare. The intensity of a visible flare is usually expressed in terms of the changes in the Hα line-width measured with Lyot Hα heliographs at intervals of a minute or so. For the present analysis the Hα line-width data obtained at the Ondrejov Observatory published by Ikeuti, Kvicala, et al (1961) were used. A dozen SID's were compared with the corresponding Hα development curves in Figure 6. Out of the twelve SID's under consideration only the SID on 25th June, 1960 ran parallel to the Hα development curve. Some of the features of this comparative study are presented in Table 2. The following points emerge:-

1) The beginning of 164 Kc/s SID's coincided in most cases with the enhancement of the Hα line-width. The lack of coincidence was either

due to the absence of information about the time of real beginning of the H_α line-width, as on 9th April and 14th August, 1960, or due to the occurrence of SID's before their previous SID's were over, e.g. on 25th June and 14th August, 1960.

FIGURE-6.

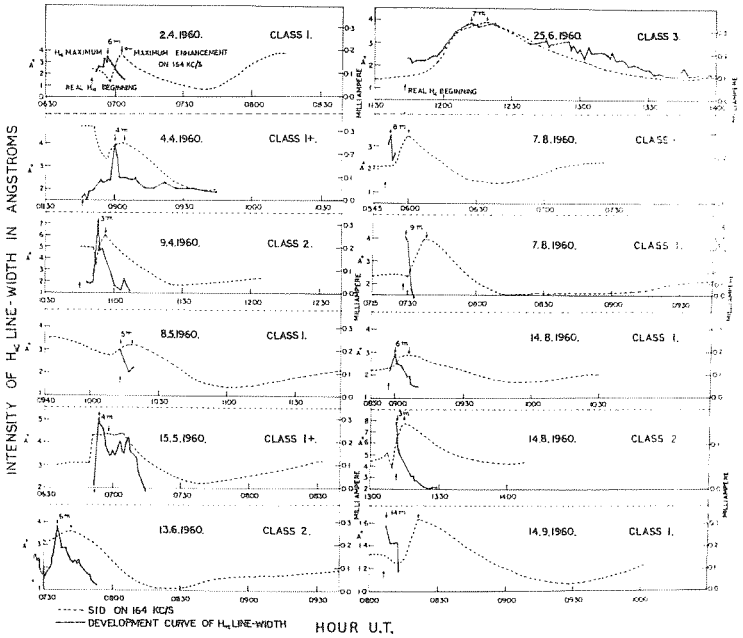


Fig. 6

Table 2

Hα 14Å-width and SID's on 104 Kc/s

Serial No.	Date	Hα flare Beg UT	Hα flare Max UT	SID on 104 Kc/s Beg UT	SID on 104 Kc/s Max UT	Delay of SID max. in min Δt
1	3-4-60	0650	0657	0650	0703	6
2	4-4-60	0946	0950	0850	0904	4
3	9-4-60	1046	1053	1051	1056	3
4	8-5-60	1013	1013	1010	1018	5
5	16-5-60	0652	0654	0651	0653	4
6	19-6-60	0725	0736	0734	0742	6
7	25-6-60	1143	1212	1153	1219	7
8	7-8-60	0650	0652	0653	0659	3
9	7-8-60	0728	0729	0730	0738	9
10	14-8-60	0657	0700	0700	0706	6
11	14-8-60	1211	1211	1207	1214	3
12	14-8-60	0806	0807	0806	0821	14

2) In all the cases the SID maximum occurred later than the flare maximum, the extent of the delay being variable from 3 to 14 minutes with an average of 6.3 minutes.

3) The end of the SID's took place much later - from about one to two hours - than that of

the H_α flares. In other words, the sluggishness of the SID's became more evident during the decay phase than during their maxima.

On the simplest interpretation, the time lag between the SID and flare maxima may mean that the ionization at the level concerned, about 70 - 75 km, builds up more gradually than the amount of light quanta received by the layer.

The similarity or otherwise between the shapes of SID's and H_α line-widths would depend on the relaxation time of the ionization produced by the visible flares. Recent rocket measurements of solar radiations during flares suggest however another possibility to explain the large differences between the course of increase and decrease in SID's and H_α flare intensities. X-rays of wavelength 1 - 8 A^o are able to ionise the atmosphere near the base of the D layer without affecting the higher ionosphere. Sufficient evidence exists to indicate that X-rays play an important role during SID's.

Appleton (1953) has shown that when the rate of electron production q passes through a maximum in any ionospheric layer, the resulting maximum electron density N_m will be delayed by a time given by $\frac{1}{2}\frac{1}{\alpha N}$ seconds, where α is the recombination coefficient. Making use of the time difference between flare maxima and maxima of SID's

produced by them, Bates and Seaton (1950) deduced a value of 5 x 10^{-5} cm^3 sec^{-1} for α at a height of about 70 Km utilizing 16 Kc/s phase height data of Bracewell and Straker (1949). Later, Mitra and Jones (1954) used the same and Ellison's (1950) data and obtained an average value of α to be 3.6 x 10^{-5} cm^3 sec^{-1} at about 60 Km.

8. 164 Kc/s SID's and Sudden Cosmic Noise Absorption on 25 Mc/s

The effects of solar flares on short radio waves (SWF) were first reported by Nagel (1935) and Dellinger (1935). Since then many workers have ascertained the various features of short wave fadeouts. Cosmic Radio Noise on 25 Mc/s is being recorded at Ahmedabad since 1955. Solar flare studies using these data are reported by Bhonsle (1960).

A comparative study of the solar flare effects on 164 Kc/s and 25 Mc/s (SCNA) was initiated by Professor K.R.Ramanathan. Their salient features are presented in the following paragraphs.

Figures 7 and 8 display original records on the 6th, 7th and 8th August, 1960, days which were characterised by a series of SID's. The upper records show SID's on 164 Kc/s while the lower ones show SCNA's on 25 Mc/s. The arrows indicate the start of sudden enhancements in

SOLAR FLARE EFFECT ON
COSMIC RADIO NOISE (25 Mc/S)
AND ON TASHKENT FIELD STRENGTH
ON 164 Kc/S AT AHMEDABAD

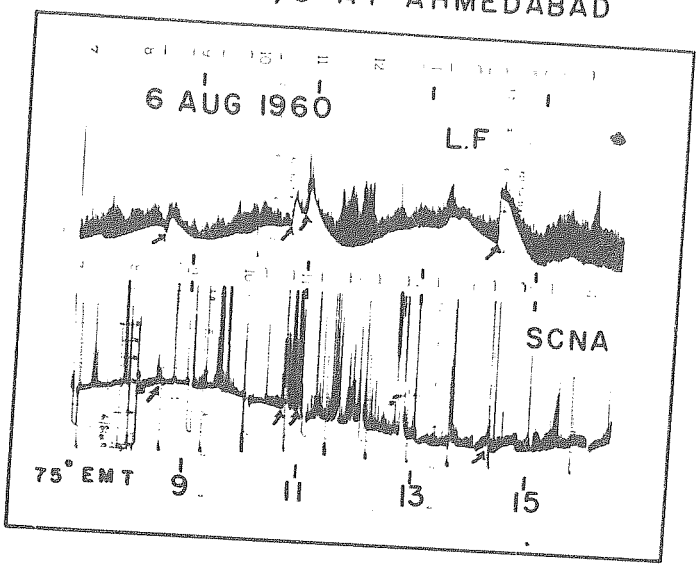


Fig. 7

the case of the low frequency and that of solar noise bursts or SCNA's in the case of cosmic radio noise. A close agreement in time of the sudden enhancements and solar noise bursts is evident. Again on the 7th August, 1960 in Figure 8 the maximum of the second SID on 164 Kc/s appeared at about 1942 hours 75° EMT. The maximum absorption of the corresponding SCNA also occurred at about the same time. A similar time

SOLAR FLARE EFFECT ON
COSMIC RADIO NOISE (25 Mc/S) AND ON
TASHKENT FIELD STRENGTH ON 164 Kc/S
AT AHMEDABAD

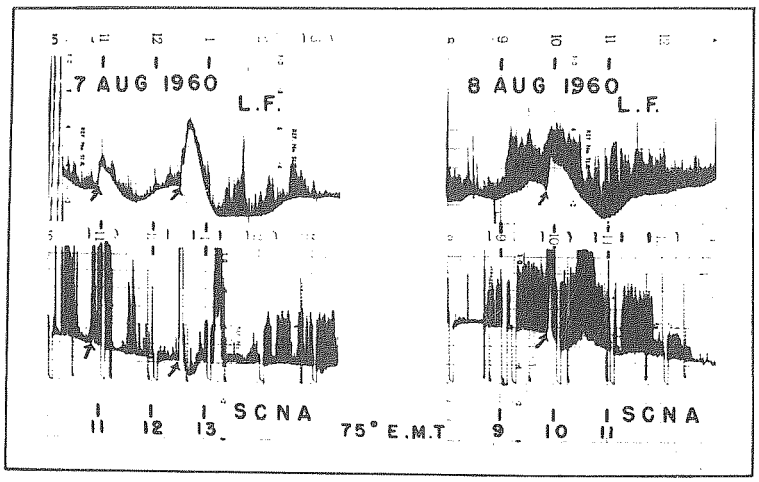
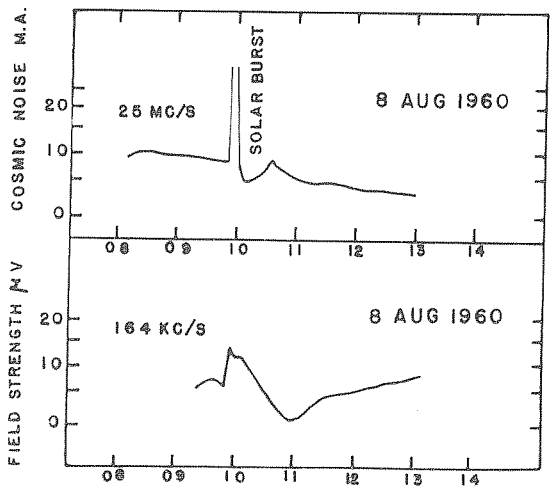


Fig. 8

coincidence was observed between the two maxima on the 8th August, though the SCNA maximum was rather difficult to pinpoint because a small portion of it was intercepted by the solar burst preceding it. This particular event is redrawn on a larger scale in Figure 9. It shows that the SCNA was complete at about 1040 hours 75° MT, while the corresponding

SID on 164 Kc/s came to the normal level about two hours later. A quantitative comparison of the durations and magnitudes of the various features of a low frequency SID and the corresponding SCNA will be made a little later.

S.I.D. EFFECTS ON
TASHKENT FIELD STRENGTH ON 164 Kc/S
AND COSMIC NOISE AT AHMEDABAD



75° E.M.T.

Fig. 9

Figure 10 shows a number of 164 Kc/s SID's on 3rd April, 4th May and 11th November, 1960 and their counterparts

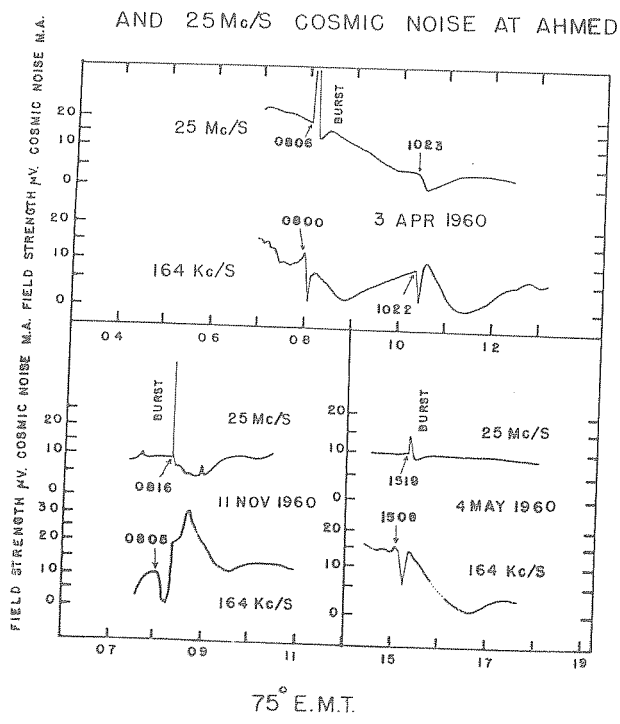


Fig. 10

on 25 Mc/s cosmic radio noise. SID's starting off with initial dips were purposely chosen. The initial dip of the first SID on the 3rd April began at 0804 hours 75°EMT, while the effect of the same time on 25 Mc/s commenced with a solar burst beginning at 0805 hours. The second SID on the same day started with an initial dip at 1023 hours. The corresponding BCNA began at 1027 hours. On the

4th May and 12th November these time differences were 9 and 11 minutes respectively. Thus it can be concluded that the initial dips in 164 Kc/s SID's appear before the 85 Kc/s record begins to show the effect of visible flares. On the contrary, the sudden enhancements and maxima in the longwave field intensity occur simultaneously with the starts and maxima of SCNA's on 85 Kc/s.

In Figure 11 a quantitative comparison of SID's and SCNA's is made on two occasions one on the 7th August and the other on the 3rd April, 1960. The changes in the intensities are expressed in terms of decibels with reference to the preflare level. The solid curves show SID's on 164 Kc/s while the dashed ones give SCNA's on 85 Kc/s. On the 7th August the maximum enhancement of the low frequency field strength was about 10 db over the preflare value, while the maximum absorption on 85 Kc/s reached a value of about 5 db below the normal level. The SCNA recovered to normal at about 1935 hours 75° EMT, while the low frequency SID was complete at about 1500 hours. The most interesting feature is the severe post-enhancement decrease on 164 Kc/s which assumed a value of about 23 db below the preflare level. Again on the 3rd April the initial dip was about 17 db and the maximum enhancement over the average level was insignificant as compared with the maximum absorption of about 3 db on 85 Kc/s. In this instance also the post-enhancement decrease on 164 Kc/s exceeded 20 db.

TASHKENT RECEPTION 164 Kc/S
AND COSMIC NOISE ON 25 Mc/S AT
AHMEDABAD IN TWO SOLAR FLARES

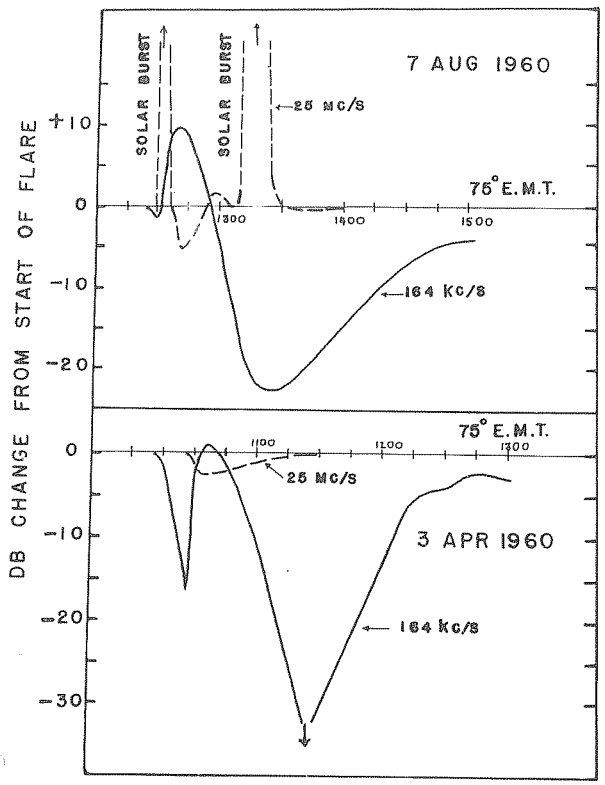


Fig. 11

Thus it is clear from this comparison that the low frequency field intensity is much more sensitive to solar flares than the 25 Mc/s cosmic radio noise both in duration as well as in magnitude. Consequently minor solar flares which produced distinct SID effects on 164 Kc/s have, on many occasions, shown hardly any deflection on the 25 Mc/s cosmic radio noise.

9. Solar and Cosmic Ray Flares

It is known that the period from 10th to 15th November, 1960 was characterised by a number of solar flares. The flare on the 15th November was a major one and is discussed here with the help of Figure 12.

SOLAR FLARE - 15 NOV 1960.
COSMIC RADIO NOISE, 25 Mc/S & TASHKENT FIELD STRENGTH, 164 Kc/S AT AHMEDABAD.
NEUTRON MONITOR INTENSITY AT DEEP RIVER, CANADA.

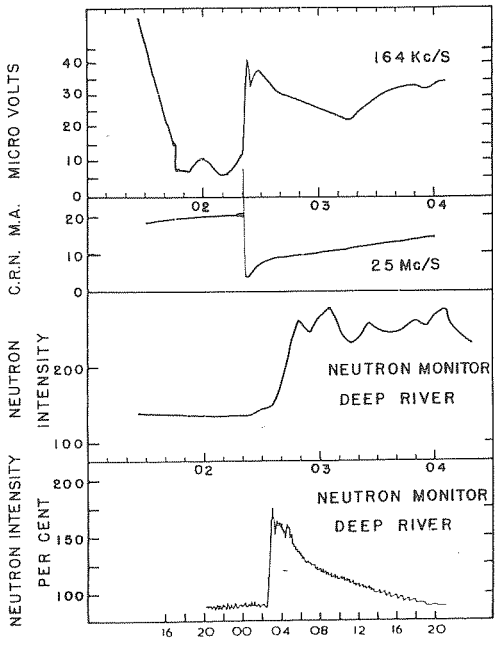


Fig. 12

The SID on 104 Kc/s and SCNA on 95 Kc/s cosmic radio noise produced by the flare are drawn one below the other. The low frequency SID has started off with a sudden enhancement beginning at 0221 hours UT. The SCNA also starts suddenly at the same time. Both the sudden enhancement as well as the start of the SCNA are characterized by unusually steep slopes of a minute or two as against 5 to 10 minutes for an average flare. Again the magnitudes of the maximum enhancement on 104 Kc/s and maximum absorption on 95 Kc/s are about 0.2 db and 7.5 db respectively. According to Thomas (1960) the average value of SCNA maximum is between one to two db only.

The third curve in Figure 12 shows the variation of the neutron monitor intensity at Deep River (60.46°N, 77.50°W), Canada, following this flare. Normally the intensity is recorded every five minutes. On this particular occasion the neutron monitor intensity is seen rising, comparatively gradually, at about 0235 hours UT, i.e. 14 minutes after the onset of the flare. Thus if we assume that the cosmic ray particles during the flare were ejected simultaneously with the relativistic radiation responsible for the low frequency SID and SCNA, then they would travel down with a velocity slightly less than one-third the velocity of light.

It is important to note that the post-enhancement decrease in the longwave field intensity on the 15th November, 1960 was almost negligible and that the daytime

intensity pattern from the instant when the SID recovered to normal resembles a typical cosmic curve.

Another cosmic ray flare was recorded on 4th May, 1960. The maximum enhancement was about 8 db which was reached within about 5 minutes. The corresponding SCNA connected with a solar burst as is seen in Figure 10.

REFERENCES

Dellinger	1935	Science, 82, 351.
Bureau	1937	Nature, Vol. 139, p.110.
Gardner	1950	Phil.Mag., 41, p.1250.
Lowe	1951	Phil.Mag., 42.
Budden, Ratcliffe and Wilkes	1959	Proc.Roy.Soc., 171A, 132.
Budden and Ratcliffe	1957	Nature, 140, 1000.
Bracewell and Straker	1949	Mon. Notices Roy.Ast.Soc., Vol. 109.
Smithlogo	1950	Nature, Lond., 165, 37.
Bracewell, Budden, Ratcliffe, Straker and Wookes.	1951	Proc.I.E.E., Part 3, Vol. 98.
Bain	1953	J.Atmosph.Terr.Phys., 3, p.141.
Wookes and Stuart	1953	Proc.I.E.E., Part 3, Vol. 99.
Ellison	1953	J.Atmosph.Terr.Phys., Vol. 4, p.236.
Friedman and Chubb	1955	Phys.Soc.(London), p. 58.
S.N.Mitra	1959	J.Inst.Telecom.Engrs., 5, 121.
Krobli, Krienla, et al	1961	IAC Vol. 12, No.5.
Appleton	1953	J.Atmosph.Terr.Phys., 3, 308.
Bates and Benton	1950	Proc.Phys.Soc., A63.
Mitra and Jones	1954	J.Geophys.Res., Vol. 59.
Ellison	1950	Publications of the Royal Observatory, Edinburgh, 1, 53.
Mogel	1950	Telefunken-Zeitung, 11, 14.
Dhonslo	1960	Proc.Ind.Acad.Sci., 51A, 150.

ooo 0 ooo

Field strength changes during solar flares on 164 Kc/s Bahlent transmissions received at Ahmedabad. All times are reckoned in minutes from starting of sudden enhancement, which will be denoted by the symbol S.S.L.F.

Serial No.	Date 1960	Time of SSLF GT	Intensity in db relative to value at beginning of S.S.L.F.			Time in minutes before or after S.S.L.F.			
			Value at beg. of initial dip.	Maximum enhancement.	Minimum after enhancement.	Beginning of initial dip	Time of maximum enhancement.	Time of minimum following enhancement.	Approximate time of recovery to normal.
1	2	3	4	5	6	7	8	9	10
1	29/3	0854	1.6	10.3	- 3.6	- 1	6	31	106
2	30/3	0706	0.0	10.6	- 10.4	0	30	100	157
3	2/4	0519	11.2	12.7	- 0.6	- 2	1	50	-
4	2/4	0653	6.0	10.9	- 2.6	- 3	5	42	67
5	2/4	0839	3.6	7.2	- 8.4	- 2	2	56	91
6	3/4	0506	20.0	15.0	+ 3.6	- 2	3	53	90
7	3/4	0527	17.0	13.0	- 15.0	- 4	9	57	123
8	3/4	1153	13.0	8.6	- 2.6	- 2	4	38	62
9	4/4	0415	3.6	1.4	- 3.4	- 3	7	32	80
10	4/4	0857	4.0	2.2	- 10.3	- 7	7	46	-

1	2	3	4	5	6	7	8	9	10
11	4/4	0851	0.0	8.0	-	0	4	31	-
12	6/4	1123	10.4	12.4	0	- 2	4	47	77
13	9/4	0818	6.8	1.4	- 7.6	- 3	2	23	74
14	9/4	1052	4.0	20.4	- 8.0	- 1	1	38	83
15	12/4	0925	0.0	5.2	- 17.0	0	8	57	110
16	20/4	0850	0.0	6.0	- 3.6	0	25	75	105
17	4/5	1015	8.6	6.2	- 17.0	- 7	4	30	115
18	8/5	1010	0.0	2.2	- 10.8	0	0	53	105
19	9/5	0218	8.8	4.2	- 8.6	- 10	19	62	114
20	9/5	1035	0.0	10.4	- 3.6	0	6	76	115
21	10/5	0212	10.4	4.4	0	- 4	6	33	93
22	12/5	0515	0.0	9.6	-	0	17	75	-
23	15/5	0850	0.0	2.4	- 9.6	0	10	47	100
24	16/5	0513	1.4	0.6	- 9.4	- 7	12	77	137
25	17/5	0855	4.8	4.8	- 12.2	- 4	10	65	105
26	23/5	0830	0.6	0.6	- 9.4	- 3	5	60	120
27	25/5	0800	2.2	2.8	- 7.4	- 6	4	60	85
28	25/5	0835	0.0	1.2	- 7.4	0	10	49	109
29	26/5	0830	0.0	1.8	- 15.6	0	32	109	144

| | | |

1	2	3	4	5	6	7	8	9	10
49	29/6	0137	6.0	18.0	+ 9.0	- 12	16	83	-
50	30/6	0354	0.0	4.8	- 14.6	0	6	69	196
51	30/6	0452	0.0	12.0	- 2.4	0	6	48	153
52	1/7	0300	3.0	10.3	- 14.0	- 3	2	111	-
53	3/7	0308	0.0	4.4	- 4.3	0	13	59	113
54	6/7	0300	0.0	4.8	- 12.0	0	17	112	145
55	6/7	0821	0.0	18.0	0.0	0	16	69	139
56	10/7	1045	0.0	6.0	- 12.0	0	8	64	135
57	15/7	0544	0.0	4.0	- 10.4	0	6	46	126
58	19/7	0446	0.3	3.4	- 20.0	- 8	9	66	134
59	20/7	1020	0.0	10.2	- 12.0	0	5	91	136
60	22/7	1945	0.0	3.6	- 6.0	0	21	58	-
61	26/7	0332	5.6	5.0	- 8.4	- 7	13	51	118
62	5/8	0754	0.0	4.6	- 10.8	0	28	87	141
63	5/8	1152	0.0	6.0	0.0	0	11	62	78
64	6/8	0330	0.0	3.0	- 6.0	0	5	40	70
65	6/8	0540	0.0	6.8	0.0	0	5	57	115
66	6/8	0818	0.0	4.8	- 12.0	0	12	-	-

| | | |

98	1/9	0520	0.0	6.0	1.4	0	23	0	0	115	
97	1/9	0530	0.0	7.4	0.0	0	23	0	0	105	
96	2/9	0540	0.0	10.0	0.0	0	22	0	0	95	
95	2/9	0557	0.0	0.0	0.0	0	15	0	0	0	
94	3/9	0607	0.0	1.4	21.2	0	15	0	0	0	
93	3/9	0625	0.0	11.6	14.0	0	15	0	0	85	
92	14/9	0645	0.0	14.0	13.0	0	15	0	0	95	
91	14/9	0655	0.0	3.6	8.8	0	22	0	0	95	
90	14/9	1005	0.0	10.0	0.0	0	23	0	0	95	
89	30/9	1115	0.0	4.4	0.0	0	23	0	0	95	
88	18/10	0505	0.0	4.4	2.8	5	23	0	0	95	
87	23/9	0537	0.0	7.6	0.0	3	23	0	0	85	
86	23/9	0545	0.0	4.0	0.0	4	23	0	0	85	
85	23/9	0551	0.0	14.0	13.0	5	23	0	0	105	
84	23/9	0604	0.0	0.0	0.0	5	23	0	0	95	
83	30/10	0715	0.0	0.0	14.0	0	23	0	0	105	
82	31/10	0110	0.0	0.0	3.6	0	23	0	0	95	
81	31/10	0508	0.0	6.0	7.4	5	23	0	0	105	

1	2	3	4	5	6	7	8	9	10
104	14/10	0722	5.6	2.0	- 8.4	- 1	4	53	53
105	15/10	0442	0.0	6.6	0.0	0	4	52	105
106	15/10	0803	5.4	4.6	- 6.0	- 3	4	47	57
107	20/10	1043	0.0	14.0	+ 3.6	0	32	55	109
108	30/10	0553	0.0	9.2	- 1.4	0	16	35	133
109	6/11	0625	11.4	18.0	- 13.2	- 4	5	17	-
110	11/11	0811	21.6	30.4	- 21.0	- 6	26	70	94
111	12/11	1001	0.0	18.0	0.0	0	19	30	125
112	14/11	0530	0.0	6.6	0.0	0	23	-	-
113	14/11	0811	0.0	9.2	- 4.0	0	7	40	65
114	15/11	0221	0.0	9.2	+ 4.6	0	23	54	-

CONTENTS

CHAPTER 4

		Page
1.	Diurnal and seasonal variations of signal amplitude	1
2.	SID effects on 164 kc/s	3
3.	Discussion	5

CHAPTER 4

SUMMARY AND DISCUSSION

In the second chapter the diurnal and seasonal behaviour of daytime field intensity of 164 Kc/s transmissions from Tashkent was studied. This was followed by an account of the effects of sudden ionospheric disturbances, following visible flares, on the long wave signal amplitudes. In the present chapter it is proposed to summarise the conclusions of those studies and make an attempt to interpret them.

The salient features of the low frequency long distance propagation are:-

1. <u>Diurnal and Seasonal variations of signal amplitude</u>

(i) In all the seasons, the night-time field strength was high and fluctuating in intensity.

(ii) The signal strength decreased rapidly at the time when solar rays first strike the D region, corresponding to a solar zenith angle of about $97^{0}30'$ throughout the year.

(iii) During summer, i.e. from June to September-October, the day-time field strength F varies with the solar zenith distance according to the relation $F \propto \cos^{n} x$,

where x is the solar zenith angle and the power n assumed an average value of 1.3. The maximum of F around noon was about 8 - 10 microvolts.

(iv) During the months other than summer, i.e. from October to April - May, the signal amplitude undergoes oscillatory changes near sunrise and sunset. There are two prominent maxima of intensity on either side of noon. These peaks glide along the daytime curve according to the position of the sun in the sky.

(v) A smooth curve drawn through the minima of intensity near sunrise and sunset and the intercept between the two main peaks around noon does not follow any simple relation of the form $F \propto \cos^n x$, connecting the field strength F to the solar zenith angle x. This basic curve in winter shows much higher intensities than those corresponding to the same solar zenith distances during summer.

(vi) The height of reflection of the low frequency wave corresponding to the start of drop in intensity at the time of layer sunrise varies irregularly from day to day, but happens to be about 70 Km on many days at the mid-point of the transmission path.

(vii) During the course of its rapid fall after layer sunrise the signal strength undergoes minima, the first minimum is regularly controlled by the position of the sun in the sky. During summer (Northern Solstice) the first minima appear

about 10 to 15 minutes earlier than ground sunrise and during winter (Southern Solstice) about 5 to 10 minutes later than ground sunrise at the mid-point of the transmission path. During the rest of the year they appear almost simultaneously with ground sunrise.

(viii) The first minimum of intensity near sunset also depends on the position of the sun, but shows more irregularity than the sunrise minimum.

c. SID effects on 164 Kc/s

(i) The effect of solar flares on the long wave field intensity manifests itself in two main types of SID's, viz. those which start off with a sudden enhancement, taking about 10 minutes on an average to reach the maximum, and those which begin with an initial dip lasting only for 3 to 5 minutes followed by a sudden enhancement. A third type of SID's appears very rarely. This is characterised by a sudden drop in intensity followed by an exponential recovery to normal.

(ii) All SID's after maximum enhancement decay gradually towards normal and continue falling below normal; after some appreciable decrease below normal, the intensity finally recovers to normal. The entire process takes about 2 to 3 hours.

(iii) SID's starting with an initial dip occur in the early morning and evening hours during winter, i.e. when the sun is

low in the sky. SID's beginning with a sudden enhancement on the other hand appear during summer and only near noon in winter.

(iv) The field intensities of initial dips depend on the solar zenith distances in the same manner in which the signal strength on a typical summer day depends, viz. $I \propto \cos^{n} \chi$.

(v) The magnitude of the post-enhancement decrease seems to be roughly correlated with the intensity of the corresponding flare. The larger the optical intensity the smaller is the decrease.

(vi) The beginning of SID's coincides with the beginning of the corresponding H_{α} flare. The SID maximum, however, lags behind the H_{α} maximum, the delay being variable from flare to flare with an average of about 6 minutes.

(vii) The initial dips in SID's on 164 Kc/s appear before the start of SCNA's on 25 Mc/s. The start and maximum of sudden enhancement coincide with the beginning and maximum of SCNA. The low frequency field intensity is much more sensitive to SID's than the short wave absorption as seen from their magnitudes and durations.

(viii) The third type of the low frequency SID's, which start with an initial dip and exponentially recover to normal without sudden enhancement, may or may not be associated with a solar burst or SCNA on 25 Mc/s.

3. Discussion

A successful attempt to interpret the results of 16 Ke/s transmission over path lengths of 90 and 535 Km was made by Bracewell and Main (1952). They explained the diurnal phase changes over 90 Km and rapid phase changes near sunrise and sunset over 535 Km in terms of two layers D_α and D_β respectively. The upper layer, D_α, is under direct solar control, while the lower one, D_β, appeared an hour before sunrise and descended to the daytime equilibrium position by sunrise.

Following this many workers explained LF and VLF observations with the help of aeronomic processes involved in the formation of the D region. The most satisfactory electron-production process to explain the general characteristics of the D region is the photo-ionization of NO by lyman alpha radiation first suggested by Nicolet (1945) who puts the peak electron density at 75 - 77 Km for the zenith sun.

On the basis of experimental observations and empirical models suggested by Nertney (1953), Hirn (1954) and Bates (1950), Houston (1953) developed a model for the D and E regions for which the main electron-production processes were assumed to be photo-ionization of NO below 100 Km by L_α (1216 A^0) and photo-ionization of O_2 above 100 Km by L_β (1026 A^0). This model agrees well with most radio measurements except for certain aspects of VLF oblique propagation.

On the basis of rocket measurements Meier (1960) showed that the single-layered D region model based on L_α photo-ionization of NO is inadequate to explain some aspects of VLF propagation. He indicated the presence of a second and lower D layer which reflects VLF waves and is produced by normal cosmic rays. The ionization conditions during solar flares are, according to Nicolet and Aikin (1960), due to X-rays of solar origin.

The oscillatory features of the 164 Kc/s signal intensities recorded at Ahmedabad during the period between the start of the sunrise effect and ground sunrise could probably be explained in terms of a sky wave composed of two components reflected by two strata similar to D_α and D_β. Aikin (1961) studied these sunrise signal strength variations and suggested that the D region at this time consists of two layers D_α and D_β. The upper one, D_α, is under solar control and is formed by the photo-ionization of NO by L_α. The lower one, D_β, is formed by cosmic rays.

The initial dips and sudden enhancements observed during SID's can also be explained on the basis of a composite D region model or a composite solar emission model as suggested by Nitta (Pennsylvania). Again it is known that the phase of a LF wave during an SID decreases continuously towards the peak of the SID and the electron density increases correspondingly. These two different behaviours of amplitude

and phase during an SID are explained by Belrose (1961) in terms of two separate changes; the first being an increase of electron density which increases the absorption, and the second an increase in the electron density gradient which improves the reflectivity for the long wave.

The post-enhancement decrease observed on 164 Kc/s needs more satisfactory explanation. One would like to understand the reason for the different recovery times taken by the LF SID's and SCNA's.

REFERENCES

Bracewell and Pain	1950	J.Atmosph.Terr.Phys., Vol. 2.
Nicolet	1955	J.Atmosph.Terr.Phys., 7, 132.
Hartney	1953	J.Atmosph.Terr.Phys., Vol. 3.
Nitta	1954	J.Atmosph.Terr.Phys., Vol. 5.
Bates	1958	J.Atmosph.Terr.Phys. (Special supplement), Vol. 6, 194.
Houston	1958	J.Atmosph.Terr.Phys., 12, 285.
Meier	1960	J.Geophys.Res., Vol.65, 2.
Nicolet and Aikin	1960	J.Geophys.Res., Vol.65, No. 5.
Aikin	1961	J.Atmosph.Terr.Phys., Vol. 23.
Peterson	1961	NBS Course in Radio Propagation Lecture No. 13, Summer.

ooo 0 ooo

CONTENTS

CHAPTER 1

		Page
1.	Cause of lunar tides in the ionosphere	2
2.	Analysis of ionospheric data for the effect of lunar tidal oscillations	3
3.	Methods of analysis	4
4.	General survey of the lunar variations in the F_2 layer of the ionosphere	6

CHAPTER 1

INTRODUCTION

Analogous to oceanic and atmospheric tides, there are periodic oscillations of ionospheric parameters, e.g. maximum electron density of an ionospheric region and its height, whose magnitudes are dependent on lunar time. These are known as ionospheric lunar tides.

It is well known that there are many more neutral particles than charged particles in the ionosphere, but due to the presence of the earth's magnetic field, the charged particles do not follow in detail the group motion of the neutral particles. Ionospheric phenomena, observed by vertical soundings, are dependent essentially on the distribution of charged particle density and movement of charged particles, particularly electrons. Lunar tidal oscillations affect all particles, neutral as well as charged. The lunar tidal variations deduced from ionospheric soundings by radio waves do not tell us the whole story of the lunar tidal wind, of the ionosphere.

The ionospheric lunar tide shows some interesting correlations with ionospheric and geomagnetic variations. These tidal motions undoubtedly interact with the magnetic field of the earth in the conducting regions of the upper

atmosphere. This interaction results in changes in the distribution of conductivity in the ionosphere and hence affects the magnetic field as observed at the ground.

1. Cause of lunar tides in the ionosphere

In physical terms, ionospheric lunar tides are believed to arise from the oscillatory motion of the earth's upper atmosphere due to the moon's gravitational attraction; both heights and electron densities are affected. Although the tidal oscillations of the E layer of the ionosphere could to some extent be explained on the basis of bodily motions of its charged particles, the interpretation is difficult in the case of the F_2 layer, since the charged particles at these levels do not follow in detail the group motions of neutral particles.

Martyn (1947, part I) advanced the theory that the major anomalies in the behaviour of the F_2 region of the ionosphere could be explained as being due to the action of solar atmospheric tides which may have a large amplitude at these heights. In brief, the theory said that the predominantly horizontal motion of the tides would cause large vertical movements of ionized air, because of the presence of the earth's magnetic field, and would thereby change the maximum electron density $N_{(max)}$ and height $h_{(max)}$, causing considerable deviations from a "Chapman region" distribution.

2. Analysis of ionospheric data for the effect of lunar tidal oscillations

By means of conventional vertical incidence ionosondes the critical frequencies and the virtual heights of different ionospheric layers are estimated. The maximum electron density of a layer and its critical penetration frequency for ordinary rays are related to each other through the following well known formula:-

$$N_{max} = 1.24 \times 10^4 f_0^2,$$

where the critical frequency, f_0, is expressed in Mc/s. Differentiation of both the sides of this equation leads to the following relation:-

$$\frac{200 \Delta f_0}{\text{Mean } f_0} = \frac{\Delta N_{max}}{\text{Mean } N_{max}} \quad \text{in per cent.}$$

Here Δ is the deviation from the mean value. Either $(200\ \Delta f_0/\text{Mean } f_0)$ or f_0 itself is used in the study of lunar variations in the ionosphere. In actual practice, the critical frequency f_0 is measurable to an accuracy of 0.1 Mc/s, while the virtual height h' can be read with an accuracy of about 10 Km. The height h_{max}, corresponding to the maximum electron density N_{max} of a layer, is estimated at a frequency 0.834 times f_0, assuming a parabolic electron density distribution with height.

3. Methods of analysis

For analysing geophysical data for special diurnal effects, the following methods are usually employed: a method is due to Chapman and Bartels (Geomagnetism, 1940); and a revised one due to Chapman and Miller (1940). See also Sachs (1949) and Chapman (1952). The following summarises the two methods in some detail.

(1) Chapman and Bartels method

The value of the geophysical element under investigation at each hour is subtracted from its monthly mean value for the same hour. These hourly deviations give the variation of the element freed from the average solar daily variation. The residual variations are due to secular variation, disturbance variations, as well as lunar daily variation.

These hourly deviations are rearranged according to lunar time, counting 25 solar hours to a lunar day. Each lunar day is reckoned from the lower lunar transit. This usually does not fall at an exact solar hour, and so the nearest solar hour is counted. The difference from the means for this hour, and similarly for the other 24 hours, are entered in a row on a sheet. This represents the lunar daily variation for that particular day. One more hourly deviation is added at the end of this row to eliminate any non-cyclic variations. The whole plan of this

method is to write on one sheet all the lunar hour deviations for each of the lunar days falling within a calendar month. The means of these 30 columns, reduced to 25 by eliminating the mean non-cyclic variation, will give the mean lunar daily variation for that month. The same procedure can be used for obtaining the average seasonal or annual lunar variations.

(ii) Chapman-Miller method

According to this method the geophysical data, initially expressed against solar hours, are rearranged according to lunar hours. The hourly deviations from monthly mean values are regrouped according to the corresponding lunar phases. The lunar phases for any period could be found from the geophysical lunar almanac prepared by Bartels and Fanselau (1937). The average of these data in 12 lunar age groups would give the seasonal or annual geophysical lunar variation.

After the geophysical data are analysed according to one of these methods, they are further analysed to study the probable errors involved in the analysis. The weights of the data analysed are judged from the sizes of the probable error circles or ellipses presented on harmonic dials, which are essentially vector representations of amplitudes and phases of the lunar variation having

semi-diurnal periodicity. The amplitudes and phases, in turn, are calculated by subjecting the average hourly deviations grouped into twelve lunar ages to Fourier analysis.

For the two methods discussed above, the lower transit of the real moon is taken as lunar hour 0, because the lunar effect varies with the position of the real moon, and not of the mean moon. Using the lower transits of the real moon a slightly larger variation is found than if the lower transits of the mean moon had been used, the amplitude found for the second harmonic component being about 1.4 per cent larger in the former than in the latter case. For the lunar hourly deviations, it is usual to determine only the second harmonic term, which is the harmonic term of physical interest.

4. General survey of the lunar variations in the F_2 layer of the ionosphere

It should be noted that the first coefficient of the 12 - point Fourier analysis called F_2, represents the maximum amplitude of the semi-diurnal lunar tide, and the phase t_2 represents the lunar time at which the maximum amplitude occurs. The ionospheric parameters that are considered for their variations with lunar phase are usually f_0F_2, the critical frequency of the F_2 layer

(or 100 Δf_0F_2/mean f_0F_2 in per cent), $h'F_2$ the equivalent virtual height of the layer, $h_{max}F_2$ the height of maximum electron density N_{max} of the F_2 layer.

Appleton and Weekes (1939) first demonstrated the existence of large tidal variations in the ionospheric regions. They found that the height of E region was subject to a lunar tide of amplitude 1 Km, the maximum heights being attained approximately 3/4 hour before the upper and lower lunar transits.

Martyn (1947, II) studied the Huancayo ionospheric data for the period 1942-44. He observed a large semi-diurnal lunar variation in $h_{max}F_2$ and $h'F_2$, the variation in the former being twice as large as that in the latter. The phase of $h'F_2$ was retarded almost an hour on that of $h_{max}F_2$. The data were divided into three groups, (a) Southern solstice, (b) Northern solstice, and (c) Equinoxes. He showed that the variation in group (a) was about twice that in group (c) for h' and more than about four times as great for h_{max}. The equinoctial amplitudes lay between those for the groups (a) and (b). The lunar tide in f_0F_2 showed a strong semi-diurnal harmonic of half amplitude 0.10 Mc/s, the phase occurring at 4.3 lunar hours. Martyn (1947) further studied the variation of the F_2 layer lunar tide with solar time. From his analysis he concluded that the phase and amplitude of the semi-diurnal lunar variations in f_0F_2, $h'F_2$ and $h_{max}F_2$ at Huancayo were markedly dependent on solar

time. The half-amplitude of the variation in $h_{max}F_2$ ranged from 0.24 km at 02 hour to as much as 16 km at 16 hours, while the half amplitude density variations in N_{max} ranged from 14.6 % at 06 hour to 2 % at 07 hour.

Martyn (1947) found semi-diurnal variations in the heights and critical frequencies of the E, F_1 and F_2 regions of the ionosphere over Canberra, Australia. He concluded that ionospheric lunar variations were caused by ionic drifts under the action of the 'dynamo' electric forces, and not by simple tidal rise and fall of isobaric surfaces.

Nellish and Gautier (1949) showed lunar effects in the midday critical frequency of the F_2 layer, over Huancayo, Peru. At the December solstice, minimum values of the critical frequency were observed four days after new and full moon and maximum value four days after the quarters, while at the June solstice this occurred two days earlier. The range from maximum to minimum in the critical frequency was about twice as great around the December solstice as it was around the June solstice.

Nellish and Gautier (1949) used ionospheric data at Huancayo, Christmas Is. (Geog. 1.9°N, 157.3°W), Leyte (Geog. 11.0°N, 125°E), Trinidad (Geog. 10.6°N, 61.2°W) and Maui (Geog. 20.8°N, 156.5°W). From the results of these magnetic equatorial stations, Nellish and Gautier

concluded that the amplitude of f_0F_2 at solar noon had large maxima about two days after the lunar quarters.

Osborne (1952) analysed midday values of f_0F_2 at Singapore for the period from November 1943 to June 1951 inclusive. Since the ionospheric conditions over Singapore differ very much during the two solstices and the equinoxes, he studied the lunar tides in f_0F_2 separately for these seasons. He showed that a minimum in f_0F_2 a few days after the full moon was clearly evident during December and June solstices and also during the equinoctial months. Again in the June solstice, there was also a well marked minimum after the new moon. The Singapore equinoctial variation of f_0F_2 for the period under consideration was nearly half that obtained during the equinoxes at Huancayo during 1941-44, a period near sunspot minimum.

Durkaud (1951) studied Huancayo f_0F_2 data at different solar hours and concluded that the semidiurnal lunar tide was largely pronounced during day time, being practically negligible at night. He found that the amplitude of the lunar tide in f_0F_2 during day time was about four times as great as the one calculated from all-day f_0F_2.

Kotadia and Ramanathan (1956) studied variations with lunar phase of F_2 parameters at Indian stations, viz.

Bombay, Madras and Tirunchirapalli during the low sunspot years 1964-65. The point of interest emerging from this investigation was that while the semi-diurnal lunar tidal oscillations at Ahmedabad and Bombay agreed in phase with those observed at middle latitudes, the phase reversed in direction between Bombay and Madras.

Duncan (1966) briefly summarised the global distribution of lunar variations of the height and electron density of the F_2 region. He concluded that the height variation had an amplitude from 1 to 3 km and a phase giving maximum height at 06 lunar hours at moderate latitudes and at 09 lunar hour at the geomagnetic equator. The amplitude of f_0F_2 varied from 3 to 4 per cent., its phase being at 00 lunar hours at moderate geomagnetic latitudes and 04 lunar hours at equatorial geomagnetic latitudes.

Brown (1966) studied the lunar variations of h_mF_2, the semi-thickness Y_mF_2, f_0F_2 and $h'F_2$ for the period December 1951 to April 1964 at Kodaikanal. He pointed out that they exhibited marked seasonal variations of both amplitude and phase. The mean annual amplitude of f_0F_2 lunar tide was 0.119 Mc/s with its phase occurring at 3.3 lunar hours. Similarly the amplitude of h_mF_2 was 7.74 km and its phase at 8.1 lunar hours. The seasonal change in f_0F_2 tide was very regular. At the northern solstice, the amplitude was much bigger than that at southern solstice, the phase lagging by about two hours. At equinoxes, amplitude and phase had

intermediate values. In the case of $h_E F_2$, there was an appreciable increase in amplitude during the months around northern solstice, and an advance of about one hour in phase in the months around southern solstice. Though the noon tides at Ibadan and Huancayo were very similar, their seasonal variations were quite different. The seasonal changes of phase and amplitude of $f_0 F_2$ were comparable with those shown by Martyn (1943) at Canberra.

As for the luni-solar variations, the lunar tides in the F_2 layer over Ibadan showed large changes in both amplitude and phase. For all parameters the amplitude tended to be maximum at about midday, i.e. when the height of the layer was greatest. These luni-solar variations were similar to those at Huancayo shown by Martyn (1947). Brown and Martyn found that the luni-solar tide in $f_0 F_2$ showed a very regular change of phase, which, after a rapid change after sunrise, underwent a steady phase retardation of about one half lunar hour per solar hour throughout the rest of the day and night. It was shown by Martyn and Brown that the phase difference between $h_M F_2$ and $f_0 F_2$ varied regularly with height. From this observation they calculated the effective recombination coefficient α and the attachment coefficient α' which agreed well with those calculated by other methods.

All these analyses have indicated very large lunar tides at stations close to the geomagnetic equator. Besides

general agreement in the phase reversal of ionospheric lunar tides between moderate latitude stations and equatorial stations there are certain disparities between the phases of lunar tides at stations having the same geomagnetic latitudes. For instance, recent analyses of the lunar variations at Singapore, Ibadan and Bombay have indicated non-agreement in the phase of the variation at stations having the same geomagnetic latitudes.

Rastogi (1961) investigated this point by studying lunar variations in the midday critical frequency of the F_2 layer during November 1952 to October 1956 at Leopoldville (Geom. lat. = 8.1^0S). He found that the lunar variation at Leopoldville was totally out of phase with that at Madras (Geom. lat. = 8.1^0N). The phase of the lunar variation at Leopoldville (Mag. lat. = 18^0S) was, however, very nearly the same as that at Ahmedabad (Mag. lat. = 18^0N). This suggested that the stations having the same magnetic latitude rather than the same geomagnetic latitude experienced similar variation of f_0F_2.

In an extensive analysis of the phase and amplitude of f_0F_2 lunar variations, Rastogi (1961) compared the data from 10 stations within about $\pm 40^0$ latitude during a period of low sunspot activity. From Figure 1 it is seen that the change-over from the equatorial type, with the phase occurring at 04 lunar hour, to the high-latitude one, with the phase at 10 lunar hour, takes place near $\pm 11^0$ magnetic latitude.

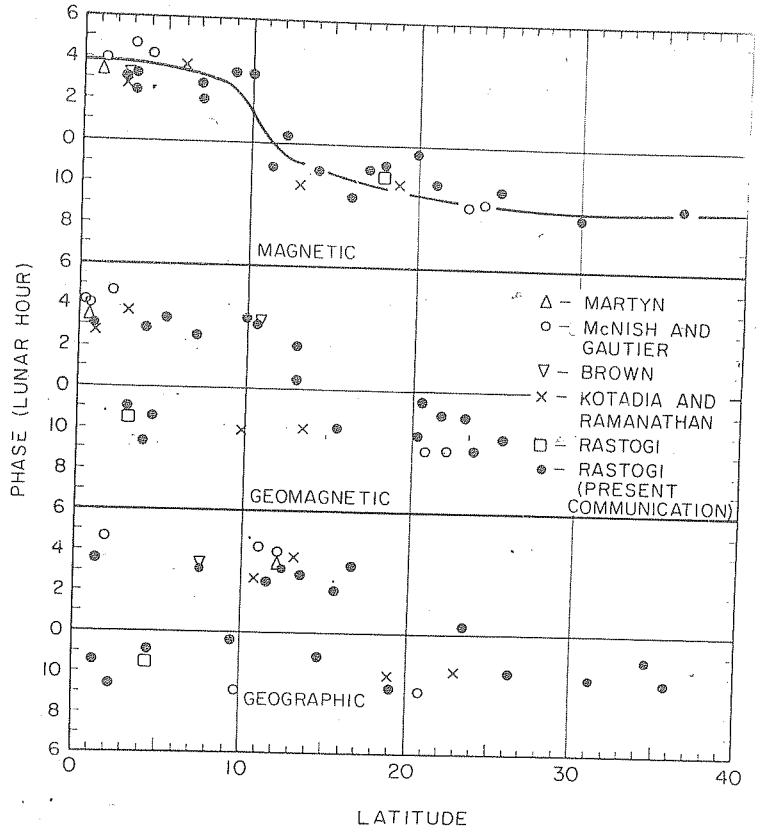


Fig. 1

Figure 1 shows that the semi-diurnal amplitude has a sharp maximum on the magnetic equator, and two broad maxima at about $\pm$ 20° magnetic latitude, which are closely associated with the maxima in the variation of mean f_0F_2 with latitude.

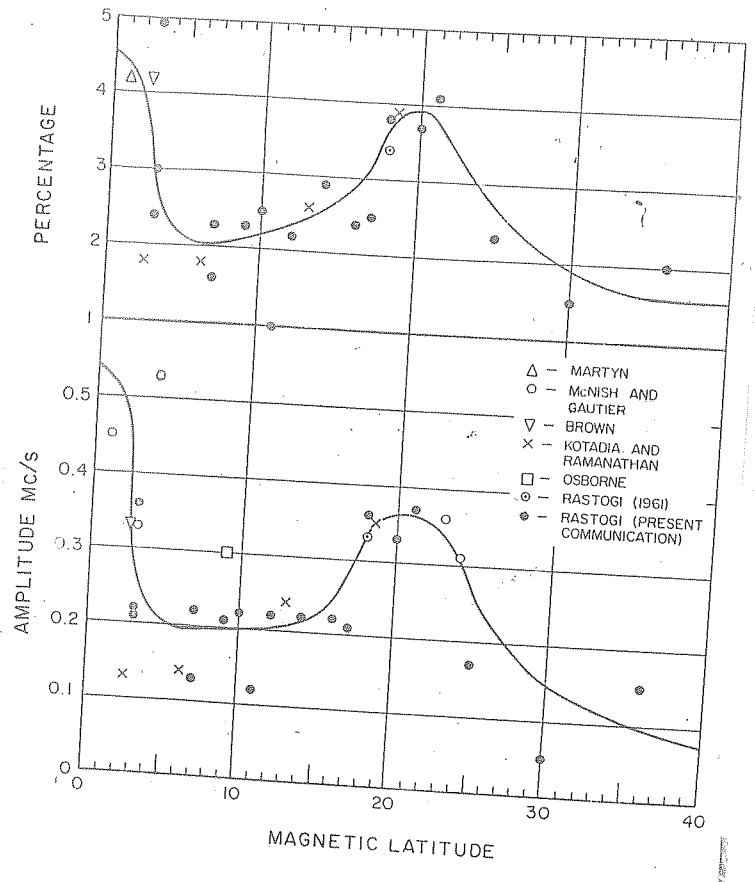


Fig. 8

He concluded that the phase was dependent on the magnetic latitude and not on the geomagnetic or the geographic latitude as seen from Figure 1.

Rastogi (1962) showed longitudinal dependence of the lunar semi-diurnal variations in the midday F_2 and h_pF_2

characteristics during 1957-58 for the two chains of equatorial stations in South America (Chimbote, Huancayo, Chiclayo and Talara) and India (Trivandrum, Kodaikanal, Tiruchirapalli and Madras). The amplitude of the semi-diurnal lunar variation in f_0F_2 showed a sharp maximum over the magnetic equator for both the zones. However, the maximum amplitude in the South American zone was about 0.60 Mc/s while in the Indian zone it was only about 0.33 Mc/s.

To understand the lunar variations in f_0F_2 at low latitudes and their interrelations with the development of the abnormal equatorial belt of the F_2 region, Rastogi (1960) selected three low latitude stations, viz. Panama, Huancayo and Buenos Aires, all in the same longitudinal zone. From the analysis of their data during the period 1956-58 he concluded that the lunar perturbation in f_0F_2 at low latitudes was closely associated with the diurnal development of the anomalous equatorial belt of the F_2 region. Again the large amplitudes of the lunar tide in f_0F_2 at tropical latitudes were associated with processes which are responsible for higher values of f_0F_2 at these latitudes during the afternoon hours.

In the light of these investigations it was thought worthwhile to undertake a detailed study of the behaviour of the semidiurnal lunar tides in f_0F_2 at Ahmedabad (a northern tropical latitude station), Panama (also a northern

tropical latitude station), Huancayo (an equatorial station) and Buenos Aires (a southern tropical latitude station). The results of this study will be presented in the following two chapters.

Martyn	1947	(Part I). Proc.Roy.Soc. A, 190, 241.
Chapman and Bartels	1940	Geomagnetism, Clarendon Press, Oxford.
Chapman and Miller	1940	Mon.Not.Roy.Ast.Soc. Geophys. Suppl., 4.
Yabsley	1940	Aust.J.Sci.Res. A, 3, 1 - 33.
Chapman	1952	Aust.J.Sci.Res. A, 5, 318 - 328.
Bartels and Fanselau	1937	Zeit.Geophysik, 13, 821 - 838.
Appleton and Weekes	1939	Proc.Roy.Soc. A, 171 - 197.
Martyn	1947	(Part II). Proc.Roy.Soc. A, 190, 370 - 388.
Martyn	1948	(Part III). Proc.Roy.Soc. A, 194, 429 - 444.
Mellen and Gautier	1949(a)	J.Geophys.Res., 54, 101 - 125.
Mellen and Gautier	1949(b)	J.Geophys.Res., 54, 303 - 304.
Osborne	1952	Nature, 169, 661 - 662.
Durrant	1951	J.Atmosph.Terr.Phys., 1, 349 - 352.
Rotadia and Ramanathan	1950	Proc.Ind.Acad.Sci., 43, 324 - 330.
Duncan	1950	Aust.J.Phys., 9, 119 - 136.
Brown	1956	J.Atmosph.Terr.Phys., 9, 144 - 154.
Rastogi	1961(a)	Nature, 190, No.4780, 214 - 216.
Rastogi	1961(b)	J.Atmosph.Terr.Phys., 22, 300 - 307.
Rastogi	1960	J.Res. NBS - D. Radio Propagation, Vol. 64D, No.5, 601 - 606.
Rastogi	1963	J.Geophys.Res., Vol. 68, 1166 - 1168.

ooo 0 ooo

Contents

CHAPTER 2

		Page
1.	Treatment of the data	1
2.	Variation with solar time of the semi-diurnal lunar tide in $f_0 J_2$ during equinoxes, winter and summer	2
3.	Secular variation of the semi-diurnal lunar tide in $f_0 J_2$ and $h_2 J_2$	10
	Appendix	13

CHAPTER 2

LUNAR TIDAL VARIATIONS IN THE F_2 LAYER OF THE IONOSPHERE OVER AHMEDABAD

1. Treatment of the data

The data used for the present analysis cover three years from March 1953 to February 1956, a period of low sunspot activity. The data of f_0F_2 and h_pF_2 were first divided into eight solar hours each of three hours duration. They were centred around 00, 03, 06, 09, 12, 15, 18 and 21 hours. The average over the three hours of, say, the 12 hour group was taken to represent the value (of f_0F_2 or h_pF_2) for that group. Deviations of f_0F_2 and h_pF_2 at these hours were then computed from their monthly mean values. Values of f_0F_2 and the corresponding h_pF_2 which were obviously affected by magnetic storms in progress at that time were discarded. To reduce the scatter of points in the average curve, any hourly deviation of f_0F_2 and h_pF_2 exceeding 20 % of its corresponding monthly mean value was assumed to be due to some unknown and random cause other than lunar tidal effect and was not included in computing the average curve. The rest of the data were then treated according to Chapman and Miller's method, described in the previous chapter, to find the amplitude and phase of the lunar tide in f_0F_2 and h_pF_2.

The analysis includes probable errors and these are shown by circles on harmonic dials. The probable error formulae are appended at the end of the chapter.

2. Variation with solar time of the semi-diurnal lunar tide in E_0F_2 during equinoxes, winter and summer

Figure 1 shows the variation with solar hour of the semi-diurnal component of the lunar tide in E_0F_2 in each season separately. Each curve represents a particular solar hour group of three hours each. The dashed lines are the smooth sine curves determined from a Fourier analysis. The most prominent feature brought out in this figure is the appreciable amplitude of the lunar tide during the sun-lit hours, particularly between 00 to 12 solar hours, irrespective of the season. During night-time and early morning hours the effect of the tide was almost negligible. These results are summarized in Table I. It is seen that during both the equinoxes and the winter (December solstice) the amplitude of the E_0F_2 lunar tide attained its maximum of 0.50 Mc/s near 12 solar hours, while in summer (June solstice) the maximum amplitude was only 0.32 Mc/s and occurred at 15 solar hour. The maximum phases during the equinoxes, winter and summer were 0.0, 10.0 and 11.7 lunar hours respectively. Percentage-wise,

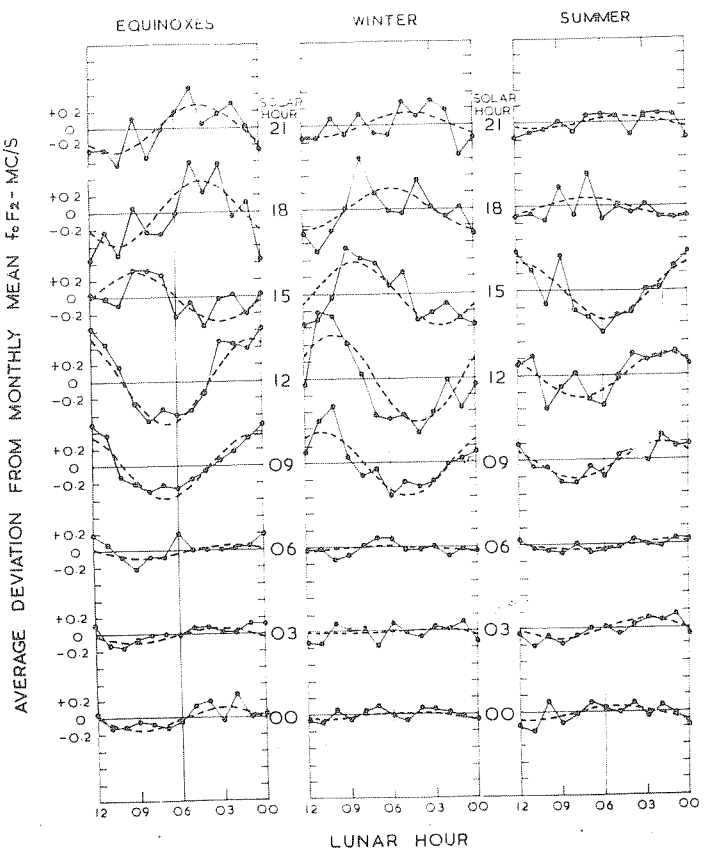


Fig. 1

the semi-diurnal E_0F_2 tide was 4.4 %, 5.0 % and 3.3 % during equinoxes, winter and summer respectively.

Figure 2 shows how the vector representing the amplitude and phase of the E_0F_2 lunar tide rotates on the harmonic dials. It may be noted that during the June

Point	Average E-W m/s	Amplitude ± m/s	Phase of max. hours	Average N-S m/s	Amplitude ± m/s	Phase of max. hours	Average Amplitude ± m/s	Phase of max. hours	Average Amplitude ± m/s	Phase of max. hours
0001	5.68	0.43 ±1	15.00	6.63	0.00 ±1	15.00	6.63	0.00 ±1	6.63	0.00 ±1
0002	5.63	0.43 ±1	15.00	6.43	0.00 ±1	15.00	6.43	0.00 ±1	6.43	0.00 ±1
0003	5.68	0.43 ±1	15.00	6.57	0.00 ±1	15.00	6.57	0.00 ±1	6.57	0.00 ±1
0004	5.67	0.43 ±1	15.00	6.63	0.00 ±1	15.00	6.63	0.00 ±1	6.63	0.00 ±1
0005	11.29	0.43 ±1	15.00	12.77	0.00 ±1	15.00	12.77	0.00 ±1	12.77	0.00 ±1
0006	5.68	0.43 ±1	15.00	6.63	0.00 ±1	15.00	6.63	0.00 ±1	6.63	0.00 ±1
0007	5.68	0.43 ±1	15.00	6.63	0.00 ±1	15.00	6.63	0.00 ±1	6.63	0.00 ±1
0008	5.68	0.43 ±1	15.00	6.63	0.00 ±1	15.00	6.63	0.00 ±1	6.63	0.00 ±1
0009	5.68	0.43 ±1	15.00	6.63	0.00 ±1	15.00	6.63	0.00 ±1	6.63	0.00 ±1
0010	5.68	0.43 ±1	15.00	6.63	0.00 ±1	15.00	6.63	0.00 ±1	6.63	0.00 ±1
0011	5.68	0.43 ±1	15.00	6.63	0.00 ±1	15.00	6.63	0.00 ±1	6.63	0.00 ±1
0012	5.68	0.43 ±1	15.00	6.63	0.00 ±1	15.00	6.63	0.00 ±1	6.63	0.00 ±1
0013	5.68	0.43 ±1	15.00	6.63	0.00 ±1	15.00	6.63	0.00 ±1	6.63	0.00 ±1
0014	5.68	0.43 ±1	15.00	6.63	0.00 ±1	15.00	6.63	0.00 ±1	6.63	0.00 ±1
0015	5.68	0.43 ±1	15.00	6.63	0.00 ±1	15.00	6.63	0.00 ±1	6.63	0.00 ±1
0016	5.68	0.43 ±1	15.00	6.63	0.00 ±1	15.00	6.63	0.00 ±1	6.63	0.00 ±1
0017	5.68	0.43 ±1	15.00	6.63	0.00 ±1	15.00	6.63	0.00 ±1	6.63	0.00 ±1
0018	5.68	0.43 ±1	15.00	6.63	0.00 ±1	15.00	6.63	0.00 ±1	6.63	0.00 ±1
0019	5.68	0.43 ±1	15.00	6.63	0.00 ±1	15.00	6.63	0.00 ±1	6.63	0.00 ±1
0020	5.68	0.43 ±1	15.00	6.63	0.00 ±1	15.00	6.63	0.00 ±1	6.63	0.00 ±1
0021	5.68	0.43 ±1	15.00	6.63	0.00 ±1	15.00	6.63	0.00 ±1	6.63	0.00 ±1
0022	5.68	0.43 ±1	15.00	6.63	0.00 ±1	15.00	6.63	0.00 ±1	6.63	0.00 ±1
0023	5.68	0.43 ±1	15.00	6.63	0.00 ±1	15.00	6.63	0.00 ±1	6.63	0.00 ±1
0024	5.68	0.43 ±1	15.00	6.63	0.00 ±1	15.00	6.63	0.00 ±1	6.63	0.00 ±1
0025	5.68	0.43 ±1	15.00	6.63	0.00 ±1	15.00	6.63	0.00 ±1	6.63	0.00 ±1
0026	5.68	0.43 ±1	15.00	6.63	0.00 ±1	15.00	6.63	0.00 ±1	6.63	0.00 ±1
0027	5.68	0.43 ±1	15.00	6.63	0.00 ±1	15.00	6.63	0.00 ±1	6.63	0.00 ±1
0028	5.68	0.43 ±1	15.00	6.63	0.00 ±1	15.00	6.63	0.00 ±1	6.63	0.00 ±1
0029	5.68	0.43 ±1	15.00	6.63	0.00 ±1	15.00	6.63	0.00 ±1	6.63	0.00 ±1
0030	5.68	0.43 ±1	15.00	6.63	0.00 ±1	15.00	6.63	0.00 ±1	6.63	0.00 ±1
0031	5.68	0.43 ±1	15.00	6.63	0.00 ±1	15.00	6.63	0.00 ±1	6.63	0.00 ±1
0032	5.68	0.43 ±1	15.00	6.63	0.00 ±1	15.00	6.63	0.00 ±1	6.63	0.00 ±1
0033	5.68	0.43 ±1	15.00	6.63	0.00 ±1	15.00	6.63	0.00 ±1	6.63	0.00 ±1
0034	5.68	0.43 ±1	15.00	6.63	0.00 ±1	15.00	6.63	0.00 ±1	6.63	0.00 ±1
0035	5.68	0.43 ±1	15.00	6.63	0.00 ±1	15.00	6.63	0.00 ±1	6.63	0.00 ±1
0036	5.68	0.43 ±1	15.00	6.63	0.00 ±1	15.00	6.63	0.00 ±1	6.63	0.00 ±1
0037	5.68	0.43 ±1	15.00	6.63	0.00 ±1	15.00	6.63	0.00 ±1	6.63	0.00 ±1
0038	5.68	0.43 ±1	15.00	6.63	0.00 ±1	15.00	6.63	0.00 ±1	6.63	0.00 ±1
0039	5.68	0.43 ±1	15.00	6.63	0.00 ±1	15.00	6.63	0.00 ±1	6.63	0.00 ±1
0040	5.68	0.43 ±1	15.00	6.63	0.00 ±1	15.00	6.63	0.00 ±1	6.63	0.00 ±1
0041	5.68	0.43 ±1	15.00	6.63	0.00 ±1	15.00	6.63	0.00 ±1	6.63	0.00 ±1
0042	5.68	0.43 ±1	15.00	6.63	0.00 ±1	15.00	6.63	0.00 ±1	6.63	0.00 ±1
0043	5.68	0.43 ±1	15.00	6.63	0.00 ±1	15.00	6.63	0.00 ±1	6.63	0.00 ±1
0044	5.68	0.43 ±1	15.00	6.63	0.00 ±1	15.00	6.63	0.00 ±1	6.63	0.00 ±1
0045	5.68	0.43 ±1	15.00	6.63	0.00 ±1	15.00	6.63	0.00 ±1	6.63	0.00 ±1
0046	5.68	0.43 ±1	15.00	6.63	0.00 ±1	15.00	6.63	0.00 ±1	6.63	0.00 ±1
0047	5.68	0.43 ±1	15.00	6.63	0.00 ±1	15.00	6.63	0.00 ±1	6.63	0.00 ±1
0048	5.68	0.43 ±1	15.00	6.63	0.00 ±1	15.00	6.63	0.00 ±1	6.63	0.00 ±1
0049	5.68	0.43 ±1	15.00	6.63	0.00 ±1	15.00	6.63	0.00 ±1	6.63	0.00 ±1
0050	5.68	0.43 ±1	15.00	6.63	0.00 ±1	15.00	6.63	0.00 ±1	6.63	0.00 ±1
0051	5.68	0.43 ±1	15.00	6.63	0.00 ±1	15.00	6.63	0.00 ±1	6.63	0.00 ±1
0052	5.68	0.43 ±1	15.00	6.63	0.00 ±1	15.00	6.63	0.00 ±1	6.63	0.00 ±1
0053	5.68	0.43 ±1	15.00	6.63	0.00 ±1	15.00	6.63	0.00 ±1	6.63	0.00 ±1
0054	5.68	0.43 ±1	15.00	6.63	0.00 ±1	15.00	6.63	0.00 ±1	6.63	0.00 ±1
0055	5.68	0.43 ±1	15.00	6.63	0.00 ±1	15.00	6.63	0.00 ±1	6.63	0.00 ±1
0056	5.68	0.43 ±1	15.00	6.63	0.00 ±1	15.00	6.63	0.00 ±1	6.63	0.00 ±1
0057	5.68	0.43 ±1	15.00	6.63	0.00 ±1	15.00	6.63	0.00 ±1	6.63	0.00 ±1
0058	5.68	0.43 ±1	15.00	6.63	0.00 ±1	15.00	6.63	0.00 ±1	6.63	0.00 ±1
0059	5.68	0.43 ±1	15.00	6.63	0.00 ±1	15.00	6.63	0.00 ±1	6.63	0.00 ±1
0060	5.68	0.43 ±1	15.00	6.63	0.00 ±1	15.00	6.63	0.00 ±1	6.63	0.00 ±1
0061	5.68	0.43 ±1	15.00	6.63	0.00 ±1	15.00	6.63	0.00 ±1	6.63	0.00 ±1
0062	5.68	0.43 ±1	15.00	6.63	0.00 ±1	15.00	6.63	0.00 ±1	6.63	0.00 ±1
0063	5.68	0.43 ±1	15.00	6.63	0.00 ±1	15.00	6.63	0.00 ±1	6.63	0.00 ±1
0064	5.68	0.43 ±1	15.00	6.63	0.00 ±1	15.00	6.63	0.00 ±1	6.63	0.00 ±1
0065	5.68	0.43 ±1	15.00	6.63	0.00 ±1	15.00	6.63	0.00 ±1	6.63	0.00 ±1
0066	5.68	0.43 ±1	15.00	6.63	0.00 ±1	15.00	6.63	0.00 ±1	6.63	0.00 ±1
0067	5.68	0.43 ±1	15.00	6.63	0.00 ±1	15.00	6.63	0.00 ±1	6.63	0.00 ±1
0068	5.68	0.43 ±1	15.00	6.63	0.00 ±1	15.00	6.63	0.00 ±1	6.63	0.00 ±1
0069	5.68	0.43 ±1	15.00	6.63	0.00 ±1	15.00	6.63	0.00 ±1	6.63	0.00 ±1
0070	5.68	0.43 ±1	15.00	6.63	0.00 ±1	15.00	6.63	0.00 ±1	6.63	0.00 ±1
0071	5.68	0.43 ±1	15.00	6.63	0.00 ±1	15.00	6.63	0.00 ±1	6.63	0.00 ±1
0072	5.68	0.43 ±1	15.00	6.63	0.00 ±1	15.00	6.63	0.00 ±1	6.63	0.00 ±1
0073	5.68	0.43 ±1	15.00	6.63	0.00 ±1	15.00	6.63	0.00 ±1	6.63	0.00 ±1
0074	5.68	0.43 ±1	15.00	6.63	0.00 ±1	15.00	6.63	0.00 ±1	6.63	0.00 ±1
0075	5.68	0.43 ±1	15.00	6.63	0.00 ±1	15.00	6.63	0.00 ±1	6.63	0.00 ±1
0076	5.68	0.43 ±1	15.00	6.63	0.00 ±1	15.00	6.63	0.00 ±1	6.63	0.00 ±1
0077	5.68	0.43 ±1	15.00	6.63	0.00 ±1	15.00	6.63	0.00 ±1	6.63	0.00 ±1
0078	5.68	0.43 ±1	15.00	6.63	0.00 ±1	15.00	6.63	0.00 ±1	6.63	0.00 ±1
0079	5.68	0.43 ±1	15.00	6.63	0.00 ±1	15.00	6.63	0.00 ±1	6.63	0.00 ±1
0080	5.68	0.43 ±1	15.00	6.63	0.00 ±1	15.00	6.63	0.00 ±1	6.63	0.00 ±1
0081	5.68	0.43 ±1	15.00	6.63	0.00 ±1	15.00	6.63	0.00 ±1	6.63	0.00 ±1
0082	5.68	0.43 ±1	15.00	6.63	0.00 ±1	15.00	6.63	0.00 ±1	6.63	0.00 ±1
0083	5.68	0.43 ±1	15.00	6.63	0.00 ±1	15.00	6.63	0.00 ±1	6.63	0.00 ±1
0084	5.68	0.43 ±1	15.00	6.63	0.00 ±1	15.00	6.63	0.00 ±1	6.63	0.00 ±1
0085	5.68	0.43 ±1	15.00	6.63	0.00 ±1	15.00	6.63	0.00 ±1	6.63	0.00 ±1
0086	5.68	0.43 ±1	15.00	6.63	0.00 ±1	15.00	6.63	0.00 ±1	6.63	0.00 ±1
0087	5.68	0.43 ±1	15.00	6.63	0.00 ±1	15.00	6.63	0.00 ±1	6.63	0.00 ±1
0088	5.68	0.43 ±1	15.00	6.63	0.00 ±1	15.00	6.63	0.00 ±1	6.63	0.00 ±1
0089	5.68	0.43 ±1	15.00	6.63	0.00 ±1	15.00	6.63	0.00 ±1	6.63	0.00 ±1
0090	5.68	0.43 ±1	15.00	6.63	0.00 ±1	15.00	6.63	0.00 ±1	6.63	0.00 ±1
0091	5.68	0.43 ±1	15.00	6.63	0.00 ±1	15.00	6.63	0.00 ±1	6.63	0.00 ±1
0092	5.68	0.43 ±1	15.00	6.63	0.00 ±1	15.00	6.63	0.00 ±1	6.63	0.00 ±1
0093	5.68	0.43 ±1	15.00	6.63	0.00 ±1	15.00	6.63	0.00 ±1	6.63	0.00 ±1
0094	5.68	0.43 ±1	15.00	6.63	0.00 ±1	15.00	6.63	0.00 ±1	6.63	0.00 ±1
0095	5.68	0.43 ±1	15.00	6.63	0.00 ±1	15.00	6.63	0.00 ±1	6.63	0.00 ±1
0096	5.68	0.43 ±1	15.00	6.63	0.00 ±1	15.00	6.63	0.00 ±1	6.63	0.00 ±1
0097	5.68	0.43 ±1	15.00	6.63	0.00 ±1	15.00	6.63	0.00 ±1	6.63	0.00 ±1
0098	5.68	0.43 ±1	15.00	6.63	0.00 ±1	15.00	6.63	0.00 ±1	6.63	0.00 ±1
0099	5.68	0.43 ±1	15.00	6.63	0.00 ±1	15.00	6.63	0.00 ±1	6.63	0.00 ±1
0100	5.68	0.43 ±1	15.00	6.63	0.00 ±1	15.00	6.63	0.00 ±1	6.63	0.00 ±1

solstice the maximum phase of the semi-diurnal component between 00 to 12 hours appeared around 08 lunar hour. This was unexpected in the case of a tropical latitude station like Ahmedabad. In all the seasons the vector rotated in the anti-clockwise direction. The sizes of the probable error circles clearly indicate that the F_0F_2 tide around 00, 08 and 06 solar hour groups are insignificant in all the three seasons. In both summer and winter,

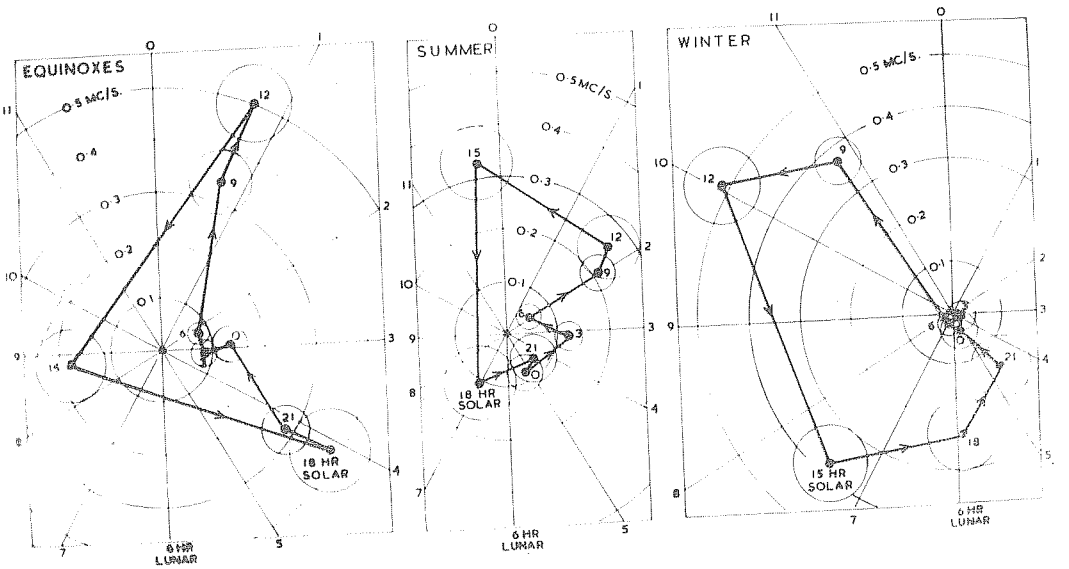
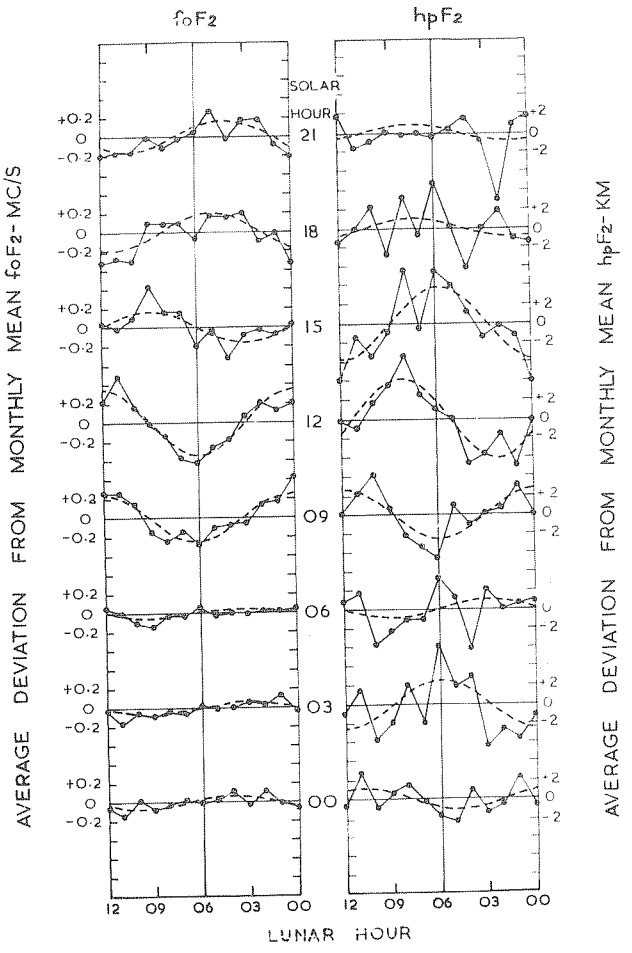


Fig. 2

the tide at 21 hours was negligible; but at the same time during the equinoxes, however, it was significantly larger.

Going back to Figure 1, if we consider any given solar hour group it is seen that the phases of the f_0F_2 tide do not vary much from each other in all the three seasons. Taking this fact into account a consolidated picture of the diurnal behaviour of the f_0F_2 lunar tide, averaged over all the three seasons, is presented in Figure 3. A similar picture of the lunar tide in the height of maximum electron density of the F_2 layer, h_pF_2, is also shown alongside. Evidently the f_0F_2 tide was significant during the period from 00 to 21 solar hours. Though the h_pF_2 deviations showed more scatter throughout the solar day it is clear that the h_pF_2 tide was also significant only during the daytime. From the harmonic dials in Figure 4 it is seen that the maximum amplitude of the f_0F_2 lunar tide occurred at 12 solar hours with its magnitude and phase 0.34 Mc/s and 11.7 lunar hours. The maximum h_pF_2 tide of 4.2 Km or 1.0% also occurred at 12 solar hours with its phase at 8.3 lunar hours. Figure 4 also shows that the phase of the f_0F_2 tide changed pretty regularly in the anti-clockwise direction throughout the day. The phase of the h_pF_2 tide, on the contrary, exhibited much randomness at 00, 03, 18 and 21 solar hours. During the rest of the day, however,



it moved in the anti-clockwise direction. From Figure 4(a) it should be noted that the phase of the f_0F_2 tide lagged behind that of the h_pF_2 tide except for the solar hours 00, 18 and 15. These results are summarised in Table II. In addition it also shows the diurnal component, P_1, of both the f_0F_2 and the h_pF_2 lunar tides. Most of the time P_1 is seen to be quite insignificant and irregular.









Fig. 4

In Figure 5 the diurnal variation of the f_0J_2 lunar tide is compared with the diurnal behaviour of f_0J_2 itself. The abscissa shows time in solar hours. Curve A represents the variation of f_0J_2 and curve B and C show the variation of the semi-diurnal component of the lunar tide in f_0J_2 expressed in No/s and percentages respectively. The vertical lines on the curve B indicate

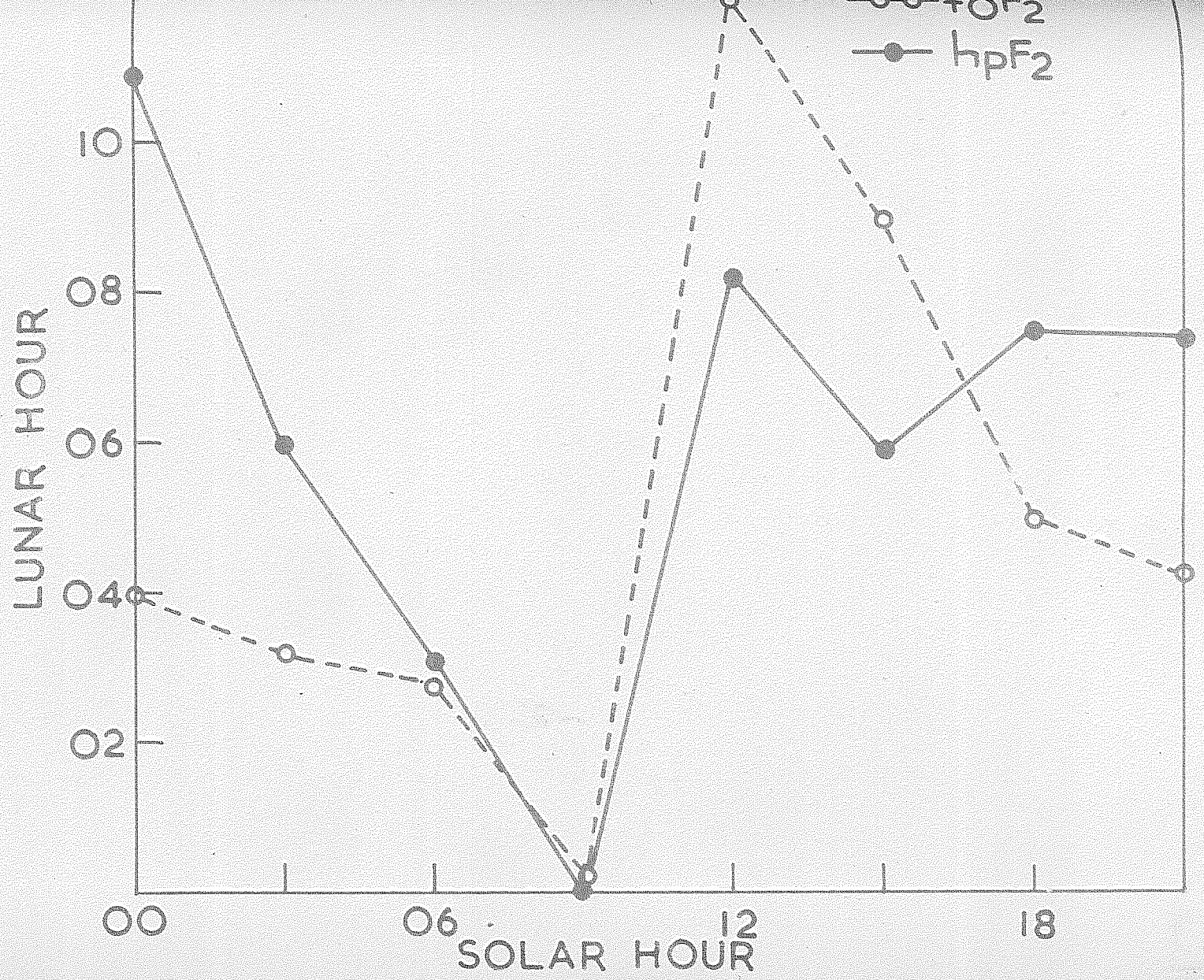


FIG. 4(a)

AMPLITUDE OF LUNAR TIDE f_0F_2

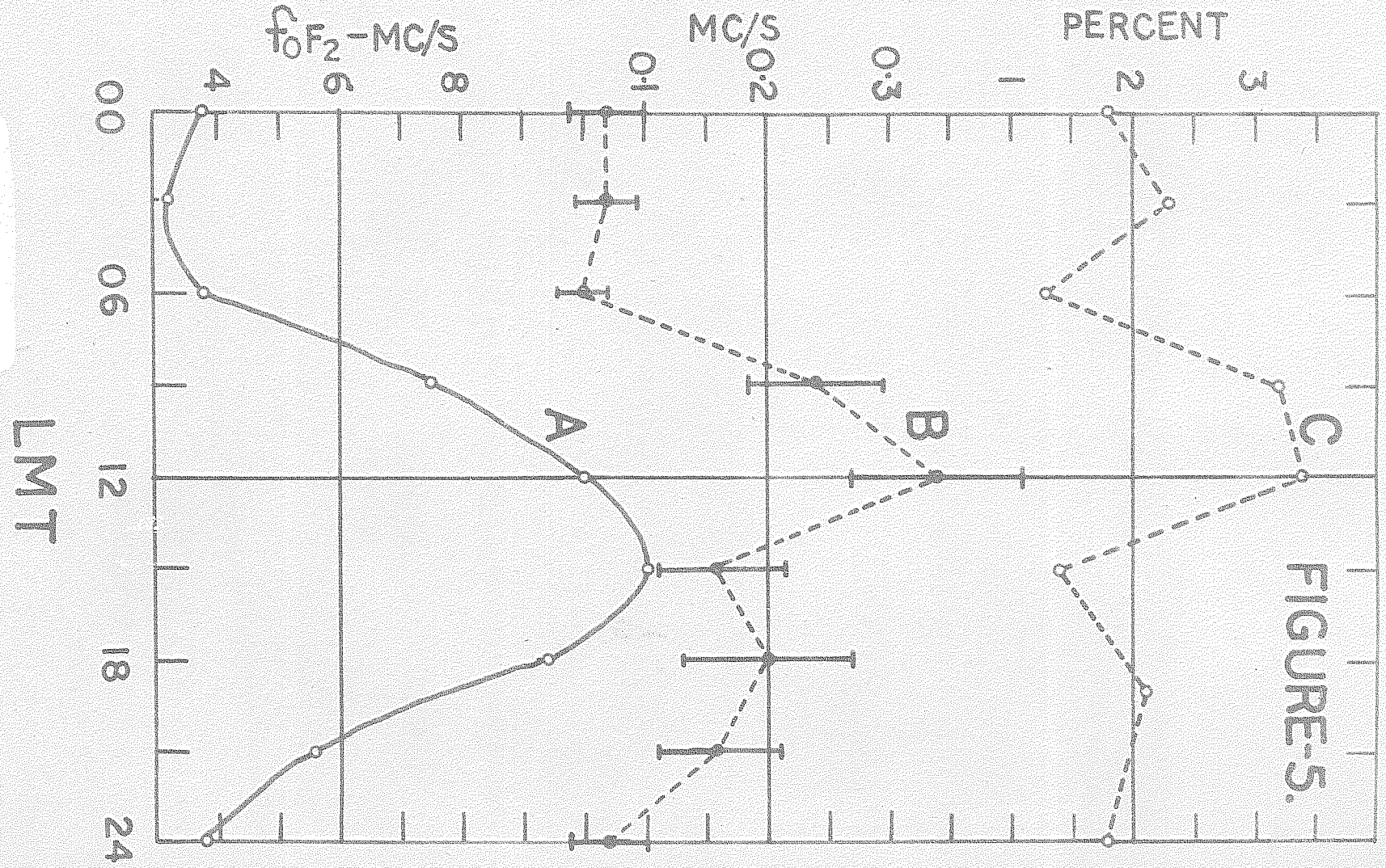


FIGURE 5.

Solar hour.	AMPLITUDE AND PHASE OF YEARLY AVERAGE h_0P_2 Average h_0P_2 Mc/s	P_1 Mc/s	t_1 Lunar hour.	P_2 Mc/s	β	t_2 Lunar hour.	AMPLITUDE AND PHASE OF YEARLY h_2P_2 Average h_2P_2 MS	P_1 MS	t_1 Lunar hour.	P_2 MS	β	t_2 Lunar hour.
2300												
0000	3.75	0.01	3.4	0.07	1.79	4.0	337	2.09	1.40	1.13	0.34	10.9
0100				±0.02								
0200												
0300	3.19	0.02	1.5	0.07	2.29	3.2	287	3.74	6.10	2.51	0.85	6.0
0400				±0.02								
0500												
0600	3.83	0.07	4.3	0.05	1.30	2.3	336	0.48	9.40	0.01	0.32	3.1
0700				±0.01								
0800												
0900	7.50	0.15	6.3	0.24	3.20	0.2	287	1.73	0.10	3.30	0.93	0
1000				±0.09								
1100												
1200	9.31	0.01	4.6	0.24	3.43	11.7	330	2.22	0.90	4.20	1.24	8.3
1300				±0.04								
1400												
1500	11.09	0.00	6.3	0.15	1.44	0.0	310	0.37	3.40	3.66	1.19	5.0
1600				±0.04								
1700												
1800	0.34	0.07	3.0	0.30	2.10	5.1	276	2.13	6.00	0.92	0.33	7.5
1900				±0.04								
2000												
2100	5.52	0.09	8.9	0.16	2.30	4.3	300	0.53	6.00	0.32	0.27	7.4
2200				±0.03								

the probable errors involved. It is seen that though the maximum of f_0F_2 occurred around 15 hour group, the maximum tide took place around 18 hour group. Again the tide in percentage was quite significant even at 21 hour when the value of f_0F_2 was comptively low.

3. Seasonal variation of the semi-diurnal lunar tide in f_0F_2 and h_pF_2

It is worthwhile to see the behaviour of the tides in f_0F_2 and h_pF_2 in different seasons averaged over all solar hours. Figure 6 shows the seasonal behaviour of the f_0F_2 and h_pF_2 tides together with their annual averages. The f_0F_2 tides in winter and equinoxes had nearly equal amplitudes but were almost in phase opposition. It is therefore the summer tide which is mostly responsible for determining the annual average tide in f_0F_2 with an amplitude of 0.05 Mc/s and phase 1.6 lunar hours. It may be worth recalling some earlier work in this context. Ikral (1956) and Rossolance and Klein (1960) computed the semi-diurnal lunar tide in f_0F_2 at Calcutta and Leopoldville respectively. The all-day annual average tide had phase of 6.0 and 6.8 lunar hours respectively. In contrast, Rastogi (1961) got 10.6 lunar hours as the phase of the annual average lunar tide in mid-day f_0F_2 at Leopoldville. This latter value of the phase is expected for a tropical latitude station. Thus it would appear desirable to compute the

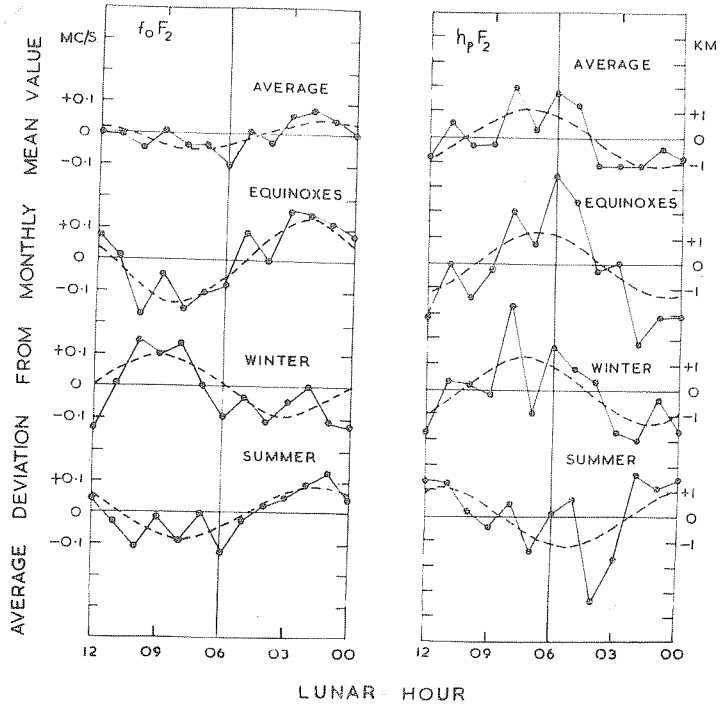


Fig. 6

annual average tides around a specific hour only, preferably midday, and not for all the solar hours. In the case of h_pF_2, the lunar tides in the equinoxes and winter possess nearly the same amplitudes occurring at almost the same lunar hour. The tide in summer, on

the other hand, has a very different phase. The average h_pF_2 lunar tide, therefore, had an amplitude of 1.20 km at 7.3 lunar hours. These results are summarized in Table III.

Table III

	f_0F_2			h_pF_2		
Season	Average f_0F_2 Mc/s	P_2 in Mc/s	t_1 Time of max. Lunar Hr	Average h_pF_2 Km	P_2 in Km	t_2 Time of max. Lunar Hr
Equinoxes	7.20	0.14	2.2	304	1.27	6.3
Summer	6.89	0.03	1.7	324	1.17	11.3
Winter	6.21	0.00	0.0	282	1.30	7.4
Average	6.87	0.05	1.3	305	1.25	7.3

APPENDIX

FORMULA FOR PROBABLE ERRORS OF AMPLITUDE AND PHASE

Standard procedures as given by Whittaker and Robinson (1944) were used. The lunar semi-diurnal wave (period of 12 lunar hours) is given by

$$R \sin\left(\frac{\pi t}{6} + \alpha\right) = a \cos(\pi t/6) + b \sin(\pi t/6)$$

where R is the amplitude, t is the time in lunar hours, α is the phase, and a and b are the cosine and sine coefficients for the 12-hour wave obtained by a Fourier analysis of the means of the $\Delta f_0 F_2$ values for each integral lunar hour. t = 0 corresponds to an upper or lower culmination of the moon at the longitude of the station.

The variances of a and b are:

$$\sigma_a^2 = (1/6)^2 \sum_{p=0}^{11} \sigma_p^2 \cos^2(\pi p/6)$$

and $$\sigma_b^2 = (1/6)^2 \sum_{p=0}^{11} \sigma_p^2 \sin^2(\pi p/6),$$

where p is the lunar hour and σ_p^2 is the variance of the mean value of $\Delta f_0 F_2$ for that hour.

For simplicity, the weighted mean variance $\bar{\sigma}^2$ for all lunar hours was substituted for σ_p^2 in the above formulae. Thus if

$$\sigma_\epsilon^2 = \left(\sum_{p=0}^{11} n_p \sigma_p^2 \right) \Big/ \sum_{p=0}^{11} n_p$$

where n_p is the number of values of $\Delta t_{o\,3}^p$ for the lunar hour p, then

$$\sigma_a^2 = (1/6)^2 \sigma_\epsilon^2 \sum_{p=0}^{11} \cos^2(\pi p/6) = \sigma_\epsilon^2/6$$

and $$\sigma_b^2 = (1/6)^2 \sigma_\epsilon^2 \sum_{p=0}^{11} \sin^2(\pi p/6) = \sigma_\epsilon^2/6$$

Then, provided that $\sigma_R << R$ the variances of R and α are given approximately by

$$\sigma_R^2 = \sigma_a^2 = \sigma_b^2 = \sigma_\epsilon^2/6$$

and $$\sigma_\alpha^2 = (\sigma_R / R)^2.$$

Assuming that R and α are normally distributed (approximately valid if $\sigma_R << R$), their probable errors are approximately

$$q_R = 0.675 \sigma_R = 0.275 \sigma$$

and $q_\alpha = q_R / R$ radians.

In lunar hours, q_α is

$$q_\alpha = (6/\pi)(q_R/R) = 1.01\, q_R / R.$$

REFERENCES

Baral	1963	J.Technol., Calcutta, 1, 175 - 177.
Bossolasco and Elena	1960	Geofisica Pura e Applicata, 46, 167 - 178.
Bastogi	1961	Nature, Vol. 190, No.4770, 214 - 215.
Whittaker and Robinson	1944	The Calculus of Observations., 4th Ed. (Blackie and Son, Ltd., London and Glasgow).

ooo 0 ooo

CONTENTS

CHAPTER 2

		Page
1.	Treatment of the data	1
2.	Lunar variations in f_0F_2 over Nairobi	2
3.	Variation of the lunar tide in f_0F_2 during December solstice, equinoxes and June solstice	2
4.	Seasonal variation of the lunar tide at 00, 06, 12 and 18 solar hours	10
5.	Lunar variations in f_0F_2 over Kisumuyo	13
6.	Variation of the lunar tide in f_0F_2 during December solstice, equinoxes and June solstice	14
7.	Seasonal variation of the lunar tide at 00, 06, 12 and 18 solar hours	21
8.	Lunar variations in f_0F_2 over Huancayo	24
9.	Variation of the lunar tide in f_0F_2 during the December solstice, equinoxes and June solstice	25
10.	Seasonal behaviour of the lunar tide around 00, 06, 12 and 18 solar hours	31
11.	The diurnal component of the lunar tide in f_0F_2	35

CHAPTER 3

LUNAR TIDAL OSCILLATIONS IN THE CRITICAL FREQUENCY f_0F_2 OF THE F_2 LAYER OF THE IONOSPHERE OVER PANAMA (9.4°N, 70.6°W), HUANCAYO (12° 02'S, 75° 20'W) AND BUENOS AIRES (34°36'S, 58° 30'W).

1. Treatment of the data

The f_0F_2 data were first arranged according to solar hours. Hourly deviations Δf_0F_2 were then computed from the monthly means for the same hours. These deviations were rearranged according to decreasing order of the phase of the moon, μ, as suggested by Chapman and Miller for determining the effect of the lunar tide. As mentioned in the previous chapter, values of the deviations of f_0F_2 during magnetic storms were omitted. Also, deviations exceeding 30 % of their respective monthly mean values of f_0F_2 were excluded. For all the three stations considered, both the quantity and quality of data were reasonably satisfactory. Average deviation curves were therefore computed for each solar hour separately. Both the diurnal as well as the semi-diurnal components of the lunar tide in f_0F_2, together with the times of their maxima (phases) were computed for all the three stations. We shall first consider the semi-diurnal component only.

The data of the three stations will be discussed one by one and the various aspects of the lunar perturbations in f_0F_2 over each of them presented.

2. Lunar variations in f_0F_2 over Panama

The data analysed refer to the low sunspot activity period 1953-55.

3. Variation of the lunar tide in f_0F_2 during December solstice, equinoxes and June solstice

The behaviour of the semi-diurnal component of the lunar tide at each solar hour was studied by grouping the hourly deviations in f_0F_2. This was done for winter, summer and equinoxes. Figure 1 shows the situation in the December solstice. The abscissae gives the lunar hour while the ordinates give the average deviations in Mc/s. There are 24 curves corresponding to the 24 solar hours. The histograms are the actual deviations in f_0F_2 around each lunar hour and the smooth curves running through them are the built-up curves computed from the 24-hourly and 12-hourly components. It is seen from this diagram that the tidal effect is significant between 08 and 20 solar hours. It is obvious that from 01 to 07 solar hours, the tide was almost negligible. The amplitude of this essentially semi-diurnal tide varied from 0.02 Mc/s or 0.6 % at 01 solar hour to a

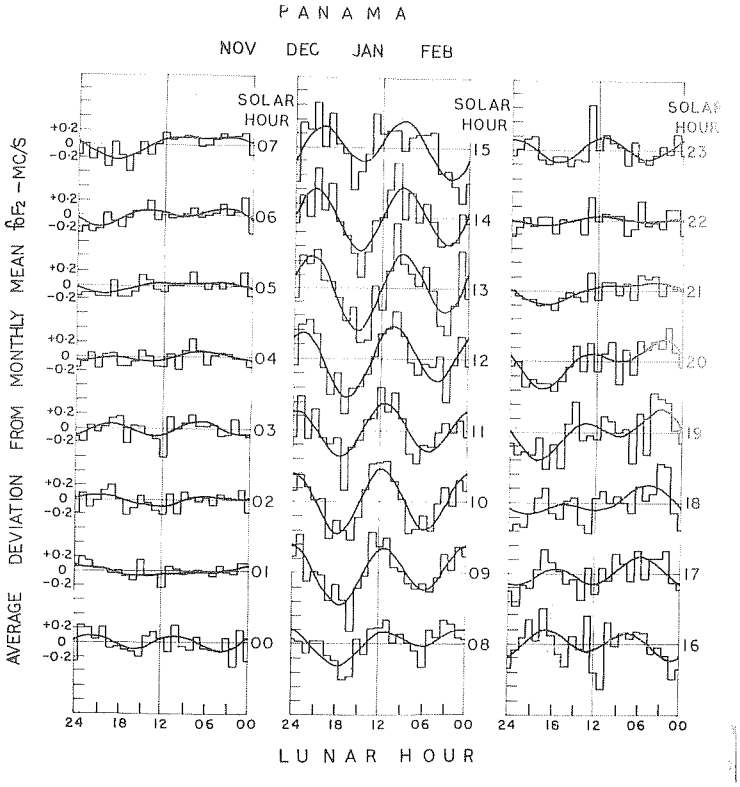


Fig. 1

maximum of 0.47 Mc/s or 6.3 % at 23 solar hour. Their corresponding phases were 10.1 and 9.4 lunar hours respectively.

During the equinoxes (Figure 2) though the tidal effect was seen almost throughout the day, it was particularly significant between 08 to about 23 solar hours.

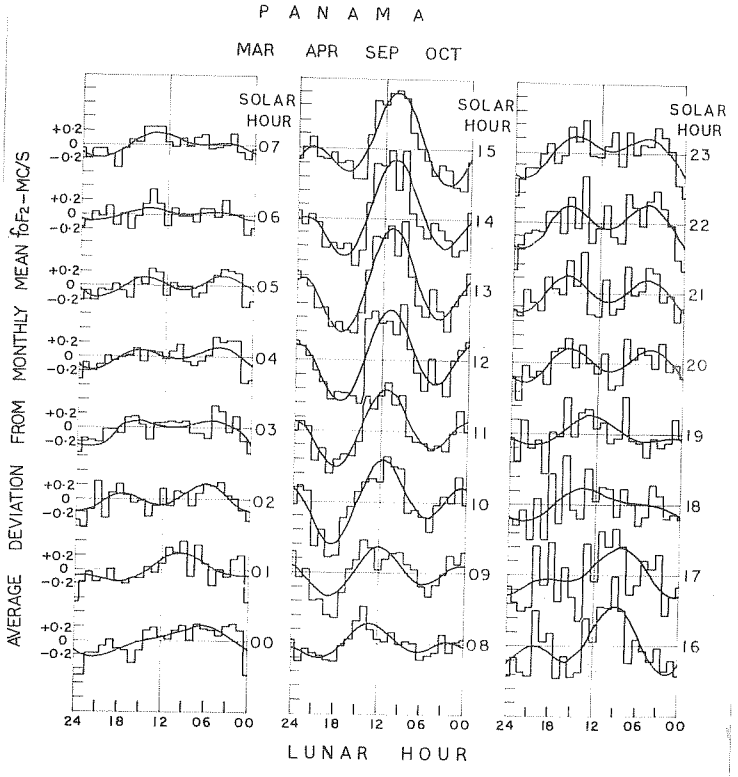


Fig. 2

The amplitude of the tide varied from a minimum of 0.06 Mc/s at 00 hour to a maximum of 0.49 Mc/s at 13 solar hour. Their respective phases were 4.5 and 11.1 lunar hours. In terms of percentage, a minimum tide of 0.9 % occurred at 18 solar hour while the maximum tide of 6.0 % occurred at 22 hour.

Figure 3 shows the behaviour of the lunar tide during the June solstice. It is seen that the tide was generally small as compared with that during the December solstice and equinoxes. The minimum tide of 0.05 Mc/s occurred at 08 solar hour while the maximum of 0.31 Mc/s happened at 16 hour, their respective phases being

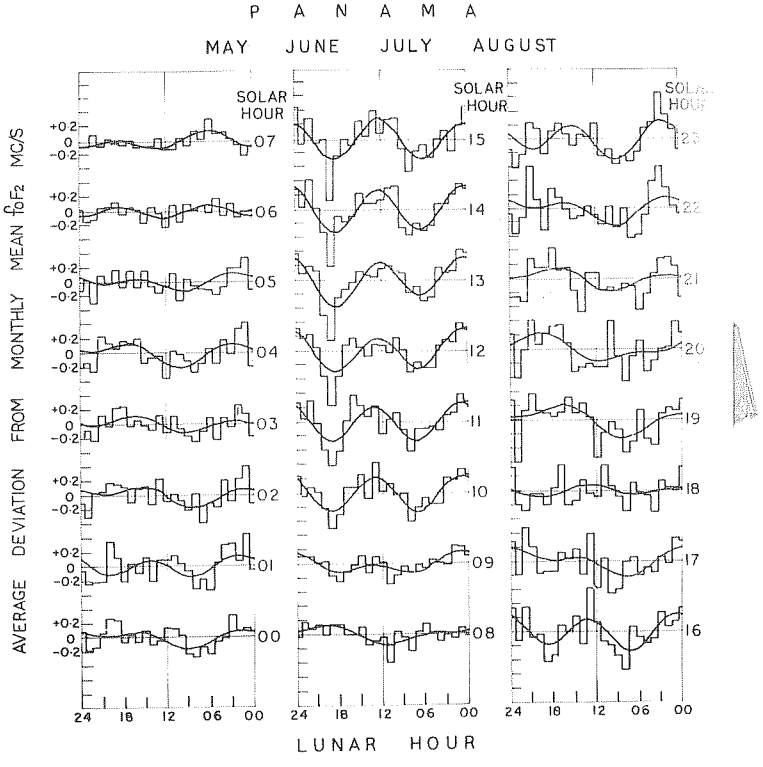
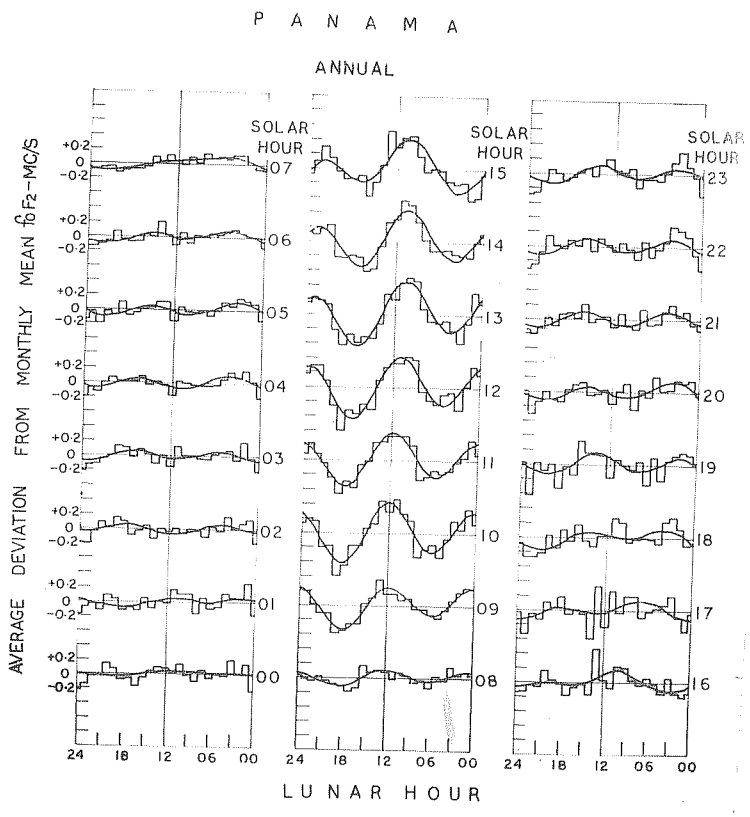


Fig. 3

0.5 and 0.00 lunar hours. In percentage, the minimum tide of 0.6 % and the maximum tide of 4.8 % occurred at 18 and 23 solar hours respectively.

A consolidated average picture of the diurnal variation of the f_0F_2 lunar tide is displayed in Figure 4.



Mo

Fig. 4

The tidal effect was more conspicuous between about 08 to 22 solar hours than for the rest of the day. The minimum tide of 0.01 Mc/s occurred at 00 solar hour and the maximum tide of 0.35 Mc/s occurred at 12 hour, their phases being 0.2 and 11.3 lunar hours respectively. The maximum percentage tide of 4.4 % took place at 10 solar hour. These results are summarised in Table I.

The diurnal behaviour of the lunar tide in f_0F_2 in the three seasons and during the whole year is shown in Figure 5 in the form of harmonic dials. The vector representing the amplitude and phase of the semi-diurnal lunar tide, rotates in the anti-clockwise direction during the December solstice and equinoxes, particularly in the daytime. The phase, during these two seasons, was regular from about 07 to about 13 solar hours. In contrast, during the June solstice, the vector was very small in magnitude and random in phase.

In Figure 6 the annual variation with solar time of the semi-diurnal lunar tide in f_0F_2 expressed in Mc/s and in percentage is shown (dotted curves) along with the corresponding f_0F_2 curve (solid curve). Though the general appearance of these curves is roughly the same, they exhibit certain differences. The maximum of the f_0F_2 curve appeared around 15 hour, whereas the tidal effect, both in Mc/s and in percentage, attained its

	Equinoxes				December Solstice				June Solstice				Annual			
Sol. Hr. t	Aver-age f_0^2 Mc/s	P_2 Mc/s	%	t_2 lunar hour. K	Aver-age f_0^2 Mc/s	P_2 Mc/s	%	t_2 lunar hour. K	Aver-age f_0^2 Mc/s	P_2 Mc/s	%	t_2 lunar hour. K	Aver-age f_0^2 Mc/s	P_2 Mc/s	%	t_2 lunar hour. K
00	4.4	0.06	1.4	4.5	3.6	0.11	3.1	10.0	5.1	0.06	1.2	1.3	4.4	0.01	0.2	0.3
01	4.3	0.07	1.6	9.9	3.3	0.02	0.6	10.1	4.8	0.12	2.5	2.1	4.1	0.04	0.9	0.3
02	3.8	0.14	3.7	5.6	3.1	0.04	1.3	7.3	4.3	0.08	1.9	2.3	3.7	0.06	1.4	5.6
03	3.1	0.08	2.9	4.4	2.7	0.10	3.7	7.1	4.0	0.06	1.5	3.7	3.3	0.06	1.8	5.2
04	2.8	0.11	3.8	4.2	2.5	0.04	1.6	6.3	3.8	0.09	2.4	4.1	3.1	0.07	2.3	4.5
05	2.7	0.15	4.4	3.5	2.5	0.03	1.2	2.5	3.4	0.07	2.1	3.1	2.9	0.07	2.4	3.2
06	3.1	0.05	1.6	3.8	2.9	0.03	1.1	3.2	3.5	0.07	2.0	3.1	3.2	0.05	1.6	4.2
07	5.3	0.08	1.5	2.2	5.3	0.06	1.1	0.7	4.9	0.09	1.9	3.4	5.1	0.03	0.6	2.5
08	6.2	0.15	2.5	1.4	6.3	0.17	2.5	0.0	5.3	0.05	0.9	0.5	6.1	0.08	1.3	0.7
09	7.2	0.24	3.3	0.4	8.0	0.35	4.7	11.7	5.8	0.09	1.6	1.3	6.9	0.24	3.5	0.2
10	8.4	0.30	4.0	0.2	8.6	0.42	4.9	11.8	6.2	0.25	4.0	1.1	7.7	0.34	4.4	0.2
11	9.4	0.36	3.8	11.7	8.8	0.33	3.8	11.5	7.1	0.25	3.5	1.2	8.4	0.30	3.6	12.0
12	10.2	0.45	4.4	11.3	8.3	0.43	4.9	10.6	8.1	0.26	3.2	0.8	9.0	0.35	3.9	11.9
13	11.0	0.48	4.5	11.1	8.3	0.47	5.3	0.4	9.0	0.29	3.2	0.6	9.6	0.34	3.5	10.8
14	11.5	0.43	3.7	10.3	8.2	0.43	4.7	0.2	9.7	0.31	3.2	0.6	10.1	0.30	3.0	10.6
15	11.8	0.30	2.6	10.2	8.2	0.25	2.3	8.7	10.1	0.23	2.7	0.5	10.4	0.25	2.4	10.3
16	11.8	0.27	2.3	9.0	8.1	0.17	1.9	7.6	10.4	0.22	2.1	1.4	10.4	0.07	0.7	9.0
17	11.8	0.16	1.4	4.7	8.4	0.16	2.0	5.0	10.2	0.10	0.9	1.3	9.9	0.03	0.3	6.9
18	9.7	0.00	0.0	3.0	8.0	0.12	1.5	4.7	9.6	0.06	0.6	1.2	9.1	0.03	0.0	3.6
19	7.5	0.10	1.3	1.2	5.3	0.21	4.0	2.5	8.4	0.00	1.1	3.4	7.1	0.12	1.7	2.4
20	6.3	0.20	3.2	4.1	4.1	0.15	4.4	2.1	7.2	0.07	0.9	7.3	5.9	0.09	1.5	3.7
21	5.4	0.21	3.9	5.0	3.5	0.05	1.4	1.7	6.3	0.03	1.2	4.6	5.0	0.10	2.0	4.5
22	4.7	0.24	5.0	5.0	3.5	0.00	0.9	0.3	5.6	0.11	1.0	3.3	4.6	0.10	2.2	4.3
23	4.4	0.19	4.3	4.7	3.6	0.13	4.2	11.6	5.3	0.22	4.2	3.2	4.4	0.10	2.3	3.1

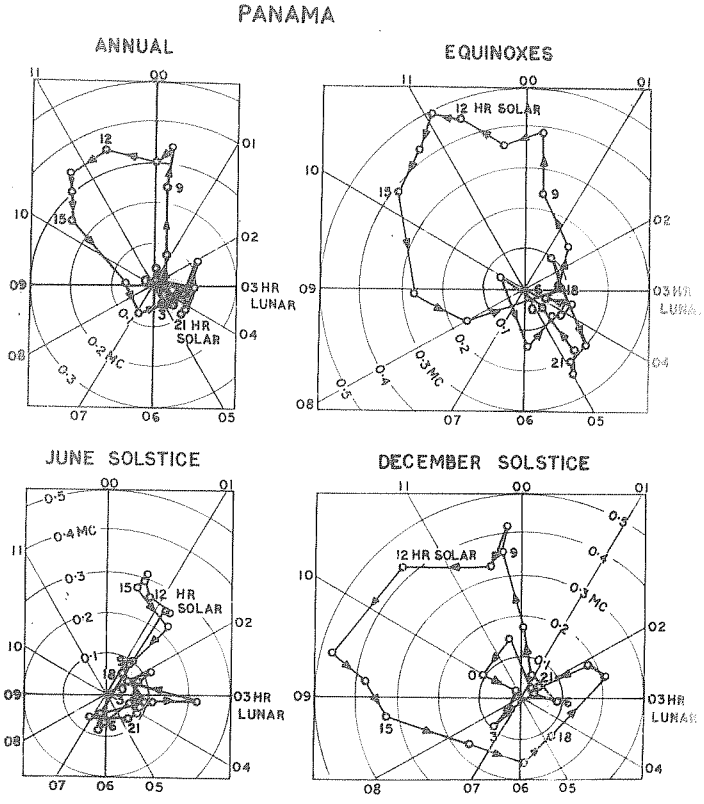


Fig. 5

maximum between 10 to 12 hours. Again, it is noteworthy that though the tide in absolute units around 05 hour was only about 0.07 Mc/s, the tide at the same time expressed in percentage was about 2.4 %. It may be noted that the F_2 - layer critical frequency itself assumed a low value of about 3.0 Mc/s at that time. For the same reason the lunar tide at 23 hour was about 3.3 % and its actual magnitude about 0.1 Mc/s.

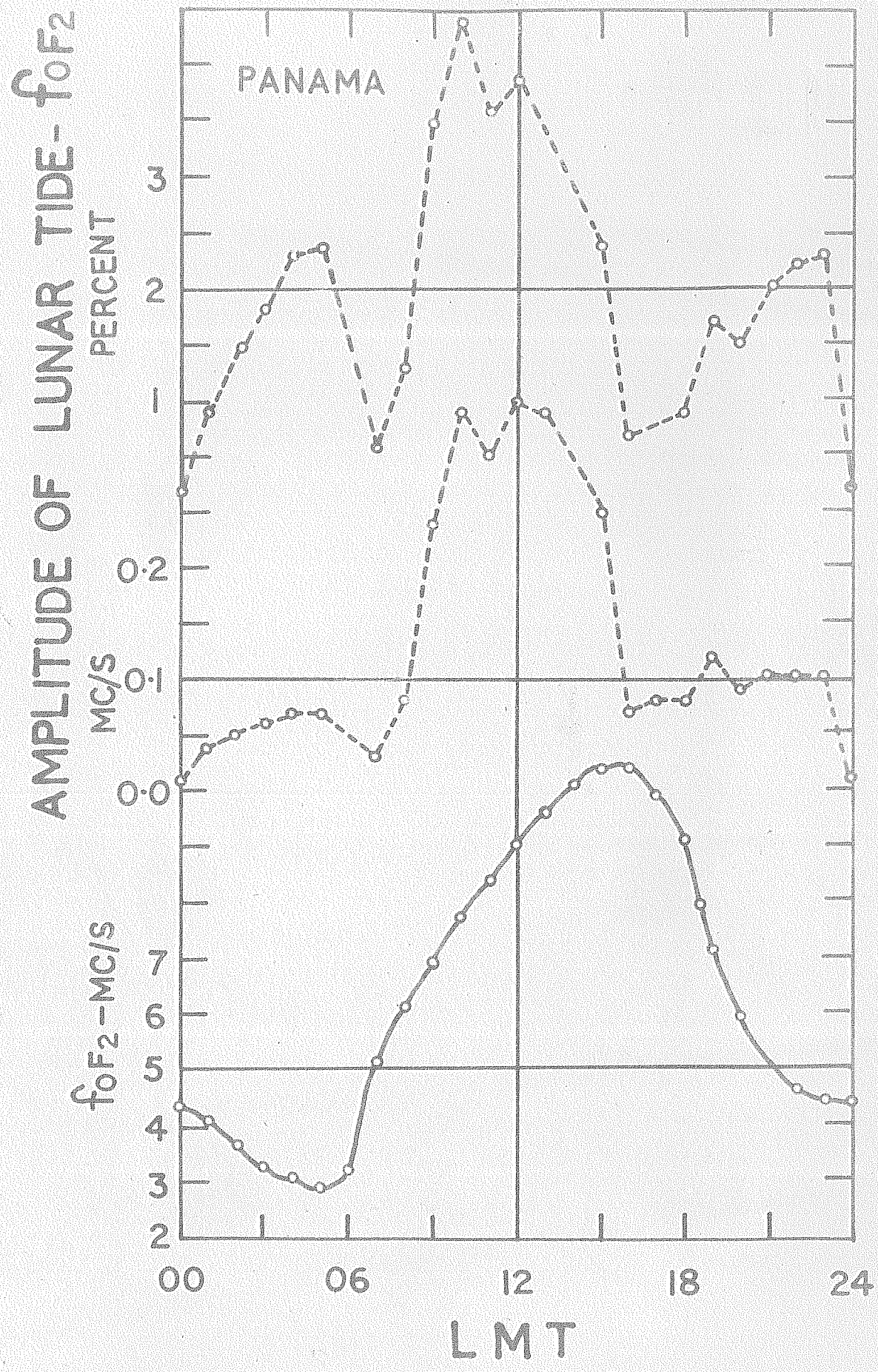

AMPLITUDE OF LUNAR TIDE- f_0F_2
PANAMA
PERCENT
MC/S
f_0F_2 - MC/S
3
2
1
0·2
0·1
0·0
7
6
5
4
3
2
00
06
12
18
24
LMT

FIG. 6

4. Seasonal variation of the lunar tide at 00, 06, 12 and 18 solar hours

The previous analysis has shown how the semi-diurnal lunar tide varied during the equinoxes and the two solstices. In order to study how the tide behaved in any given month four groups of three hours each were formed. They were one around midnight (23, 00, 01), one around sunrise (05, 06, 07), one around mid-day (11, 12, 13) and the fourth around sunset (17, 18, 19). Figure 7 shows the situation. The important features are summarised in Table II. It could be seen that almost throughout the year the tidal influence was more obvious around 12 hour group than at any other time. Again the maximum tide of 0.75 Ms/s or 8.3 β occurred around noon in the month of February with its phase at 11.3 lunar hour. The minimum tide of 0.17 Ms/s or 3.3 β around noon happened in July at 1.0 lunar hour. It is also seen from Table II that the tidal effect exhibited much more randomness in phase during the 00, 06 and 18 hour groups than during the 12 hour group. For this reason the tidal picture around noon only was returned in Figure 8 in the form of a harmonic dial. The Roman figures indicate the months. Two main groups were clearly evident, viz. the one consisting of November, December, January and February, and the other formed by May, June, July and August. The December solstitial months lay in the fourth

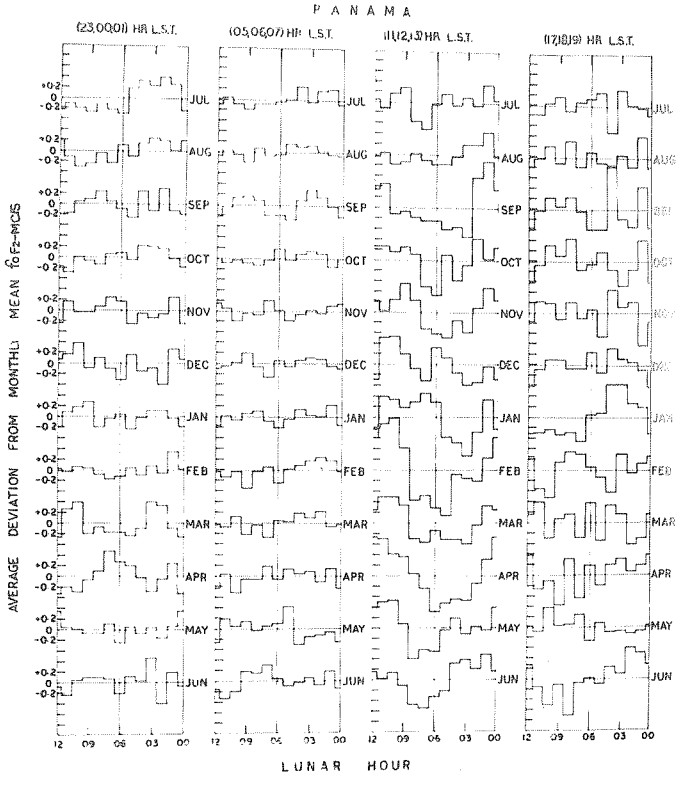


Fig. 7

quadrant, whereas the June solstitial ones lay in the first quadrant of the dial. The equinoctial months were located between these two. Though not perfectly uni-directional the vector rotated anti-clockwise during most of the months.

	(23, 00, 01) Sol. Hr.				(05, 06, 07) Sol. Hr.				(11, 12, 13) Sol. Hr.				(17, 18, 19) Sol. Hr.			
Month	Average f_0F_2 Mc/s	P_2 Mc/s	%	t_2 Lunar hour.	Average f_0F_2 Mc/s	P_2 Mc/s	%	t_2 Lunar hour.	Average f_0F_2 Mc/s	P_2 Mc/s	%	t_2 Lunar hour.	Average f_0F_2 Mc/s	P_2 Mc/s	%	t_2 Lunar hour.
Jan.	3.5	0.06	1.7	10.9	2.5	0.05	1.5	1.5	6.0	0.32	5.3	0.2	5.5	0.45	6.9	3.2
Feb.	3.3	0.11	3.3	0.7	5.2	0.16	5.0	2.7	9.0	0.75	8.3	11.3	7.9	0.06	0.3	6.1
Mar.	3.8	0.13	3.9	0.7	3.4	0.12	3.5	6.7	9.5	0.42	4.2	11.0	8.5	0.05	0.5	7.5
Apr.	5.3	0.22	4.3	6.1	3.8	0.12	3.2	4.1	9.9	0.65	6.6	11.0	9.4	0.23	2.4	2.4
May.	5.3	0.09	1.7	11.7	4.0	0.14	3.5	7.7	8.3	0.36	4.1	12.0	8.7	0.12	1.2	0.1
Jun.	5.3	0.05	0.9	5.4	4.1	0.13	2.9	6.4	7.9	0.41	5.2	1.4	8.1	0.42	4.5	3.5
Jul.	5.0	0.30	6.0	2.5	3.3	0.13	3.4	5.3	7.5	0.17	2.3	1.0	8.0	0.03	0.9	6.3
Aug.	4.6	0.13	3.3	2.7	3.3	0.03	2.1	3.3	8.1	0.19	2.3	1.5	8.6	0.07	0.7	10.7
Sep.	4.5	0.05	1.1	6.9	3.3	0.07	1.3	0.5	10.2	0.46	4.5	0.1	9.7	0.03	0.3	10.0
Oct.	3.9	0.15	3.9	4.1	3.9	0.00	2.3	4.2	10.3	0.33	3.1	11.7	8.0	0.10	2.1	3.3
Nov.	3.4	0.03	2.4	8.6	4.0	0.03	0.8	0.2	9.7	0.33	3.9	10.9	7.2	0.04	0.6	7.4
Dec.	3.7	0.16	4.3	10.5	3.6	0.02	0.6	3.1	8.7	0.35	2.0	3.9	5.9	0.12	2.0	5.2

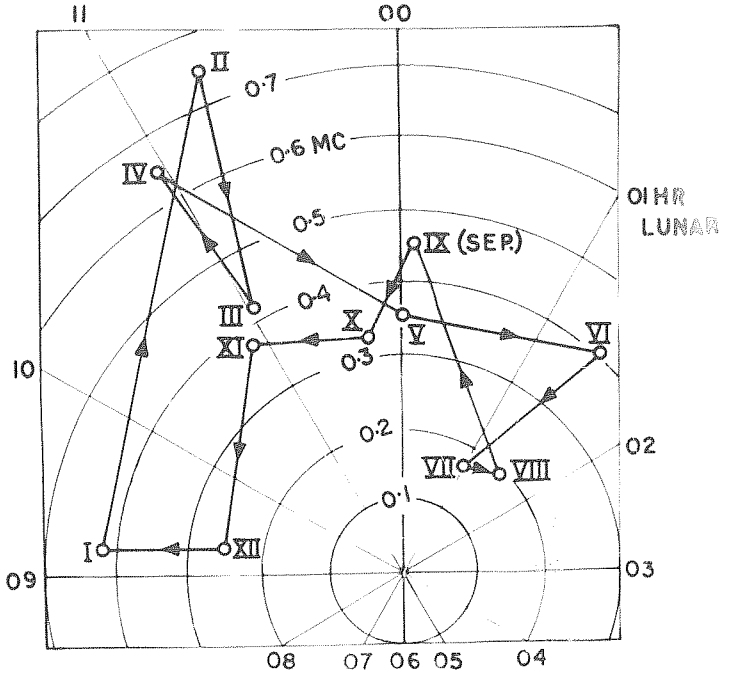


Fig. 8

5. Lunar variations in f_0F_2 over Huancayo

The F_2 - layer critical frequency data used were those from 1951 through 1956.

6. Variation of the lunar tide in f_0F_2 during December solstice, equinoxes and June solstice

Figure 9 shows the tidal variations during the December solstice. Except for the hours from 04 to 08 the tidal effect was quite significant in amplitude and regular in phase. During the night hours, viz., between 21 to 05 much scatter was evident. The tidal amplitude

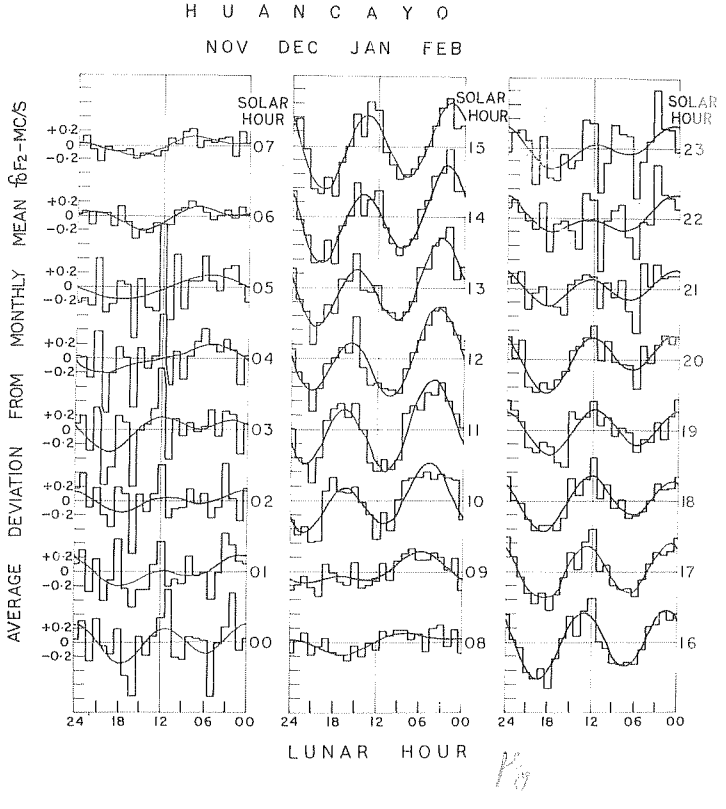


Fig. 9

varied from 0.01 Mc/s or 0.4 % at 05 solar hour to a maximum of 0.58 Mc/s or about 5.8 % around 14 hour. Their phases were 0.1 and 2.3 lunar hours respectively. It should be noted that at 05, 06, 07 and 08 solar hours the tidal influence was essentially diurnal.

The tidal behaviour during the equinoxes and June solstice is shown in Figures 10 and 11 respectively.

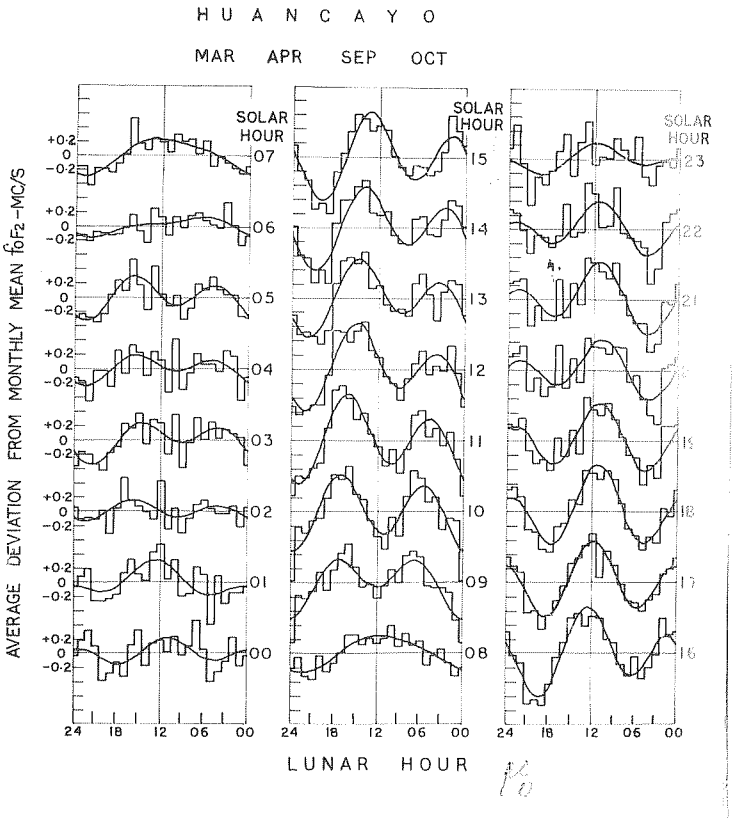


Fig. 10

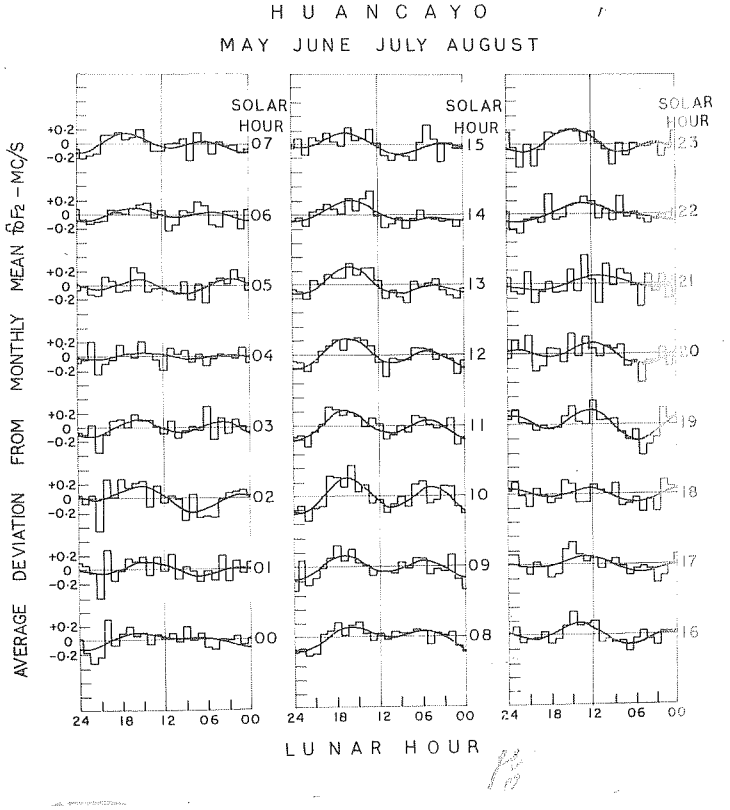


Fig. 11

Both the figures show that the scatter of the deviations became prominent from about 20 to about 05 solar hours. During the equinoxes the range of the amplitude was from a minimum of 0.03 Mc/s or 0.3 % at 08 hour to a maximum of 0.47 Mc/s or 5.7 % at 11 hour. Their phases were 6.9 and 4.7 lunar hours respectively. Similar to Parwan the

lunar influence on f_0F_2 at Huancayo during the June solstice was seen (Figure 11) to be small compared with those during the December solstice and equinoxes. The minimum amplitude of 0.03 Mc/s or 0.5 % occurred around 22 hour with its phase at 3.0 lunar hour. The maximum amplitude in absolute units happened at 10 hour with its phase at 4.3 lunar hour. The amplitude of the tide expressed in percentage, however, was 2.2 % at 05 hour having its phase at 3.1 lunar hour.

Figure 12 exhibits the variation with solar time of the semi-diurnal lunar tide in f_0F_2 averaged over all the three seasons. The tidal effect was significant throughout except for 06, 07 and 08 solar hours. The annual average tidal amplitude ranged from a minimum of 0.03 Mc/s or 0.4 % at 08 hour to a maximum of 0.27 Mc/s or 4.6 % at 11 hour, their respective phases being 5.1 and 4.6 lunar hours. The details concerning the above analysis are presented in Table III.

Figure 13 summarizes these results by way of vector representation. From the December solstice, equinoxes and annual diagrams it is evident that the semi-diurnal lunar tide assumed significant amplitude from about 09 to about 23 solar hours, and that its phase was centred around 05 lunar hour. The vector rotated in the anti-clockwise direction. During the June solstice, however,

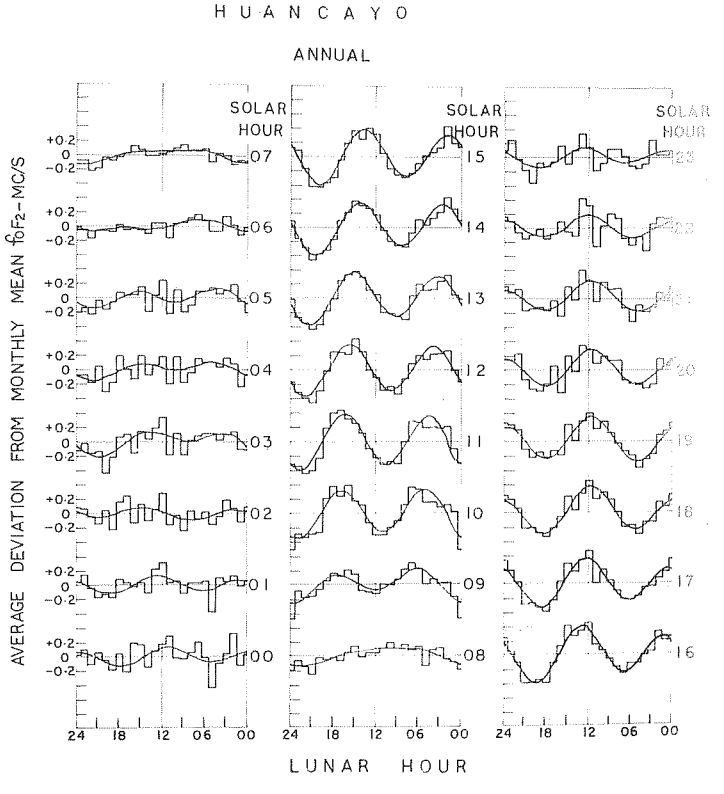


Fig. 12

the vector had almost negligible amplitude with its sense of orientation being quite random.

It is interesting to see how the variation with solar time of the lunar tide in f_0F_2 expressed in absolute units as well as in percentage compares with the

Sol. Nr.	Equinoxes: Aver-age f_0F_2 Mc/s	Equinoxes: P_2 Mc/s	Equinoxes: P_2 %	Equinoxes: t_2 lunar hour.	December Solstice: Aver-age f_0F_2 Mc/s	December Solstice: P_2 Mc/s	December Solstice: P_2 %	December Solstice: t_2 lunar hour.	June Solstice: Aver-age f_0F_2 Mc/s	June Solstice: P_2 Mc/s	June Solstice: P_2 %	June Solstice: t_2 lunar hour.	Annual: Aver-age f_0F_2 Mc/s	Annual: P_2 Mc/s	Annual: P_2 %	Annual: t_2 lunar hour
t				μs				μs				μs				μs
00	7.3	0.13	1.8	11.0	5.7	0.23	4.0	11.5	4.9	0.05	1.0	4.7	5.9	0.10	1.7	11.4
01	6.6	0.12	1.8	0.4	5.1	0.11	2.2	0.4	4.6	0.07	1.5	2.1	5.4	0.10	1.9	0.3
02	5.6	0.11	2.0	3.0	4.3	0.09	2.1	11.3	4.3	0.10	2.3	2.6	4.7	0.06	1.3	2.4
03	4.5	0.19	4.2	3.3	2.4	0.14	4.1	0.9	3.8	0.09	2.4	4.0	3.9	0.11	2.8	2.7
04	3.8	0.14	3.7	4.2	3.1	0.06	1.9	3.6	3.2	0.03	0.9	2.7	3.4	0.08	2.4	3.9
05	3.3	0.23	7.0	4.2	2.7	0.01	0.4	6.1	2.8	0.09	3.2	3.1	2.9	0.10	3.4	4.0
06	4.6	0.05	1.1	4.6	4.9	0.08	1.6	3.4	5.0	0.06	2.0	4.6	4.2	0.04	0.9	6.0
07	7.3	0.05	0.7	3.8	7.2	0.04	0.6	9.3	5.4	0.09	1.7	5.3	6.6	0.04	0.6	5.3
08	8.0	0.03	0.3	6.3	8.4	0.05	0.6	0.7	6.3	0.10	1.5	5.0	7.0	0.03	0.4	5.1
09	9.0	0.20	2.2	6.1	8.0	0.11	1.2	5.6	7.2	0.12	1.7	5.4	8.4	0.17	2.0	5.8
10	8.7	0.44	5.0	5.4	8.0	0.37	4.6	4.5	7.1	0.30	3.8	4.8	8.2	0.33	4.0	5.0
11	8.3	0.47	5.7	4.7	8.7	0.50	5.7	4.3	6.9	0.15	2.2	5.2	8.0	0.37	4.6	4.6
12	8.2	0.41	5.0	3.7	8.8	0.47	5.3	3.7	6.8	0.14	2.1	4.3	7.9	0.33	4.2	3.9
13	8.4	0.38	4.5	3.3	8.9	0.48	5.4	3.0	6.8	0.13	1.8	4.2	8.0	0.32	4.0	3.2
14	8.6	0.42	4.8	2.6	9.2	0.53	5.8	2.8	6.9	0.07	1.0	4.1	8.2	0.33	4.0	2.5
15	8.9	0.47	5.3	1.7	9.5	0.58	6.5	1.7	7.1	0.08	1.1	3.9	8.5	0.34	4.0	1.8
16	9.0	0.45	5.0	1.1	9.6	0.44	4.6	1.4	7.3	0.10	1.4	1.5	8.6	0.33	3.8	1.3
17	9.0	0.42	4.7	0.3	9.5	0.39	4.1	0.9	7.3	0.07	0.9	0.5	8.6	0.29	3.3	0.6
18	8.9	0.44	5.0	11.5	9.5	0.31	3.3	0.7	7.3	0.08	1.1	0.9	8.6	0.28	3.1	12.0
19	8.6	0.38	4.5	11.4	9.1	0.28	3.1	12.0	6.7	0.15	2.2	12.0	8.1	0.26	3.2	11.7
20	8.2	0.28	3.5	10.9	8.5	0.31	3.6	0.6	6.4	0.10	1.6	11.4	7.7	0.21	2.7	11.7
21	8.2	0.34	4.2	11.2	7.9	0.20	2.5	0.7	6.4	0.04	0.6	12.0	7.5	0.17	2.3	11.7
22	8.1	0.26	3.2	11.5	7.4	0.16	2.2	0.8	6.9	0.03	0.5	3.0	7.2	0.12	1.8	0.2
23	7.8	0.12	1.5	0.6	6.8	0.13	2.0	0.4	5.1	0.12	2.4	2.9	6.6	0.12	1.8	1.1

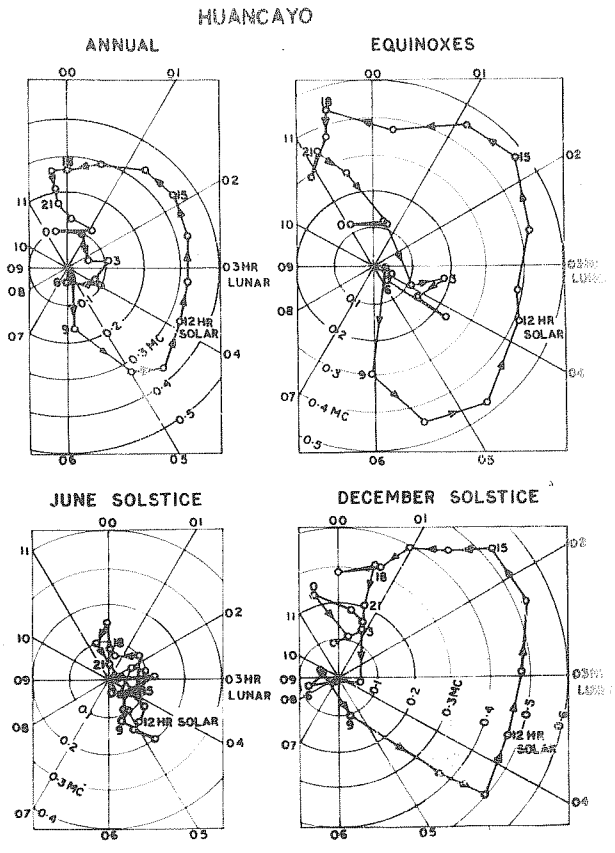


Fig. 13

diurnal variation of the F_2-layer critical frequency itself. In Figure 14 the solid curve shows the variation of f_0F_2 with the local time at Huancayo, and the dotted ones show the amplitude variation. In general they go parallel with each other. Around 06 hour, however, the

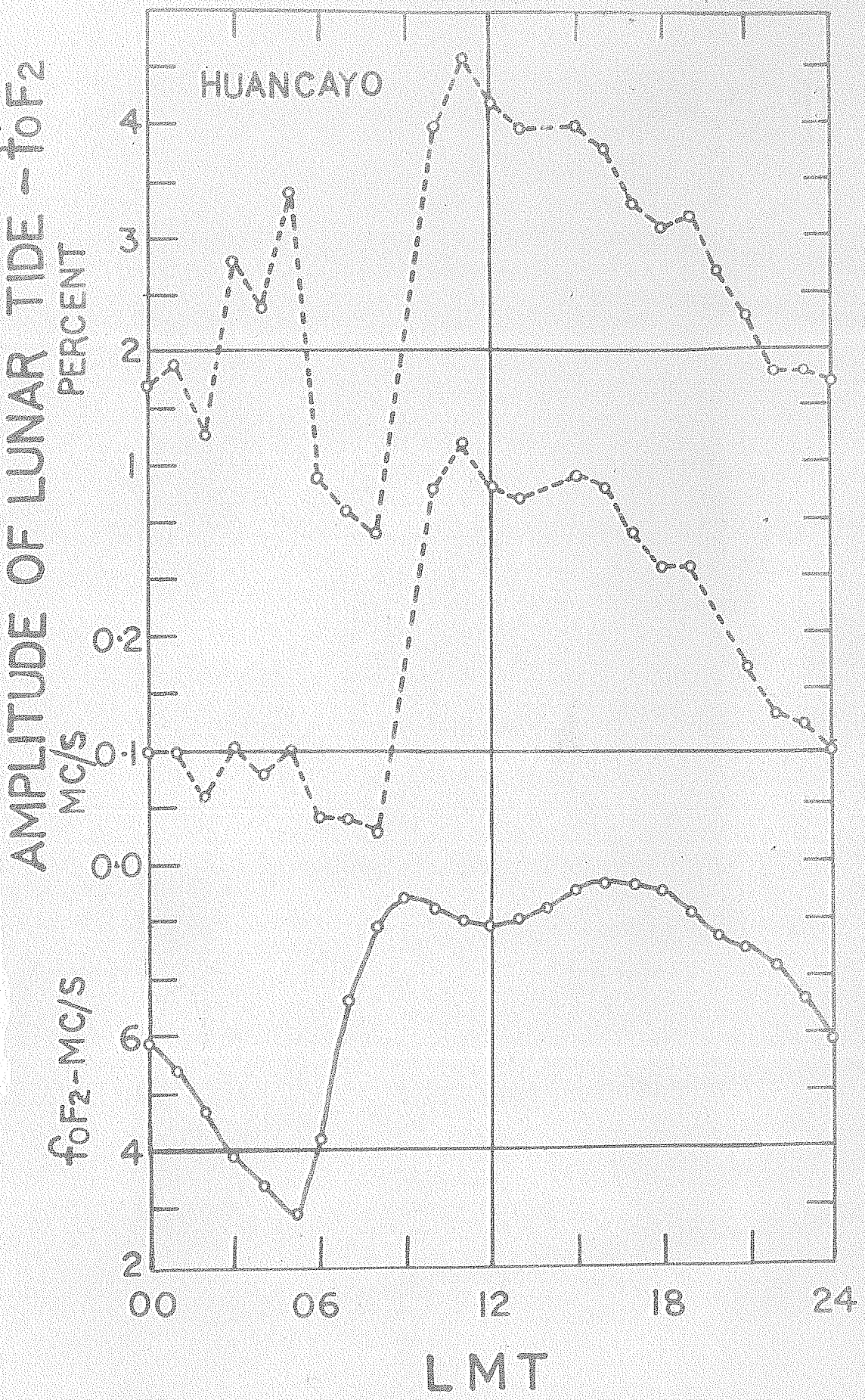

HUANCAYO
AMPLITUDE OF LUNAR TIDE - foF2
foF2-MC/S
MC/S
PERCENT
4
3
2
1
0·2
0·1
0·0
6
4
2
00
06
12
18
24
LMT

FIG. 14

percentage tide attained a peak of about 3.4 %, similar to the one in the case of Bunaun. The reason is also the same, viz. the value of $f_0 f_2$ at this time was very low, about 3.0 Mc/s.

7. Seasonal variation of the lunar tide at 00, 06, 12 and 18 solar hours

Figure 15 shows the behaviour of the tide for each month separately during 00, 06, 12 and 18 solar hour groups. The semi-diurnal tide was prominent during 12 and 18 hours. Around 00 and 06 hours, however, the tidal effect was obvious only during the December solstice and equinoxes. These results are shown in Table IV. It is seen that around 12 hour the maximum tide of 0.60 Mc/s or 7.0 % occurred in October at 9.9 lunar hour. The percentage tide of 7.0 % happened in February also. The minimum amplitude of 0.0 Mc/s or 1.4 % occurred in July. Around 00 hour the maximum tidal amplitude of 0.64 Mc/s or 8.6 % happened in November at 11.2 lunar hour.

Figure 16 reproduces the tidal picture around 12 hour in the form of a harmonic dial. The Roman numbers indicate the months. It is clearly brought out that the phase of the lunar tide changed only between 02 to 03 lunar hours. Again the June solstitial months formed the lowest amplitude group, while the December

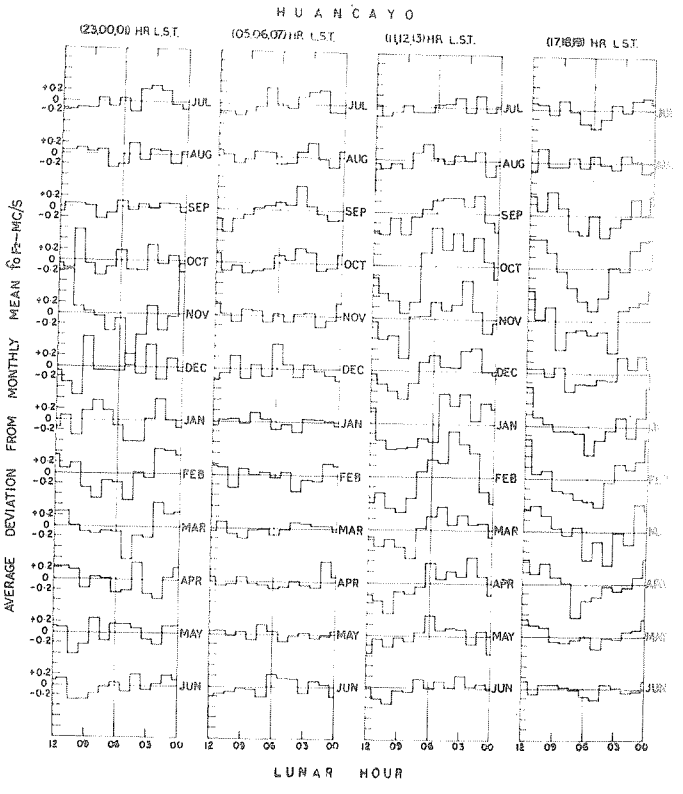


Fig. 13

solstitial ones formed the highest amplitude group; the equinoctial months, except October, assumed amplitudes intermediate between the two former groups.

(23. 00. 01) Sol.Str. (05. 05. 07) Mol.Str. (11. 12. 13) Sol. Ir. (17. 18. 19) Sol. Ir.

Month	Ave. P_o	ΔP_o	Ave. P_o	ΔP_o	Ave. P_o	ΔP_o	Ave. P_o	ΔP_o	Ave. P_o	ΔP_o
Jan.	5.0	0.19	5.9	0.5	4.5	0.05	1.7	0.2	5.9	0.2
Feb.	5.5	0.57	5.7	0.7	4.9	0.00	1.7	0.2	5.7	0.2
Mar.	5.5	0.38	4.0	12.0	4.9	0.00	1.7	0.2	5.8	0.2
Apr.	7.9	0.13	10.7	1.3	4.9	0.00	1.7	0.2	5.8	0.2
May	5.2	0.08	1.2	0.8	4.1	0.04	1.9	0.2	5.8	0.2
Jun.	4.5	0.14	8.1	2.3	3.5	0.10	4.9	0.2	5.8	0.2
Jul.	3.7	0.15	3.2	3.5	3.5	0.10	4.9	0.2	5.8	0.2
Aug.	5.2	0.04	0.8	12.8	3.5	0.04	1.1	0.2	5.8	0.2
Sep.	6.2	0.05	0.7	1.9	4.0	0.05	5.3	0.2	5.8	0.2
Oct.	8.0	0.05	0.8	15.0	5.7	0.05	0.8	0.2	5.8	0.2
Nov.	6.5	0.04	6.9	11.2	5.2	0.11	0.8	0.2	5.8	0.2
Dec.	5.5	0.12	2.2	3.7	5.0	0.11	0.8	0.2	5.8	0.2

Month	Ave. P_o	ΔP_o	Ave. P_o	ΔP_o	Ave. P_o	ΔP_o	Ave. P_o	ΔP_o	Ave. P_o	ΔP_o
Jan.	5.0	0.12	2.2	3.7	5.0	0.11	0.8	0.2	5.8	0.2
Feb.	5.5	0.13	2.2	3.7	5.0	0.11	0.8	0.2	5.8	0.2
Mar.	6.0	0.04	6.9	11.2	5.2	0.11	0.8	0.2	5.8	0.2
Apr.	6.5	0.05	0.8	15.0	5.7	0.05	0.8	0.2	5.8	0.2
May	6.0	0.05	0.7	1.9	4.0	0.05	5.3	0.2	5.8	0.2
Jun.	5.2	0.04	0.8	12.8	3.5	0.04	1.1	0.2	5.8	0.2
Jul.	4.5	0.14	8.1	2.3	3.5	0.10	4.9	0.2	5.8	0.2
Aug.	3.7	0.15	3.2	3.5	3.5	0.10	4.9	0.2	5.8	0.2
Sep.	5.2	0.04	0.8	12.8	3.5	0.04	1.1	0.2	5.8	0.2
Oct.	6.0	0.05	0.7	1.9	4.0	0.05	5.3	0.2	5.8	0.2
Nov.	5.2	0.04	0.8	12.8	3.5	0.04	1.1	0.2	5.8	0.2
Dec.	5.5	0.12	2.2	3.7	5.0	0.11	0.8	0.2	5.8	0.2

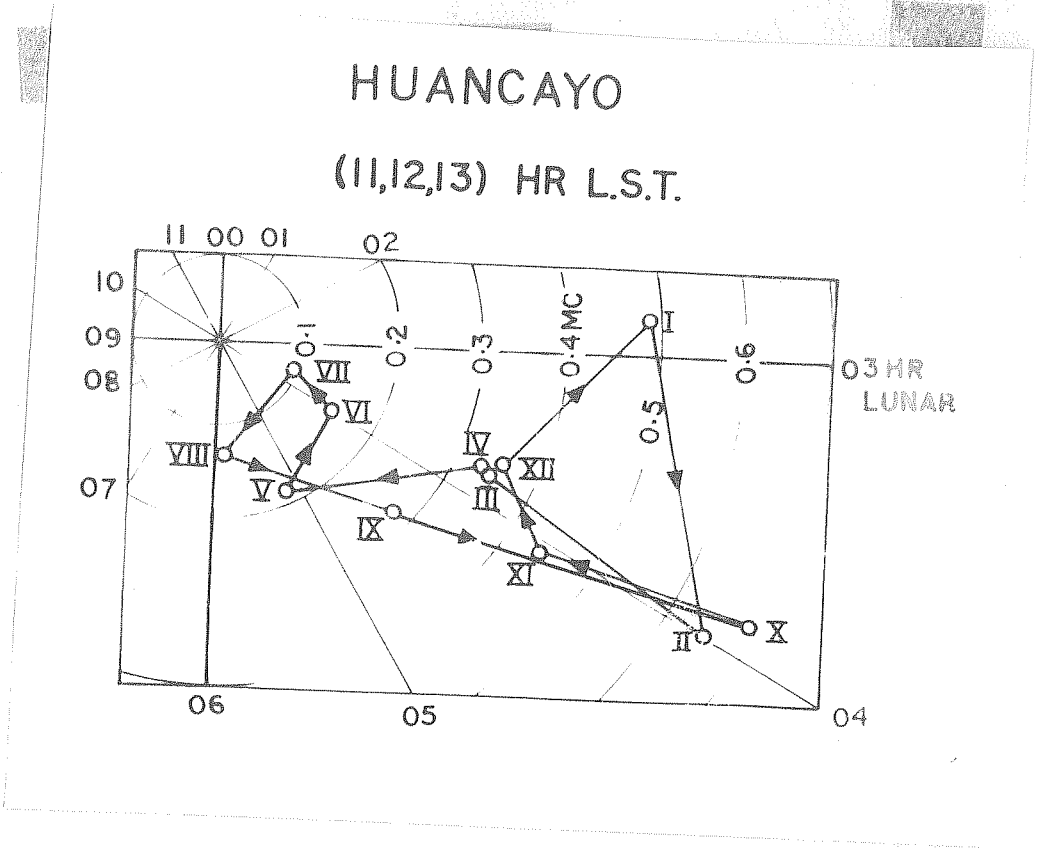


Fig. 16

6. Lunar variations in f_0F_2 over Ibadan Africa

Four years' data from 1958 through 1965 were used in this case.

9. Variation of the lunar tide in f_0F_2 during the December solstice, equinoxes and June solstice

The variation of the lunar tide with solar time during the December solstice and equinoxes is shown in Figures 17 and 18 respectively. During both these seasons

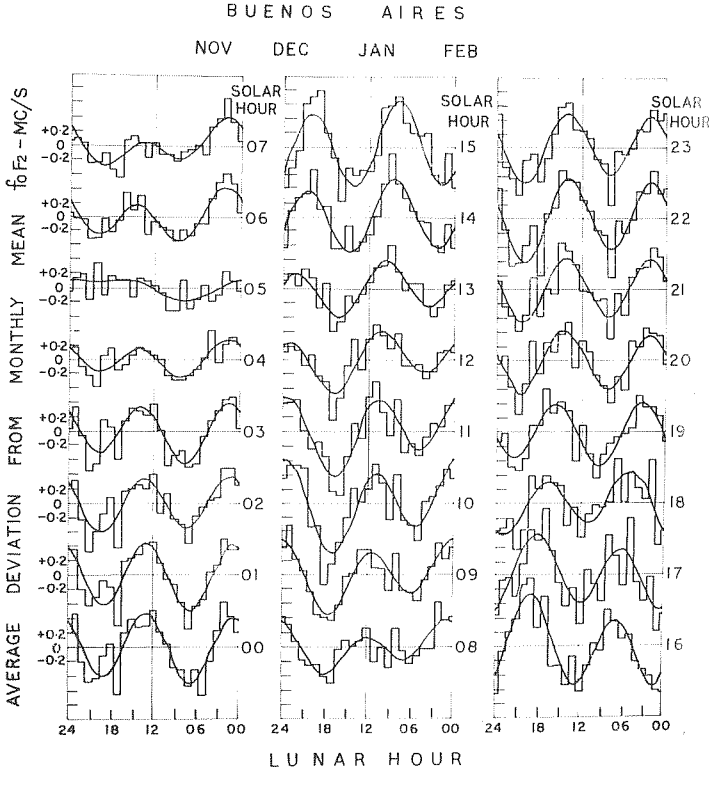


Fig. 17

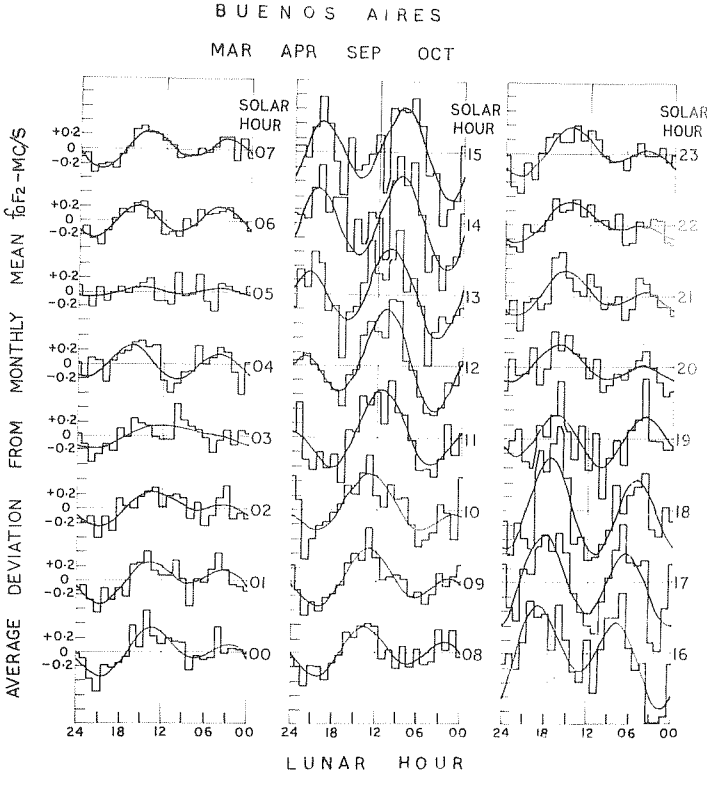


Fig. 18

the lunar tidal effect was quite large for all the solar hours except for the hour 05 for the December solstice and around 04 hour for the equinoxes, when the amplitudes were comparatively very small. During the December solstice the maximum amplitude of 0.56 Mc/s occurred around 15 hour

with its phase at 7.8 lunar hour, while the minimum amplitude of 0.05 Mc/s or 1.0 % happened at 05 hour with its phase at 1.0 lunar hour. The amplitude range during the equinoxes was from a minimum of 0.03 Mc/s or 0.7 % at 03 hour to a maximum of 0.33 Mc/s or 7.3 % at 13 hour. Their respective phases were 2.1 and 5.2 lunar hours.

The tidal amplitudes during the June solstice were generally small as is seen from Figure 19. A minimum

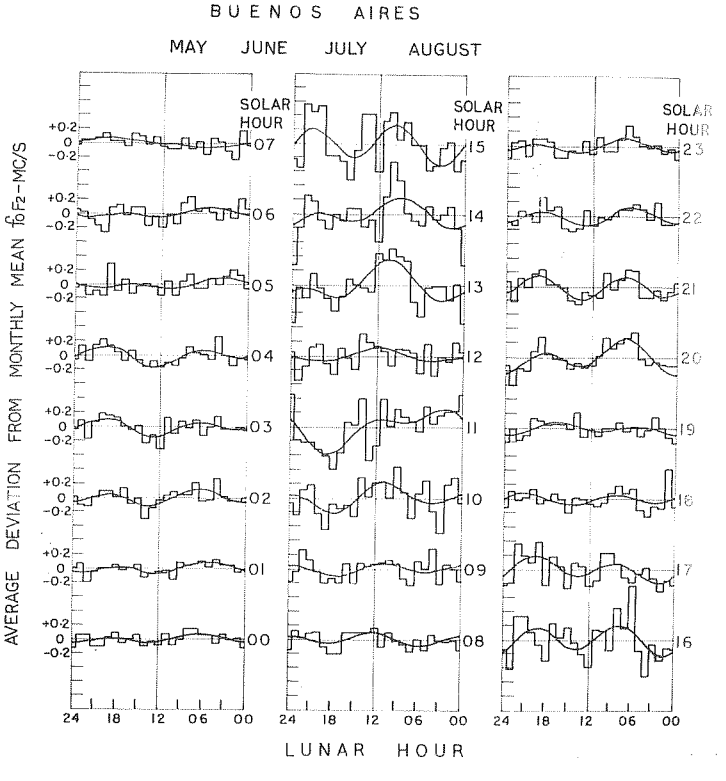


Fig. 19

amplitude of 0.01 Mc/s or 0.2 % occurred at 07 hour and a maximum tide of only 0.03 Mc/s appeared at 15 hour, with their phases at 8.4 and 0.4 lunar hours respectively.

The tidal perturbations in f_0F_2 averaged over all the three seasons are presented in Figure 20. The figure clearly shows that the amplitude of the tide was minimum

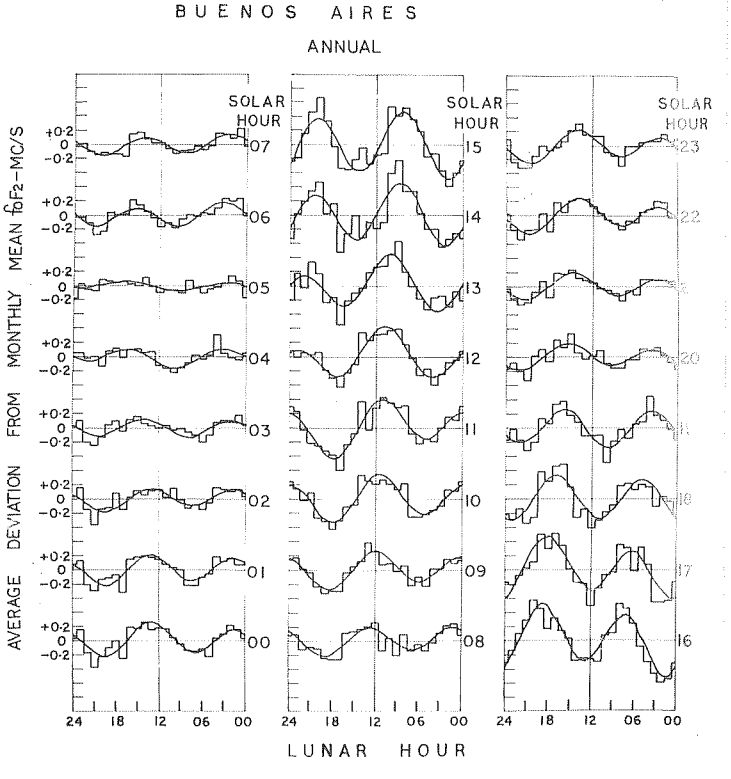
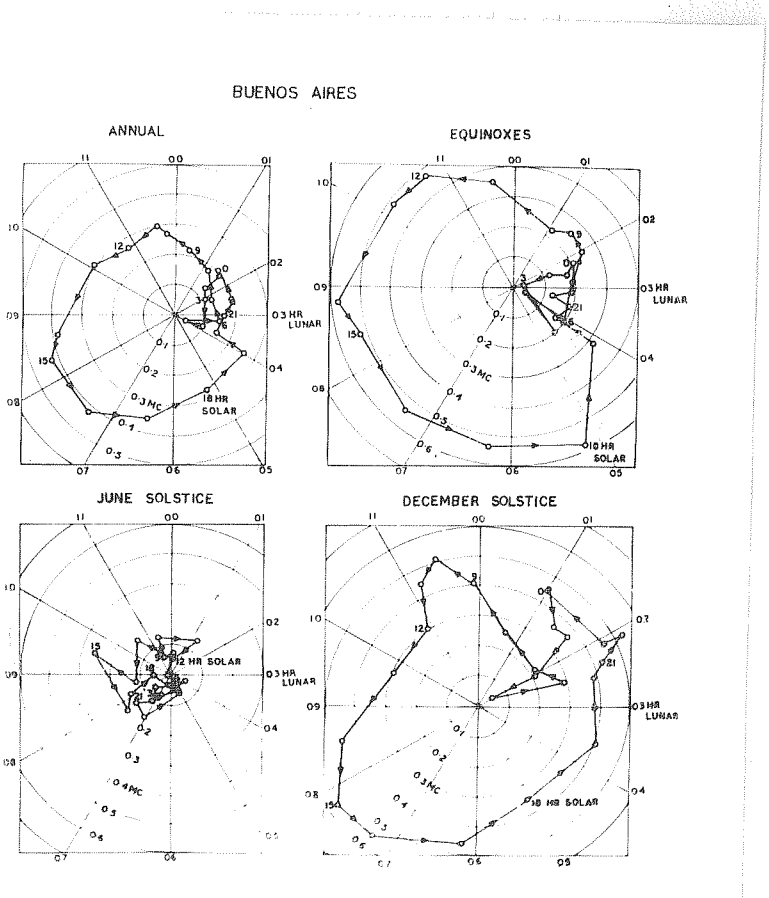


Fig. 20

(0.04 ke/s or 1.1 %) at 05 hour and maximum (0.43 ke/s or 6.0 %) around 15 hour, their phases being 4.0 and 8.0 lunar hours. These results are given in Table V.

Figure 21 summarizes the above results by means of harmonic dials. During the December solstice, equinoxes and the annual plots it is obvious that the main



	Equinoxes				December Solstice				June Solstice				Annual			
Sol. Hr.	Average f_0F_2 Mc/s	P_2 Mc/s	P_2 %	t_2 Lunar hour.	Average f_0F_2 Mc/s	P_2 Mc/s	P_2 %	t_2 Lunar hour.	Average f_0F_2 Mc/s	P_2 Mc/s	P_2 %	t_2 Lunar hour.	Average f_0F_2 Mc/s	P_2 Mc/s	P_2 %	t_2 Lunar hour.
00	4.3	0.21	4.9	2.2	6.2	0.45	7.3	1.0	2.9	0.04	1.4	6.3	4.5	0.30	4.4	1.4
01	4.3	0.18	4.2	2.6	6.0	0.45	7.5	1.0	2.9	0.06	2.1	5.3	4.4	0.19	4.3	1.6
02	4.4	0.12	2.7	3.3	5.9	0.36	6.1	1.4	3.0	0.08	2.7	6.8	4.4	0.13	3.0	1.6
03	4.6	0.03	0.7	2.1	5.5	0.37	6.7	1.8	2.9	0.09	3.1	7.0	4.3	0.11	2.6	2.1
04	3.9	0.20	5.1	4.0	5.0	0.21	4.2	2.0	2.9	0.09	3.1	6.0	5.0	0.16	3.6	3.8
05	3.8	0.04	1.1	3.9	5.1	0.05	1.0	1.9	2.6	0.05	1.9	3.9	3.7	0.04	1.1	4.0
06	4.4	0.20	4.6	4.2	5.2	0.29	5.6	2.5	2.6	0.04	1.6	5.3	4.3	0.15	3.5	3.3
07	5.7	0.18	3.3	2.5	6.2	0.22	3.5	1.6	4.2	0.01	0.2	3.4	5.4	0.13	2.4	2.3
08	6.4	0.25	3.9	2.0	6.6	0.30	4.6	0.6	5.1	0.07	1.4	0.2	6.0	0.16	2.6	1.2
09	7.1	0.36	5.7	1.5	7.2	0.41	5.7	11.9	5.6	0.06	1.1	11.3	6.6	0.22	3.3	0.4
10	7.8	0.23	2.9	1.1	7.9	0.51	6.5	11.4	6.2	0.13	2.1	11.6	7.3	0.37	5.7	11.8
11	8.3	0.36	4.1	11.6	8.8	0.46	5.1	11.1	6.7	0.14	2.1	1.2	8.1	0.30	3.7	11.6
12	8.3	0.47	4.8	10.7	8.6	0.31	3.2	10.9	6.8	0.05	0.8	0.2	8.3	0.27	3.1	10.8
13	10.3	0.48	4.7	10.2	10.1	0.30	3.0	0.7	7.1	0.16	2.3	10.5	9.3	0.21	3.3	10.1
14	10.4	0.57	5.5	9.8	10.4	0.46	4.4	8.5	7.4	0.12	1.6	8.5	9.4	0.30	4.1	8.7
15	10.2	0.58	5.1	9.4	10.4	0.56	5.4	7.8	7.4	0.26	3.5	9.4	9.3	0.42	4.6	8.3
16	9.5	0.54	5.7	7.0	9.8	0.55	5.6	7.3	6.7	0.10	2.3	7.2	8.7	0.43	5.0	7.4
17	8.0	0.54	6.1	6.3	8.0	0.46	5.1	6.2	5.8	0.15	2.6	8.2	7.0	0.36	4.6	6.5
18	6.0	0.53	7.3	5.2	8.3	0.35	4.3	5.1	4.6	0.06	1.3	0.0	7.0	0.30	4.3	5.2
19	6.6	0.32	4.8	4.3	7.7	0.41	5.3	5.6	4.0	0.07	1.8	5.3	6.1	0.26	4.3	4.0
20	5.6	0.17	3.0	4.3	7.0	0.30	5.6	2.5	3.9	0.17	4.4	7.0	5.5	0.15	2.7	3.8
21	5.1	0.19	3.7	3.9	6.6	0.43	6.5	2.3	3.6	0.15	4.2	7.7	5.1	0.16	3.1	3.1
22	4.7	0.13	2.8	3.4	6.4	0.53	8.3	2.1	3.3	0.11	3.3	6.8	4.9	0.19	4.0	2.6
23	4.6	0.19	4.1	3.1	6.3	0.46	7.3	2.1	3.0	0.07	2.3	7.6	4.6	0.19	4.1	2.5

bulk of the vector loops lay around 07 to 08 lunar hours. The vector rotated essentially in the anti-clockwise direction. The loops began to be formed at about 08 solar hour and was completed at about 22 hour, thus exhibiting the tidal influence for a longer duration than those at Panama and Huancayo. Alike those in the latter two cases, the June solstice showed very small tidal amplitudes with very random phase variation.

A comparison of the variation of the annual average amplitude of the tide, expressed both in Mc/s and in percentage, was made with the diurnal variation of the corresponding f_0F_2 and is shown in Figure 22. Though the f_0F_2 peak took place at 14 hour local time, the maximum amplitude of the tide (1.3 Mc/s or 5 %) occurred only around 16 hour. Over Buenos Aires, in contrast to Panama and Huancayo, there was a sharp minimum of about 1.1 % at 06 solar hour even though the value of f_0F_2 at that time was only about 3.7 Mc/s.

10. Seasonal behaviour of the lunar tide around 00, 06, 12 and 18 solar hours

The behaviour of the semi-diurnal tide in different months and for 00, 06, 12 and 18 hour groups is shown in Figure 23 and its various coefficients are given in Tm/ The tidal effect was generally larger around 12 and ?

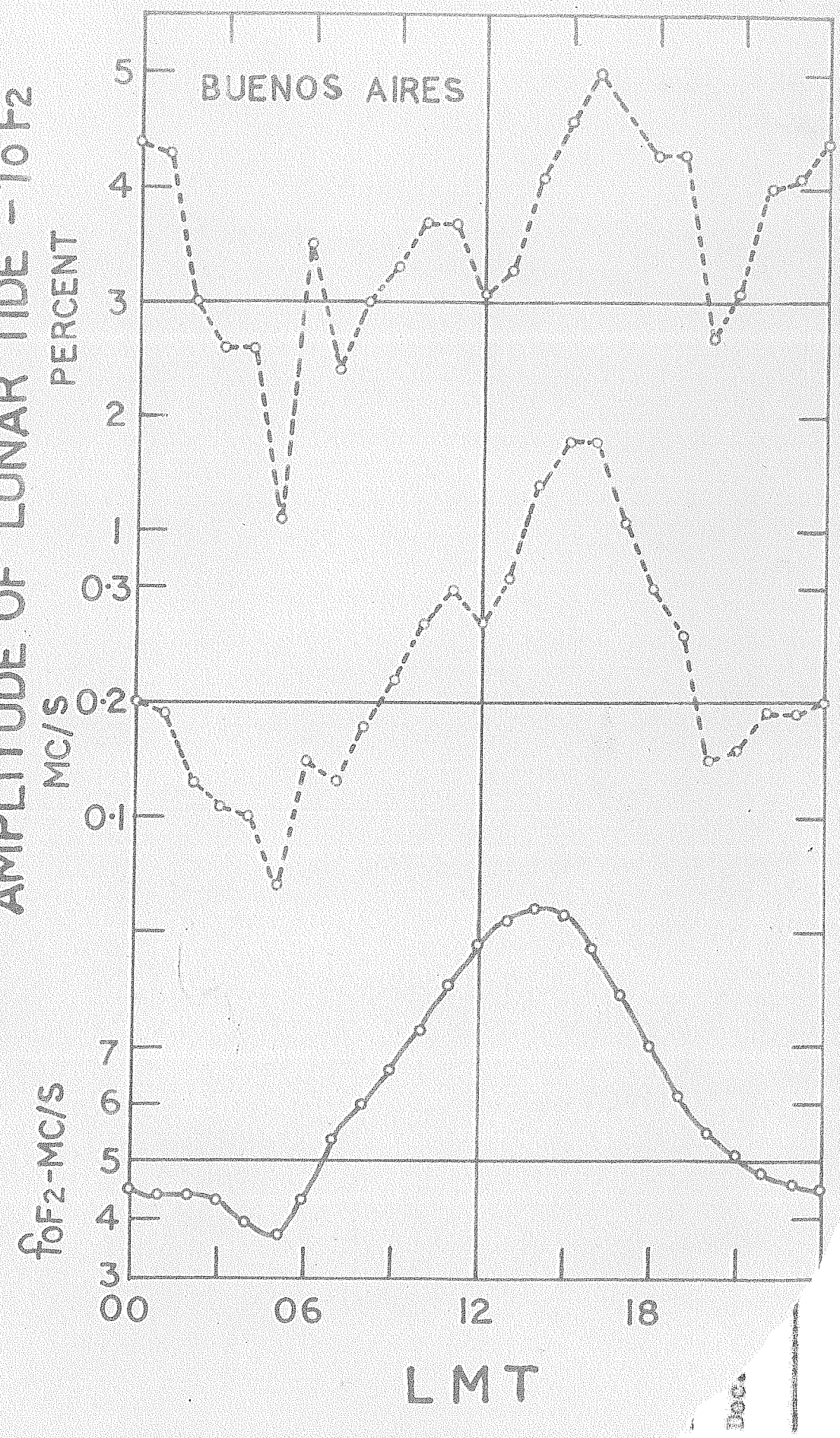

AMPLITUDE OF LUNAR TIDE - foF2
BUENOS AIRES
PERCENT
MC/S
foF2-MC/S
5
4
3
2
1
0·3
0·2
0·1
7
6
5
4
3
00
06
12
18
LMT

FIG. 22

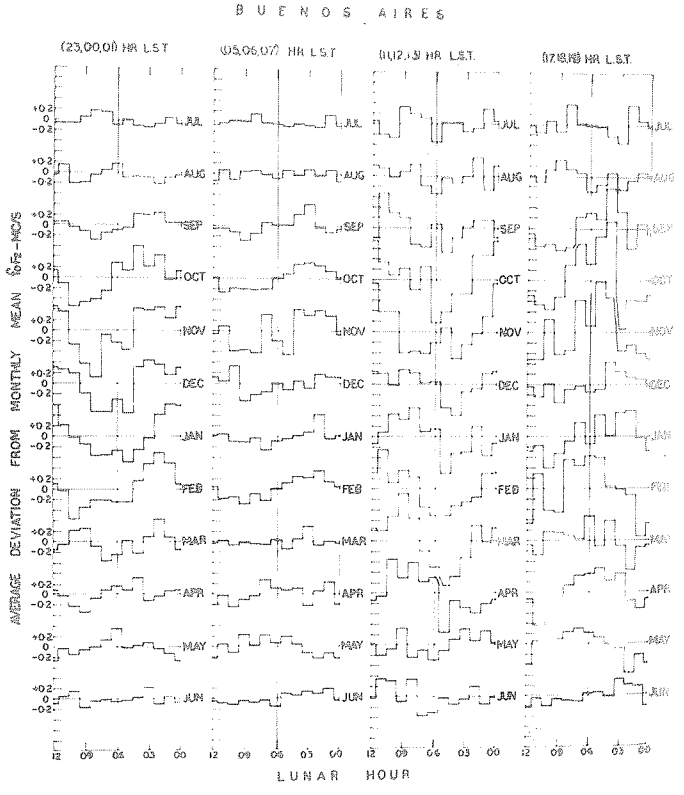


Fig. 23

than during the remaining hours. From Table VI it is seen that generally minimum amplitudes occurred in one of the June solstitial months and maximum amplitudes occurred in one of the December solstitial months or equinoctial months.

	(33, 00, 01) Sol. Hr.				(05, 06, 07) Sol. Hr.				(11, 12, 13) Sol. Hr.				(17, 18, 19) Sol. Hr.			
Month	Average f_0F_2 Mc/s	P_2 Mc/s	P_2 %	t_2 Lunar hour.	Average f_0F_2 Mc/s	P_2 Mc/s	P_2 %	t_2 Lunar hour.	Average f_0F_2 Mc/s	P_2 Mc/s	P_2 %	t_2 Lunar hour.	Average f_0F_2 Mc/s	P_2 Mc/s	P_2 %	t_2 Lunar hour.
Jan.	5.7	0.43	8.4	0.5	5.1	0.15	2.9	1.9	8.8	0.36	4.1	0.9	7.6	0.38	5.0	3.9
Feb.	5.5	0.47	8.5	2.2	4.9	0.28	5.7	2.7	8.6	0.49	5.7	10.9	8.2	0.55	6.7	6.2
Mar.	4.4	0.15	3.4	0.4	3.8	0.05	1.3	2.8	8.3	0.00	6.5	10.3	8.3	0.34	2.9	6.9
Apr.	3.7	0.14	3.8	4.0	3.9	0.11	2.8	5.1	8.3	0.45	4.3	8.3	6.3	0.46	7.3	5.2
May	3.2	0.15	4.7	5.7	3.5	0.17	4.9	7.0	7.5	0.15	2.0	1.5	4.9	0.32	6.5	7.5
Jun.	2.7	0.03	1.1	2.5	3.7	0.11	4.1	6.6	6.5	0.13	2.8	11.1	4.5	0.16	3.6	6.4
Jul.	2.8	0.03	2.9	8.3	2.8	0.05	1.8	9.5	6.3	0.05	0.8	9.5	4.7	0.07	1.5	9.1
Aug.	2.9	0.04	1.4	6.4	3.5	0.02	0.6	4.0	7.1	0.13	1.8	11.6	5.0	0.14	2.8	9.6
Sep.	3.9	0.19	4.9	2.1	4.2	0.13	4.3	4.9	9.2	0.23	3.0	11.5	6.6	0.40	6.1	4.3
Oct.	5.6	0.41	7.9	3.2	5.5	0.27	4.9	3.0	10.6	0.59	5.6	11.9	10.0	0.65	6.5	5.3
Nov.	6.6	0.53	8.0	1.8	6.4	0.31	4.9	2.4	10.5	0.44	4.2	12.0	9.1	0.52	5.7	5.5
Dec.	6.7	0.45	6.7	1.1	6.4	0.15	2.3	0.9	10.0	0.20	2.0	10.3	8.4	0.22	2.6	3.1

The behaviour of the tide around 12 hour is represented on a harmonic dial in Figure 24. The phase was limited almost within the fourth quadrant (09 - 12 lunar hour) of the dial. The June solstitial months formed a group representing the smallest amplitude period. Again the equinoctial months showed larger amplitude than the December solstitial ones.

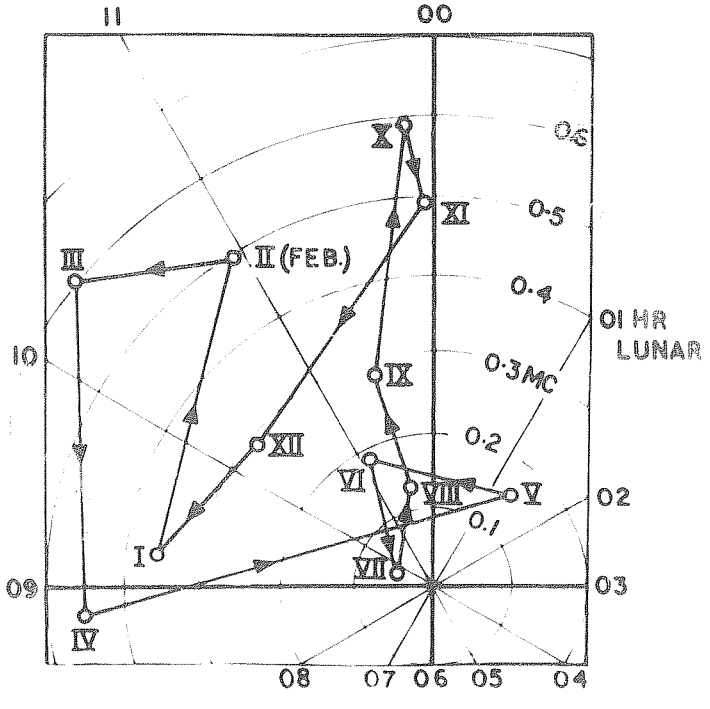


Fig. 24

In the case of Buenos Aires only the amplitude of the lunar tide around 00 hour in f_0F_2 was found comparable with that around 12 hour. For this reason the variation of the tide around 00 hour in different months was redrawn on a harmonic dial in Figure 26. Here also the December solstitial group showed the largest amplitudes while the June solstitial ones formed the smallest amplitude group. The equinoctial period had intermediate amplitudes. In contrast to the 12 hour group, most of the months were located in the first quadrant (00 - 03 lunar hour).

11. The diurnal component of the lunar tide in f_0F_2

While computing the various coefficients of the lunar tide it was observed that the magnitude of its diurnal component amount a value which was occasionally significant as compared with that of the semi-diurnal component. Though the physical significance of the diurnal periodicity of lunar tides is rather difficult to understand, a brief account of its order of magnitudes for all the three stations under consideration is presented below.

In Figures 26, 27 and 28 the amplitude and phase of the diurnal component of the lunar tide in f_0F_2 over Panama, Huancayo and Buenos Aires respectively is shown in vectorial form. In each case the data were divided into two groups, viz. the day group (solid circles) from 07 to 19 hours and

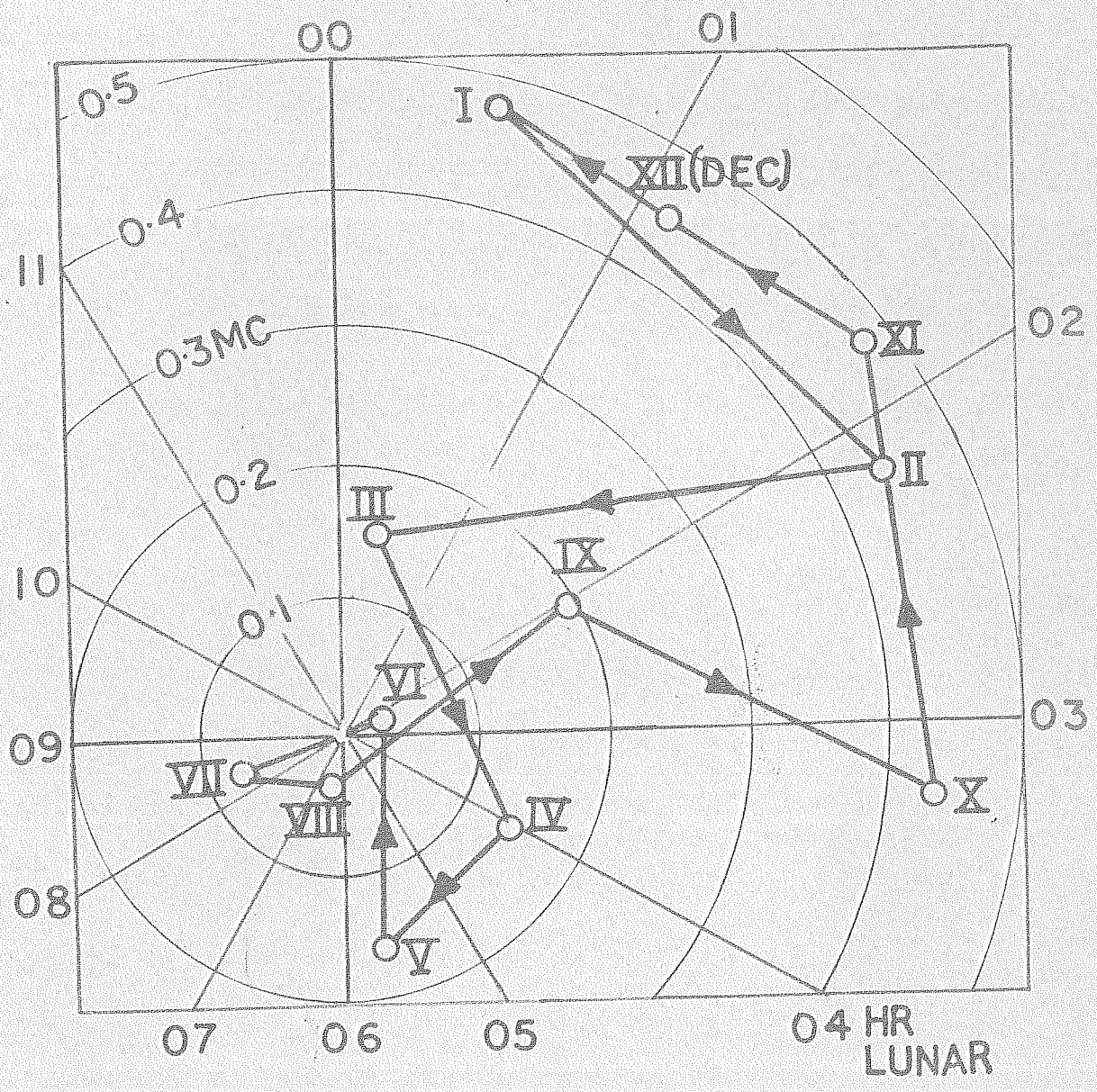

BUENOS AIRES
(23,00,01) HR L.S.T.
00
01
02
03
04 HR
LUNAR
05
06
07
08
09
10
11
0·5
0·4
0·3MC
0·2
0·1
I
II
III
IV
V
VI
VII
VIII
IX
X
XI
XII(DEC)

FIG. 25

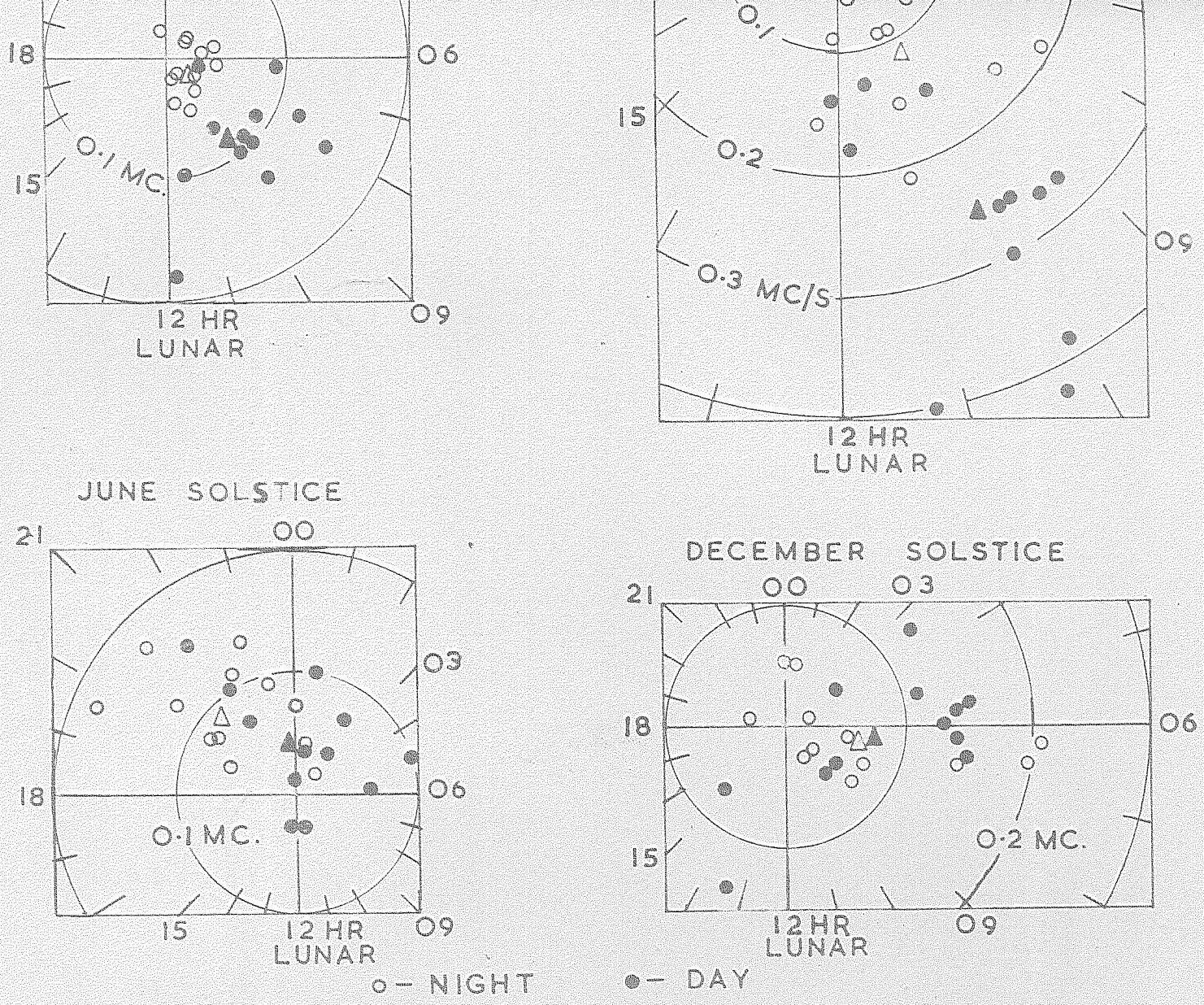
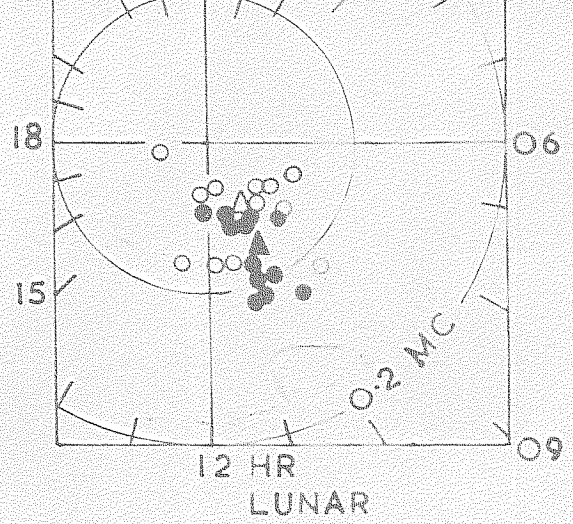
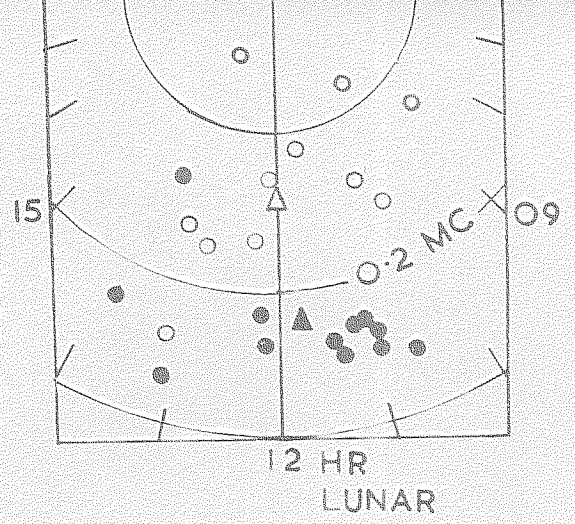
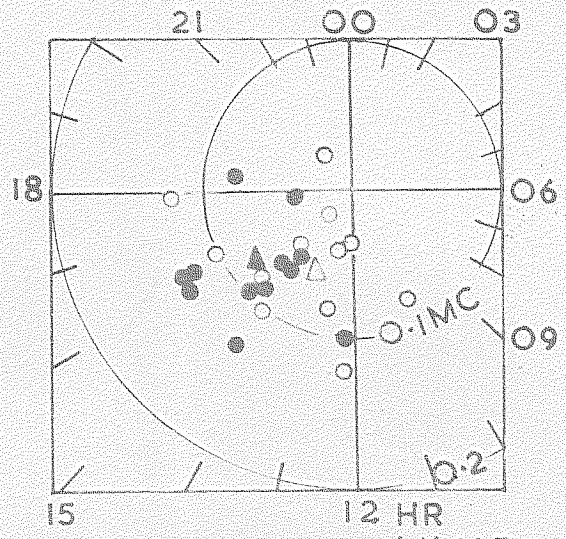

18
06
15
0·1 MC.
12 HR
LUNAR
09
0·1
15
0·2
09
0·3 MC/S
12 HR
LUNAR
JUNE SOLSTICE
21
00
03
18
06
0·1 MC.
15
12 HR
LUNAR
09
DECEMBER SOLSTICE
21
00
03
18
06
0·2 MC.
15
12 HR
LUNAR
09
○ – NIGHT
● – DAY

FIG. 26

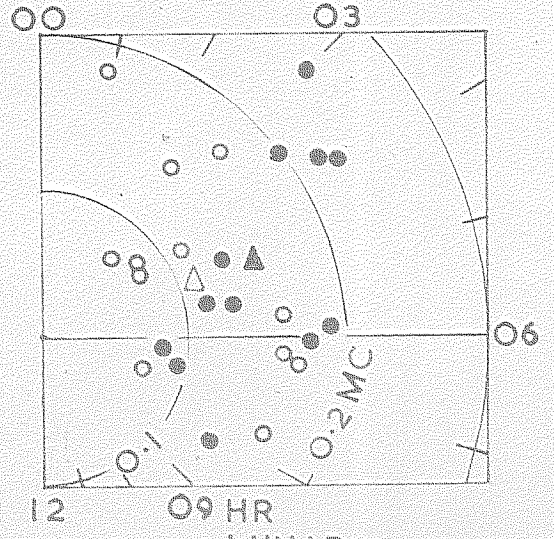




JUNE SOLSTICE

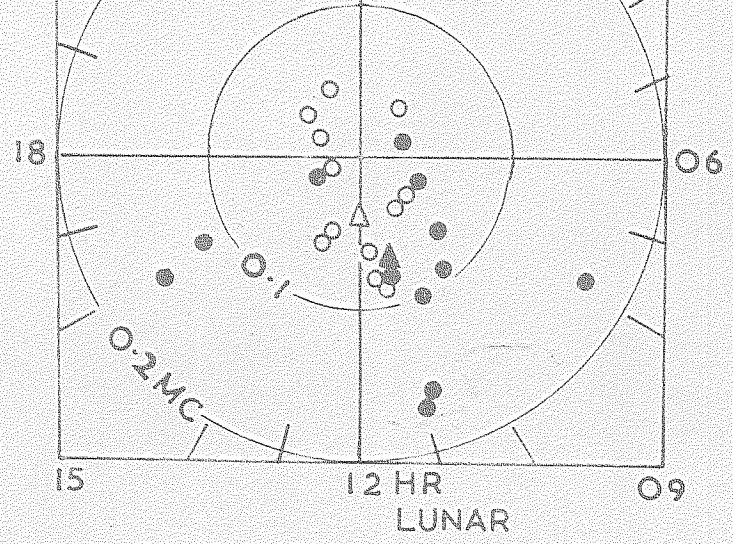


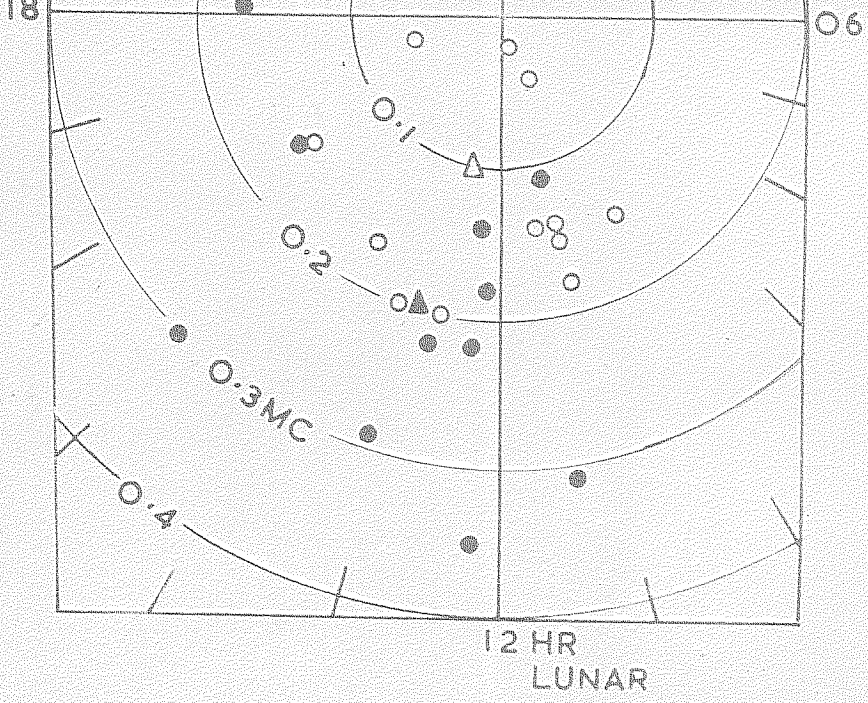
DECEMBER SOLSTICE



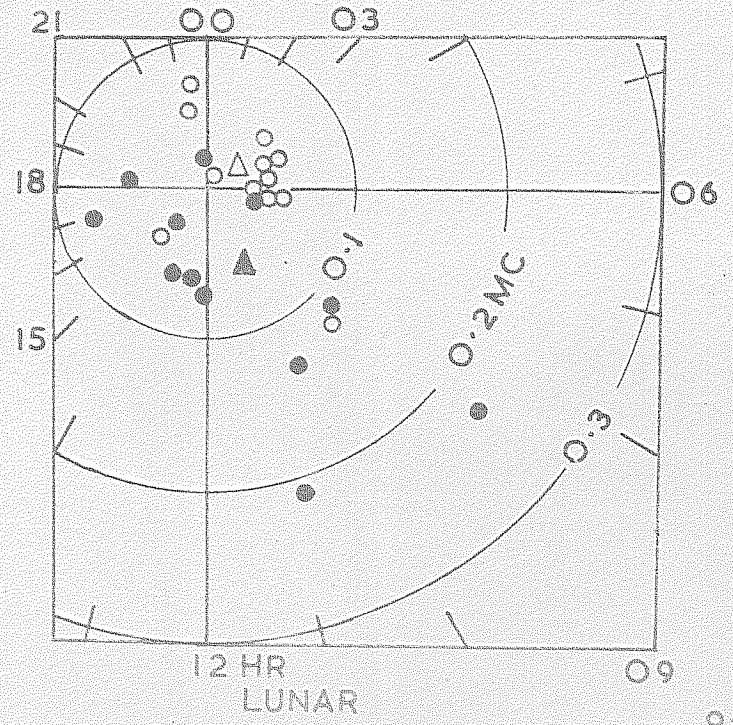
○—NIGHT ●—DAY

FIG. 27

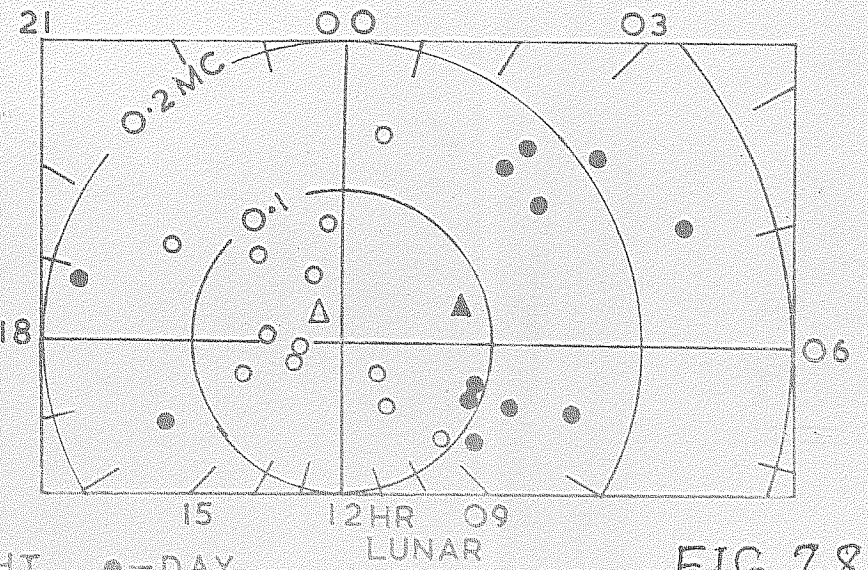




JUNE SOLSTICE



DECEMBER SOLSTICE



○—NIGHT ●—DAY

FIG. 28

the night group (hollow circles) from 19 - 00 hours. The centres of gravity of the mass plots are shown by solid and hollow triangles for day and night respectively. The results of this analysis are given in Tables VII, VIII and IX for Panama, Ibadanayo and Buenos Aires respectively.

Broadly, it is seen that the amplitude of the diurnal component of the tide attained appreciable magnitudes during the equinoxes and the December solstice for all the stations. At times they were even almost equal to the corresponding semi-diurnal component. For instance, in the case of Buenos Aires the diurnal component during the equinoxes had amplitudes of 4.8 %, 4.3 % and 4.0 % at 23, 00 and 01 hours respectively; and the corresponding values of the semi-diurnal component (Table V) were respectively 4.1 %, 4.0 % and 4.2 %. Again, the phases of the diurnal components during the equinoxes were centred around 5 to 6 lunar hours for all the three places. The plots for the June solstice show much smaller amplitudes and more random phases.

	Equinoxes				December Solstice				June Solstice				Annual			
Sol. Hr.	Aver-age f_0F_2 Mc/s	P_1 Mc/s	%	$t_{1/2}$ lunar hour.	Aver-age f_0F_2 Mc/s	P_1 Mc/s	%	$t_{1/2}$ lunar hour.	Aver-age f_0F_2 Mc/s	P_1 Mc/s	%	$t_{1/2}$ lunar hour.	Aver-age f_0F_2 Mc/s	P_1 Mc/s	%	$t_{1/2}$ lunar hour
00	4.4	0.19	4.3	4.0	3.6	0.03	0.8	9.0	5.1	0.03	1.6	10.3	4.4	0.03	0.7	4.3
01	4.3	0.17	4.0	4.4	3.3	0.06	1.8	12.0	4.8	0.04	0.8	8.3	4.1	0.04	1.0	9.2
02	3.8	0.08	2.1	4.2	3.1	0.05	1.6	8.3	4.3	0.09	2.1	10.0	3.7	0.02	0.5	11.9
03	3.1	0.09	2.9	5.1	2.7	0.02	0.7	8.2	4.0	0.06	1.5	9.7	3.3	0.02	0.6	5.9
04	2.9	0.08	2.8	4.5	2.6	0.05	2.0	8.8	3.8	0.11	2.9	11.0	3.1	0.02	0.6	1.8
05	2.7	0.06	2.2	4.7	2.5	0.07	2.8	8.9	3.4	0.07	2.1	12.0	2.9	0.03	1.0	3.0
06	3.1	0.06	1.9	5.7	2.9	0.07	2.4	4.3	3.5	0.02	0.6	1.6	3.2	0.04	1.3	4.7
07	5.3	0.13	2.5	5.7	5.3	0.15	2.8	3.0	4.8	0.06	1.3	2.9	5.1	0.09	1.8	6.1
08	6.2	0.14	2.3	6.1	6.8	0.15	2.2	2.3	5.3	0.10	1.9	10.9	6.1	0.03	0.5	3.7
09	7.3	0.15	2.1	5.1	8.0	0.11	1.4	2.5	5.6	0.10	1.8	0.3	6.9	0.09	1.3	3.2
10	8.4	0.27	3.2	4.6	8.6	0.05	0.6	4.2	6.2	0.01	0.2	11.8	7.7	0.10	1.3	4.5
11	9.4	0.36	3.8	6.0	8.8	0.06	0.7	4.7	7.1	0.04	0.6	0.5	8.4	0.10	1.2	4.8
12	10.2	0.27	2.6	4.3	8.8	0.13	1.5	3.0	8.1	0.07	0.9	1.1	9.0	0.12	1.3	3.2
13	11.0	0.37	3.4	5.0	8.9	0.13	1.5	1.8	9.0	0.10	1.1	8.5	9.6	0.15	1.6	4.0
14	11.5	0.42	3.7	5.1	9.2	0.05	0.5	1.3	9.7	0.04	0.4	1.3	10.1	0.13	1.3	4.7
15	11.3	0.40	3.4	5.6	9.2	0.14	1.6	6.7	10.1	0.03	0.3	6.0	10.4	0.13	1.7	6.0
16	11.3	0.30	2.5	5.1	9.1	0.07	0.8	7.4	10.4	0.07	0.6	10.9	10.4	0.10	1.0	5.7
17	11.2	0.26	2.3	5.0	8.4	0.09	1.1	3.1	10.2	0.15	1.5	10.3	9.9	0.07	0.7	5.0
18	9.7	0.18	1.9	5.9	8.0	0.14	1.8	2.8	9.6	0.03	0.3	6.3	9.1	0.09	1.0	4.5
19	7.5	0.16	2.1	6.2	5.3	0.20	3.4	3.3	8.4	0.18	2.1	0.3	7.1	0.04	0.6	5.7
20	6.3	0.09	1.4	6.3	4.1	0.22	5.4	3.1	7.2	0.17	2.4	10.6	5.9	0.04	0.7	2.3
21	5.4	0.09	1.7	6.1	3.5	0.14	4.0	3.4	6.8	0.12	2.0	10.2	5.0	0.03	0.4	5.1
22	4.7	0.15	3.2	5.4	3.5	0.03	0.9	5.0	5.6	0.13	2.3	11.3	4.6	0.02	0.4	6.1
23	4.4	0.21	4.8	5.5	3.6	0.03	0.8	4.6	5.3	0.09	1.7	11.5	4.4	0.03	1.1	5.3

	Equinoxes				December Solstice				June Solstice				Annual			
Sol. Hr.	Aver-age $\epsilon_0 P_2$ Mc/s	P_1 Mc/s	%	t_1 lunar hour.	Aver-age $\epsilon_0 P_2$ Mc/s	P_1 Mc/s	%	t_1 lunar hour.	Aver-age $\epsilon_0 P_2$ Mc/s	P_1 Mc/s	%	t_1 lunar hour.	Aver-age $\epsilon_0 P_2$ Mc/s	P_1 Mc/s	%	t_1 lunar hour.
00	7.3	0.08	1.1	4.9	5.7	0.08	1.4	1.9	4.9	0.08	1.6	6.5	6.0	0.06	0.9	4.7
01	6.6	0.10	2.0	6.5	5.1	0.14	2.7	1.3	4.6	0.05	1.1	7.5	5.4	0.08	0.5	5.0
02	5.5	0.06	0.9	6.8	4.3	0.08	1.9	1.7	4.3	0.12	2.8	9.0	4.7	0.08	0.6	5.8
03	4.5	0.16	3.6	5.1	3.4	0.16	4.7	3.9	3.8	0.04	1.1	6.0	3.9	0.11	2.9	4.6
04	3.8	0.11	2.8	5.3	3.1	0.17	5.5	3.2	2.8	0.02	0.6	7.3	3.4	0.07	2.1	4.4
05	3.3	0.13	3.9	6.1	2.7	0.16	5.9	2.8	2.8	0.03	1.1	10.3	2.9	0.05	1.7	4.2
06	4.6	0.12	2.6	4.4	4.9	0.11	2.2	1.9	3.0	0.04	1.3	6.5	4.2	0.06	1.4	3.6
07	7.3	0.25	3.4	5.7	7.2	0.11	1.5	2.6	5.4	0.07	1.3	7.3	6.6	0.10	1.5	5.3
08	8.6	0.25	2.9	5.5	8.4	0.13	1.5	2.7	6.3	0.10	1.5	6.1	7.9	0.12	1.5	5.0
09	9.0	0.22	2.4	6.1	8.9	0.13	2.0	3.0	7.2	0.06	0.8	7.3	8.4	0.10	1.2	6.2
10	8.7	0.14	1.6	6.9	8.5	0.19	2.1	2.9	7.1	0.07	1.0	7.7	8.2	0.06	0.7	5.3
11	8.2	0.22	2.8	6.9	8.7	0.20	2.3	1.7	6.9	0.09	1.3	7.5	8.0	0.05	0.6	6.1
12	8.2	0.27	3.3	6.6	8.8	0.25	2.8	1.5	6.8	0.12	1.5	7.6	7.9	0.05	0.8	5.6
13	8.4	0.31	3.9	6.1	8.9	0.22	2.5	1.9	6.8	0.13	1.8	8.1	8.0	0.06	0.8	5.4
14	8.6	0.23	2.7	5.6	9.2	0.23	2.5	2.0	6.9	0.12	1.7	8.0	8.2	0.07	0.9	4.6
15	8.9	0.23	2.6	5.5	9.5	0.13	1.4	2.8	7.1	0.08	1.1	8.1	8.5	0.06	0.7	5.0
16	9.0	0.26	2.9	5.3	9.6	0.09	0.9	3.4	7.3	0.08	1.1	8.0	8.6	0.11	1.3	5.3
17	9.0	0.19	2.1	5.6	9.5	0.08	0.8	3.1	7.3	0.08	1.1	7.5	8.6	0.09	1.0	5.8
18	8.8	0.24	2.7	5.7	9.5	0.13	1.4	4.1	7.3	0.04	0.6	8.9	8.5	0.11	1.3	5.4
19	8.5	0.17	2.0	6.2	9.1	0.07	0.8	3.6	6.7	0.10	1.5	8.5	8.1	0.08	1.0	6.4
20	8.2	0.18	2.2	6.5	8.5	0.16	1.9	2.1	6.4	0.08	1.4	7.6	7.7	0.08	1.0	5.6
21	8.2	0.24	2.9	6.8	7.9	0.07	0.9	1.4	6.4	0.08	1.2	5.5	7.5	0.09	1.1	6.0
22	8.1	0.17	2.1	6.7	7.4	0.18	2.4	0.5	6.0	0.12	2.0	6.1	7.2	0.08	0.8	6.3
23	7.8	0.14	1.8	6.3	6.8	0.17	2.5	1.5	5.1	0.10	2.0	7.3	6.6	0.05	0.8	4.3

	Equinoxes				December Solstice				June Solstice				Annual			
Sol. No.	Aver- age f_0F_2 Mc/s	P_1 Mc/s	%	t_1 hour.	Aver- age f_0F_2 Mc/s	P_1 Mc/s	%	t_1 hour.	Aver- age f_0F_2 Mc/s	P_1 Mc/s	%	t_1 hour.	Aver- age f_0F_2 Mc/s	P_1 Mc/s	%	t_1 hour.
00	4.3	0.18	4.2	5.5	6.2	0.07	1.1	3.4	2.9	0.03	1.0	3.0	4.5	0.06	1.3	5.9
01	4.0	0.15	3.5	5.0	6.3	0.05	0.8	2.9	2.9	0.05	1.7	2.8	4.4	0.04	0.9	4.8
02	4.4	0.15	3.4	5.5	6.9	0.03	0.5	2.2	3.0	0.05	1.7	2.5	4.4	0.04	0.9	4.3
03	4.5	0.14	3.1	5.5	5.5	0.08	1.5	10.5	2.9	0.06	2.1	11.5	4.3	0.02	0.5	8.2
04	3.9	0.06	1.5	5.3	5.0	0.08	1.6	11.3	2.9	0.07	2.4	11.7	3.9	0.05	1.3	11.0
05	3.5	0.02	0.6	5.3	5.1	0.13	2.5	10.0	2.6	0.05	1.9	1.6	3.7	0.06	0.8	9.8
06	4.4	0.04	0.9	5.3	5.3	0.14	2.4	0.4	2.6	0.04	1.5	2.7	4.3	0.04	0.9	1.3
07	5.7	0.11	1.9	5.6	6.2	0.13	2.0	1.4	4.2	0.06	1.4	9.1	5.4	0.03	0.6	3.4
08	6.4	0.14	2.2	5.7	6.6	0.16	2.4	1.6	5.1	0.03	0.6	7.5	6.0	0.04	0.7	3.7
09	7.1	0.22	3.1	6.2	7.2	0.16	2.2	1.8	5.6	0.03	0.5	6.6	6.6	0.07	1.1	4.4
10	7.6	0.29	3.7	6.6	7.6	0.21	2.7	1.8	6.3	0.11	1.8	4.4	7.3	0.09	1.2	4.8
11	8.3	0.31	3.5	5.7	8.3	0.19	2.2	2.4	6.7	0.23	3.4	3.0	8.1	0.17	2.1	4.0
12	9.2	0.35	3.6	6.1	9.6	0.16	1.7	2.0	6.8	0.07	1.0	6.0	8.8	0.17	1.9	5.8
13	10.3	0.22	2.1	6.4	10.1	0.19	1.8	2.7	7.1	0.21	3.0	5.4	9.8	0.16	1.7	5.4
14	10.4	0.14	1.3	6.2	10.4	0.00	0.0	2.6	7.4	0.13	1.8	5.1	9.4	0.10	1.0	6.2
15	10.2	0.13	1.3	6.1	10.4	0.09	0.9	3.8	7.1	0.06	0.8	6.7	9.3	0.08	0.9	5.5
16	9.5	0.30	3.2	7.5	9.8	0.13	1.3	9.4	6.7	0.06	0.9	6.2	8.7	0.15	1.7	8.0
17	8.9	0.16	1.8	8.0	9.0	0.13	1.4	8.2	5.8	0.08	1.4	8.4	7.9	0.12	1.5	8.1
18	8.0	0.17	2.1	0.0	8.3	0.11	1.3	4.3	4.6	0.02	0.4	11.0	7.0	0.03	0.4	8.1
19	6.3	0.08	1.2	10.7	7.7	0.05	0.6	11.3	4.0	0.04	1.0	7.4	6.1	0.04	0.7	10.3
20	5.6	0.15	2.7	7.9	7.0	0.04	0.6	3.3	3.9	0.12	3.1	4.6	5.5	0.06	1.1	6.8
21	5.1	0.17	3.3	7.0	6.6	0.03	0.5	4.4	3.6	0.01	0.3	5.1	5.1	0.05	1.0	6.7
22	4.7	0.20	4.3	6.6	6.4	0.09	1.4	4.5	3.3	0.04	1.2	3.1	4.8	0.08	1.7	5.7
23	4.6	0.20	4.3	6.4	6.3	0.05	0.8	4.9	3.0	0.05	1.7	3.2	4.6	0.08	1.7	5.7

CONTENTS

CHAPTER 4

		Page
(a)	Lunar tidal variations in $F_0 F_2$ and $h_y F_2$ over Ahmedabad	1
(b)	Lunar variations in $F_0 F_2$ over Puerto Rico and Huancayo	9
	Discussion	3

CHAPTER 4

SUMMARY AND DISCUSSION

In this final chapter are summarized the important points emerging out of the studies on the lunar tidal oscillations in (a) the critical frequency of the F_2 layer of the ionosphere and the height of maximum electron density over Ahmedabad, and (b) the critical frequency of the F_2 layer of the ionosphere over Panama, Huancayo and Buenos Aires. This is followed by a comparison with the results obtained by other workers and a short discussion.

(a) Lunar tidal variations in f_0F_2 and h_pF_2 over Ahmedabad

The maximum annual average amplitude of the lunar tide in f_0F_2 during March 1958 to February 1966 was 0.3% Mc/s. This occurred at about 12 solar hour and the corresponding lunar phase was 11.7 lunar hour. The maximum yearly amplitude of the tide in h_pF_2 was 4.2 Km occurring at about 12 solar hour with its phase at about 8.3 lunar hour.

The variation of the amplitude and phase of the tide in f_0F_2 with solar time was studied separately for each season. During the equinoxes, a maximum amplitude

of 0.50 Mc/s occurred at about 12 solar hour with its phase at about 0.00 lunar hour; in winter (December solstice) also, the maximum amplitude of 0.51 Mc/s was observed at about 13 solar hour with its phase at 10.0 lunar hour. During summer (June solstice), however, the maximum amplitude of 0.32 Mc/s occurred at about 15 solar hour and its phase at 11.7 lunar hour. On harmonic dials the vectors representing the amplitude and phase always rotated in the anti-clockwise direction.

Seasonally, the maximum amplitude of the lunar tide in f_0F_2 averaged over all solar hours, occurred during the equinoxes with a magnitude of 0.14 Mc/s and phase 8.2 lunar hour. The average lunar tide in h_pF_2 had its amplitude of about 1.22 Km with its phase at 7.3 lunar hour.

(b) Lunar variations in f_0F_2 over Panama, Huancayo and Buenos Aires

The variation with solar time of the semi-diurnal lunar tide in f_0F_2 was studied for each season separately and also annually. Broadly, the amplitude of the tide was maximum during the December solstice and equinoxes at all the three places and negligibly small and random in phase during the June solstice. The maximum annual average tides which occurred at Panama, Huancayo and Buenos Aires respectively were 0.35 Mc/s (6.9 %) at 12 hour, 0.37 Mc/s (4.6 %) at 11 hour and 0.43 Mc/s (6.0 %) at 10 hour. Their

respective phases were 11.3, 4.6 and 7 to 8 lunar hours. The vectors representing the amplitude and phase of the semi-diurnal lunar tide rotated in the anti-clockwise direction at all the three stations. There was a definite indication of enhanced tidal amplitudes at 03 solar hour at Panama and Huancayo. At Buenos Aires, however, the tidal effect at 03 hour was smaller.

Seasonally, the maximum amplitudes of the semi-diurnal tide in f_0F_2 happened in one of the months of the winter solstice or the equinoxes. Generally, larger tidal amplitudes were observed around 12 solar hour than those around 00, 06 and 18 hours for Panama and Huancayo. In the case of Buenos Aires, however, the amplitudes around 18 hour also were significantly large for all the months.

As for the diurnal component of the lunar tide, its amplitude at all the stations was larger during the equinoxes than during the two solstices. Their phases during the June solstice were the most random.

Discussion

Many workers have found an enhancement of lunar tidal perturbation in the F_2 layer of the ionosphere during daytime near the magnetic equator. Martyn (1947) showed that the phase and amplitude of the semi-diurnal lunar variations in f_0F_2 and h_mF_2 at Huancayo were strongly dependent on solar

time. Rastogi and Gautier (1960) analysed f_0F_2 data for a number of low latitude stations and concluded that f_0F_2 lunar tide at solar noon had large maxima about two days after each lunar quarter at stations near the magnetic equator. Rastogi (1961) found that the amplitude of lunar tide calculated from daytime f_0F_2 was much larger than that calculated from all day f_0F_2; and also that the night-time f_0F_2 at Huancayo did not show any lunar tidal variation. Brown (1960) analysed F_2 layer data for another equatorial station, viz. Ibadan. He also reported large luni-solar variations in F_2 layer parameters. He found large seasonal variations of their amplitude and phase, the latter changing considerably during the course of a solar day. All these and other similar results led to the conclusion that the large lunar F_2 variations in the magnetic equatorial zone occur only during daylight hours. In other words, luni-solar tide is predominant in this zone. According to Martyn, the vertical drift motions of charged particles caused by their horizontal movements across the horizontal lines of the magnetic field of the earth, in the presence of an electric field, are responsible for the large lunar tidal variations in the F_2 layer near the magnetic equator.

It is interesting to note that for all the stations considered here, viz. Ahmedabad, Panama, Huancayo and Huancayo alone, the amplitudes of lunar tide in f_0F_2 were much larger

during the December solstice than during the June solstice. Similar results were obtained by Bartels (1936) at Huancayo. He concluded that the amplitude of daytime f_0F_2 lunar tide at Huancayo in local summer was about five times larger than in local winter. The ratio of the amplitude of the magnetic lunar variation in summer to that in winter was about three at Huancayo. The phase of the lunar tidal variations in f_0F_2 at the places examined, namely Panama, Huancayo and Buenos Aires, was very random during the June solstice. Again, the rotation of the vector representing the amplitude and phase of lunar tide was essentially in the anti-clockwise direction for all the four stations.

Rastogi (1959) presented a qualitative general picture of the variation of the lunar tide in f_0F_2 at Panama, Huancayo and Buenos Aires. He found that the maximum lunar perturbation in f_0F_2 was felt at Huancayo at the time of the midday bite-out of f_0F_2, while at Panama and Buenos Aires it was observed at the time of the afternoon peak of f_0F_2. His point was verified quantitatively by our detailed analyses.

The maximum yearly average amplitude of the lunar tide in f_0F_2 at Panama (a northern tropical latitude station), at Huancayo (a magnetic equatorial station) and at Buenos Aires (a southern tropical latitude station) occurred at 12, 11 and 16 solar hours respectively. Now the corresponding f_0F_2 maxima at Panama and Buenos Aires occurred at about 15 solar hour, and

the maximum bite-out of f_0F_2 at Huancayo happened at about 12 hour. Thus, the maximum lunar tidal amplitudes at Huancayo and Buenos Aires occurred almost simultaneously with the afternoon bite-out of f_0F_2 and the maximum of f_0F_2 respectively. It remains to be seen whether the large lunar perturbations in f_0F_2 observed at tropical latitude stations are due to the processes which are responsible for higher values of f_0F_2 at those places.

At Panama and Huancayo large amplitudes of lunar tides in f_0F_2 were also observed at 05 hour. A similar result was reported by Martyn (1947) at Huancayo. He found that the half-amplitude of the density variations in N_{max} had a value of 14.6 % at 05 hour while it was only 2 % at 07 hour. It is difficult to understand why Buenos Aires shows reduced tidal effect around 05 hour, even though the values of f_0F_2 at all the three stations at that time are very low.

Thus, whereas Panama behaves as a tropical latitude station, with the half-amplitude of f_0F_2 lunar tide of about 0.25 Mc/s (3.9 %) at 12 hour and its phase at 11.3 lunar hour, Buenos Aires shows very different lunar tidal variations with a semi-diurnal amplitude of 0.43 Mc/s (5.0 %) at 16 hour and its phase between 7 to 8 lunar hours.

At some southern high latitude stations, Rastogi (1960) had observed abnormal features of the F_2 region of the ionosphere.

For example, in the west zone (American zone) the ionization in the F_2 region of the ionosphere at a station in the southern hemisphere was lower than that at a station of equal magnetic dip in the northern hemisphere. There was no such difference in the east zone. Again, during mid-night hours of local summer months abnormally high values of f_0F_2 were observed at the southern stations in the west zone.

Whether the anomalous behaviour of the lunar tide in f_0F_2 is connected with the anomalous behaviour of f_0F_2 itself and how far either of these is connected with the asymmetry of the geomagnetic field in the southern hemisphere are matters requiring further study.

REFERENCES

Hartree	1947	Part II. Proc.Roy.Soc., A, 190, 273 - 293.
Mellish and Gaubler	1949	J.Geophys. Res., 54, 303 - 304.
Pasquill	1951	J.Atmosph.Terr.Phys., 1, 340 - 338.
Brown	1956	J.Atmosph.Terr.Phys., 8, 144 - 154.
Bartels	1960	J.Atmosph.Terr.Phys., 1, 8 - 12.
Rastogi	1963	J.Geophys.Res., 68, No.4, 1165 - 1169.
Rastogi	1960	J.Geophys.Res., 65, No.2, 585 - 592.

000 0 000